

Characterisation of freeze dried amino acids and gelatin based rapidly disintegrating tablets

JOSEPH DARKWAH

DECEMBER 2011

**In partial fulfillment of the degree of MPhil awarded by
De Montfort University.**

i. Statement

The work presented in this thesis was carried out by the author in the Department of Leicester School of Pharmacy within the Faculty of Health and Life Sciences (De Montfort University) from October 2009 to October 2011. Unless otherwise accredited, the work was carried out by the author and has not submitted in any other form for any other degree or qualification.

ii. Acknowledgements

I would like to thank God Almighty for giving me the knowledge and strength throughout this project.

Special thanks also go to my parents Mr & Mrs Danquah, siblings and Jennifer Ekewenu for their interest shown in my work and sponsoring it. I would forever be grateful to them for all the support and advice they have given me throughout.

Thank you so much Dr Geoff Smith and Dr Irina Ermolina for your excellent support and the patience you had with me. I could not have asked for better supervisors than you. Your guidance and encouragement made stressful times easy to cope with.

iii. Abstract

Background Recent research has shown the feasibility of using individual or a combination of amino acids as a replacement component for sugars in RDT formulations. What has emerged from this work is the notion of an optimal concentration of amino acid, i.e. one that is sufficiently high to provide the desired mechanical strength but not too high to impact disintegration time.

Aim In this study, the degree of amino acid crystallinity in gelatin/amino acid based RDTs was investigated using terahertz pulsed spectroscopy. Three amino acids were investigated: alanine (89 g mol^{-1}), serine (105 g mol^{-1}), and proline (115 g mol^{-1}).

Methods The three amino acids were studied by terahertz pulsed spectroscopy (in the frequency band 0.1 to 3 THz; $3 \text{ to } 100 \text{ cm}^{-1}$), both in the pure crystalline form (as received from the manufacturer) and in the form of a co-freeze-dried matrix with gelatin (in weight fractions of 10:90, 30:70, 50:50, 70:30).

Results Each pure crystalline form of amino acid displayed one or two resonance peaks at characteristics wave numbers, which were in general agreement with the literature (with alanine at 75 cm^{-1} and 85 cm^{-1} ; proline at 48 cm^{-1} and 66 cm^{-1} and serine centred on 67 cm^{-1}). Irrespective of the amino acid in question (viz. alanine, proline, or serine) all freeze-dried formulations containing 10% amino acid and 90% gelatin were found to have no crystallinity with respect to the amino acid component. On increasing the amino acid to 30%, only those formulations manufactured from serine showed evidence of crystallisation behaviour. Only on increasing the concentration of amino acid to 50% did the spectra of alanine display the distinct absorption bands of their crystalline reference counterparts. The degree of crystallinity in serine and alanine was estimated using calibration model built from partial least square regression (PLSR). The increased concentration of alanine to 50%w/w and 70% w/w in freeze dried gelatin matrix showed an estimated degree of crystallinity to be $\sim 62\%$ and $\sim 72\%$ ($\pm 16\%$) respectively. Similarly the degree of crystallinity in 30%w/w and 50% w/w serine/gelatin freeze dried matrix were estimated to be $\sim 55\%$ and $\sim 97\%$ ($\pm 10\%$) respectively.

Discussion This work has shown a rank order of solubility within the freeze-dried gelatin matrix of proline > alanine > serine. Unsurprisingly, the same rank order exists for the aqueous solubility, with serine being the least soluble ($\sim 5 \text{ g ml}^{-1}$) and proline being the most soluble

(~162 g ml⁻¹). The impact of hydrophobic interactions between the amino acid and gelatin are therefore less dominant in defining the crystallinity of the amino acid within the freeze-dried material.

iv. Table of contents

Table of Contents

| | | |
|------------|---|------|
| i. | Statement | i |
| ii. | Acknowledgements..... | ii |
| iii. | Abstract..... | iii |
| iv. | Table of contents | v |
| v. | List of Figures | viii |
| vi. | List of Tables | xii |
| Chapter 1. | Introduction | 2 |
| 1.1 | Background | 3 |
| 1.1.1 | Rapidly Disintegrating Tablets | 3 |
| 1.1.2 | Summary for technologies used in making RDTs..... | 9 |
| 1.1.3 | Hypothesis..... | 10 |
| 1.1.4 | Amino acids and gelatin | 11 |
| 1.2 | Physical Properties of freeze dried RDTs | 19 |
| 1.2.1 | Moisture content and Glass transition | 19 |
| 1.2.2 | Mechanical properties of freeze-dried product..... | 19 |
| 1.3 | Some quantification techniques used to determine crystallinity..... | 20 |
| 1.3.1 | Thermal analysis..... | 21 |
| 1.3.2 | Spectroscopic Techniques..... | 22 |
| 1.4 | Data processing for quantitative analysis – Regression analysis | 1 |
| 1.4.1 | Linear regression (LR)..... | 1 |
| 1.4.2 | Partial Least squares regression (PLSR) | 2 |
| Chapter 2. | Aim of the Project | 6 |
| 2.1 | Objectives..... | 6 |

| | |
|---|----|
| • Phase I Method Development | 6 |
| • Phase II Development and Validation of the Calibration Model | 6 |
| • Phase III Determining unknown crystallinity in freeze dried gelatin/amino acids | 6 |
| Chapter 3. Experimental Section | 7 |
| 3.1 Materials | 7 |
| 3.2 Equipment and software | 7 |
| 3.2.1 Equipment/Data acquisition | 7 |
| 3.2.2 Software/Data processing..... | 7 |
| 3.3 Methods..... | 8 |
| 3.3.1 Preparation of Solutions | 8 |
| 3.3.2 Colorimetry measurements | 8 |
| 3.3.3 Method Development for THz Measurements: Freeze Drying..... | 9 |
| 3.3.4 Method Development for THz Measurements: Pellet Preparation..... | 9 |
| 3.3.5 Pellet Preparation for Crystalline Amino Acids and Freeze-Dried Amino Acids . | 11 |
| 3.3.6 THz measurements | 12 |
| 3.3.7 Peak Area Analysis | 12 |
| Chapter 4. Results..... | 15 |
| 4.1 Phase I - Method development | 15 |
| 4.1.1 Pellet Preparation | 15 |
| 4.1.2 Effects Pellet Thickness | 16 |
| 4.1.3 Particle size effects..... | 18 |
| 4.1.4 Basic Terahertz Absorption features..... | 20 |
| 4.2 Phase II – Development and Validation of the Calibration Model | 24 |
| 4.2.1 THz Measurements of Sucrose | 24 |
| 4.2.2. Testing Calibration Model..... | 27 |
| 4.3 Calibration models of amino acids..... | 30 |
| 4.3.1 THz Measurements | 30 |

| | | |
|-------------|--|----|
| 4.3.2 | Partial Least Squares Regression | 34 |
| 4.4 | Phase III– Crystallinity in freeze dried gelatin/amino acid..... | 39 |
| 4.4.1 | Colorimetric measurements | 39 |
| 4.4.2 | THz measurements | 39 |
| 4.4.3 | Determining degree of crystallinity using PLSR | 41 |
| Chapter 5. | Discussions | 43 |
| 5.1 | THz studies of;..... | 43 |
| 5.1.1 | Crystalline amino acids and gelatin individually in polyethylene | 43 |
| 5.1.2 | Freeze dried amino acids/gelatin in polyethylene..... | 44 |
| 5.2 | Calibration models | 47 |
| 5.3 | Degree of crystallinity in freeze dried amino acids..... | 48 |
| Chapter 6. | Conclusion..... | 49 |
| Chapter 7. | Future work..... | 50 |
| Chapter 8. | References | 55 |
| Appendix I | | 64 |
| Appendix II | | 66 |

v. List of Figures

| | |
|---|----|
| Figure 1. Diagram of the technologies currently used for producing commercial RDTs..... | 4 |
| Figure 2. Schematic summary of the technologies used in making rapidly disintegrating tablets and the design options for enhancing the final product quality attributes. | 11 |
| Figure 3. The molecular structure of an α amino acid in the <i>L</i> - stereoisomeric form..... | 12 |
| Figure 4. The molecular structure of alanine (Circled is the neutral non polar organic constituent)..... | 14 |
| Figure 5. The molecular structure of <i>L</i> -proline which indicates a cyclic side chain..... | 15 |
| Figure 6. The molecular structure of <i>L</i> -serine indicating methoxyl side chain..... | 16 |
| Figure 7. Differential scanning calorimetry thermogram of crystal <i>L</i> -serine. Highlighted areas corresponding to melting endothermic peak and decomposition exotherm. | 22 |
| Figure 9. Typical Raman spectra of <i>L</i> -serine and gelatin indicating the distinctive absorption bands. (Insert spectra features at the (I) terahertz domain and (II) portions of the mid IR). Absorption spectra measured at Nottingham University..... | 24 |
| Figure 10. Terahertz absorption spectra of <i>L</i> -leucine and <i>L</i> -lysine offset from 5 cm ⁻¹ . The spectra of leucine have been shifted upwards 0.5 units for clarity. The distinctive absorption bands are marked with + for leucine and * for lysine. | 26 |
| Figure 11. Three different positions on the sample where THz measurements was taking. | 12 |
| Figure 12. Estimating peak area using (A) Linear function baseline (B) Polynomial function baseline..... | 14 |
| Figure 13. The optical delay response from varying the compression force used to produce amino acid/polyethylene pellets. The spectra presented are average of three different measurements from different positions..... | 15 |
| Figure 14. The average thickness of polyethylene pellets against weight | 16 |
| Figure 15. Terahertz waveform and scanner position of different concentration of pellets. Arrows show the spurious internal reflections from the air-pellet interface for the three thinnest pellets (prepared from 200, 250 and 300 mg PE)..... | 16 |
| Figure 16. Log of the peak height against the thickness of the diluent..... | 17 |
| Figure 17. Difference between the sample spectrum of 300 mg tablet with pellet thickness of 3.24 mm and 400 mg with pellet thickness of 3.66 mg. The ripples in the absorption spectrum will cause further issues when recording the spectra from the amino-acid containing samples. | 18 |

| | |
|--|----|
| Figure 18. Terahertz absorption spectra of <i>L</i> -alanine indicating the effects of varying the particle size. Each spectrum is the average of three spectra recordings from three different positions..... | 19 |
| Figure 19. THz absorption spectra of 10% w/w sucrose in PE pellet between 5 cm ⁻¹ and 95 cm ⁻¹ . The data presented is the average of three measurements from three different areas of the pellet. | 20 |
| Figure 20. THz absorption spectra of 10% w/w FREEZE DRIED sucrose in PE pellet between 5 cm ⁻¹ and 95 cm ⁻¹ . The data presented is the average of three measurements from three different areas of the pellet..... | 21 |
| Figure 21. THz absorption spectra of 10% w/w <i>L</i> -alanine in PE pellet between 5 cm ⁻¹ and 95 cm ⁻¹ . The data presented is the average of three measurements from three different areas of the pellet. | 21 |
| Figure 22. THz absorption spectra of 10% w/w <i>L</i> -proline in PE pellet between 5 cm ⁻¹ and 95 cm ⁻¹ . The data presented is the average of three measurements from three different areas of the pellet. | 22 |
| Figure 23. THz absorption spectra of 10% w/w <i>L</i> -serine in PE pellet between 5 cm ⁻¹ and 95 cm ⁻¹ . The data presented is the average of three measurements from three different areas of the pellet. | 22 |
| Figure 24. THz absorption spectra of 10% w/w gelatin in PE pellet between 5 cm ⁻¹ and 95 cm ⁻¹ . The data presented is the average of three measurements from three different areas of the pellet. | 23 |
| Figure 25. Terahertz absorption spectra of three different partitions of polycrystalline sucrose. Each absorption spectrum is an average of three repeated measurements from three separate positions of the pellets..... | 25 |
| Figure 26. Calibration model based on linear regression of the estimated peak area for polycrystalline sucrose against the actual concentrations with 95% prediction bands. | 26 |
| Figure 27. Calibration model based on partial least square regression of the predicted concentration for polycrystalline sucrose against the actual concentrations with 95% prediction bands..... | 27 |
| Figure 28. Calibration model based on linear regression of the estimated peak area for polycrystalline sucrose against the actual concentrations with 95% prediction bands fitted with the predicted concentrations in samples prepared with unknown active proportions..... | 28 |

| | |
|---|----|
| Figure 29. Calibration model based on partial least square regression of the predicted concentration for polycrystalline sucrose against the actual concentrations with 95% prediction bands fitted with the predicted concentrations in samples prepared with unknown active proportions. | 29 |
| Figure 30. THz terahertz absorption spectra of crystalline <i>l</i> -alanine for three separate partitions. Each individual spectrum is an average of three repeated measurements per each sample for each separate partition..... | 31 |
| Figure 31. THz absorption spectra of crystalline <i>l</i> -proline for three separate partitions. Each individual spectrum is an average of three repeated measurements per each sample for each separate partition. | 32 |
| Figure 32. The terahertz absorption spectra of crystalline <i>l</i> -serine for three separate partitions. Each individual spectrum is an average of three repeated measurements per each sample for each separate partition..... | 33 |
| Figure 33. PLSR calibration model of the predicted concentration for <i>l</i> -alanine against the actual concentrations with 95% confidence interval bands..... | 34 |
| Figure 34. PLSR calibration model of the predicted concentration for <i>l</i> -alanine against the actual concentrations with 95% prediction bands. The model is fitted with the predicted concentrations in samples prepared with unknown alanine concentrations. | 35 |
| Figure 35. PLSR calibration model of the predicted concentration for <i>l</i> -proline against the actual concentrations with 95% confidence interval bands..... | 35 |
| Figure 36. PLSR calibration model of the predicted concentration for <i>l</i> -proline against the actual concentrations with 95% prediction bands. The model is fitted with the predicted concentrations in samples prepared with unknown proline concentrations..... | 36 |
| Figure 37. PLSR calibration model of the predicted concentration for <i>l</i> -serine against the actual concentrations with 95% confidence interval bands..... | 37 |
| Figure 38. PLSR calibration model of the predicted concentration for <i>l</i> -serine against the actual concentrations with 95% prediction bands. The model is fitted with the predicted concentrations in samples prepared with unknown proline concentrations..... | 38 |
| Figure 39. Terahertz absorption spectra of freeze dried gelatin and individual <i>l</i> -alanine. Each spectrum is the average of 6 repeated measurements from different areas across the pellet. | 39 |
| Figure 40. Terahertz absorption spectra of freeze dried gelatin and individual <i>l</i> -proline. Each spectrum is the average of 6 repeated measurements from different areas across the pellet. | 40 |

| | |
|--|----|
| Figure 41. Terahertz absorption spectra of freeze dried gelatin and individual <i>L</i> -serine. Each spectrum is the average of 6 repeated measurements from different areas across the pellet. 40 | |
| Figure 42. PLSR calibration model of the predicted concentration for <i>L</i> -alanine against the actual concentrations with 95% prediction bands. The model is fitted with the predicted degree of crystallinity in samples prepared with freeze dried gelatin/alanine..... 41 | 41 |
| Figure 43. PLSR calibration model of the predicted concentration for <i>L</i> -serine against the actual concentrations with 95% prediction bands. The model is fitted with the predicted degree of crystallinity in samples prepared with freeze dried gelatin/serine. 42 | 42 |

vi. List of Tables

| | |
|---|----|
| Table 1. Summary of the modified technologies used to produce commercial RDTs (Fu et al., 2004) | 5 |
| Table 2. Some examples of commercially available, preapproved or submitted RDT products. Table reproduced from (Fu et al., 2004)..... | 9 |
| Table 3. Summary of some basic properties of the selected amino acids (National Institute of Standards and Technology, 2011)..... | 17 |
| Table 4 Summary of some technologies used to study the physical properties and quantify degree of crystallinity | 27 |
| Table 5. An example of K-fold CV of three datasets | 3 |
| Table 6 compares linear regression with partial least square regression analysis..... | 4 |
| Table 7. List of the equipment used for this project..... | 7 |
| Table 8. Preparation of amino acids solutions based on the addition of a known weight of amino acid to a fixed weight (100 g) of a 5% gelatin solution. The effective concentration has been calculated assuming that gelatin reduces the available water activity by 10%. Comparison of this effective concentration with the literature value of aqueous solubility shows whether the amino acid concentration would exceed the theoretical solubility threshold..... | 8 |
| Table 9. Composition of the different freeze-dried formulations studied | 11 |
| Table 10. Partition into three datasets of the concentration range for 400 mg Pellets manufactured for each material under test. | 13 |
| Table 11. Estimated scores from principal component analysis (PCA) using the dimension reduction from the dot product | 26 |
| Table 12. For a function of $f(x) = p_1 \cdot x + p_2$, the following parameters were estimated for the three different partitions. The average of the RMSE of these estimates is used as the prediction errors..... | 27 |
| Table 13. Parameters used for CV against their respective test sets | 27 |
| Table 14. Comparing the predicted concentrations using linear regression and PLSR calibration models for pellets prepared with unknown concentrations of sucrose..... | 28 |
| Table 15. Estimated functions of the three different partitions used for L-alanine in cross validation. | 34 |
| Table 16. Comparing the actual concentration and the predicted concentrations of samples prepared with unknown proportions of L-alanine. | 34 |

| | |
|--|----|
| Table 17. Estimated functions of the three different partitions used for l-proline in cross validation | 36 |
| Table 18. Comparing the actual concentration of unknown proline samples with the expected and predicted concentrations using PLSR calibration model | 36 |
| Table 19. Estimated functions of the three different partitions used for l-serine in cross validation | 37 |
| Table 20. Comparing the actual concentration of unknown samples with the expected and predicted concentrations using PLSR calibration model | 37 |
| Table 21. Parameters generated from quantitative models using PLSR. All values are expressed in terms of amino acid concentration %w/w..... | 38 |
| Table 22. Colorimetric absorbance recorded for the solution of gelatin, and amino acid/gelatin. | 39 |
| Table 23. Summary of the degree of crystallinity estimated from the PLSR calibration models built from the related crystalline amino acids (n=3, and RMSE 0.16%, 0.20%, and 0.10% for the respective models of alanine, proline and serine)..... | 42 |

Chapter 1. Introduction

The most popular medicinal dosage form, making up to 50 – 60% for all prescribed and widely accepted by patients, is tablet (Thakur and Kashi, 2011). The United States Pharmacopoeia describes tablets to be solid dosage forms containing medicinal substances with the inclusion or omission of suitable diluents (United States Pharmacopeial Convention, 2009). They may be classed based on the method of manufacture e.g. compression or moulded. Tablets have many characteristic advantages and disadvantages when compared to other formulations like liquids or powder dosage forms. Some of these advantages include an ability to offer the most accurate dose in drug administration compared to all other formulation types. Depending on the formulation design and manufacturing process, tablets can be modified to release the drug at the required time i.e. sustained release. The product taste can also be masked to enhance patient acceptability and compliance.

Although most drug manufacturer's targets the oral route, and is the patient preferred method, there are some major disadvantages that render this administration route unfavourable. Some of these disadvantages include some patients' inability to swallow, drug degradation in the acidic stomach environment, availability of good clean water, and the therapeutic onset. The drug bioavailability in the gastrointestinal tract (GIT) determines its therapeutic efficiency. Drug bioavailability may be influenced by either the physiochemical properties of the drug molecule, choice of excipients, or the route of administration. The therapeutic onset period is critical in treating patients with chronic ailments like coronary related conditions or diabetics. The compression forces used during manufacture of conventional tablets might result in poor disintegration and delayed dissolution profiles, thus slowing the therapeutic onset when compared with liquid dosage forms. Furthermore, some patients suffer from some discomfort or pain when swallowing, medically referred to as dysphagia. About 35% of the population suffer from this condition, of which 30 - 40% are elderly and 18 - 20% are people in long term care facilities (Lindgren and Janzon, 1991, Sastry et al., 2000). This problem leads to high incidence of patients non-compliance resulting in ineffective drug therapy; a situation which is more common in paediatric and geriatric patients (Seager, 1998). Some drug molecules, mostly proteins, may be unsuitable for administration via the oral route due to acid degradation and may also be susceptible to liver deactivation during first pass metabolism in the liver increasing risks of toxicity and side effects.

As a result of these disadvantages associated with conventional tablets, it has become imperative for researchers and drug manufacturers to develop better alternatives which incorporate most of the advantages of conventional tablets whilst reducing the disadvantages to the minimum. This has led to a current shift in industrial and academic research dedicated to developing oral route medication intended for buccal, sublabial or sublingual disintegration which will avoid gastric absorption. Such formulations may widely be referred to as fast dissolve, rapid dissolve, quick melt and rapidly disintegrating tablets with the function and the concept being similar.

1.1 Background

1.1.1 Rapidly Disintegrating Tablets

Over the past three decades, orally disintegrating tablets or rapidly disintegrating tablets (RDTs) have received considerable pharmaceutical and academic attention (Hirani et al., 2009, Sastry et al., 2000). The European Pharmacopoeia (Council of Europe, 2001) adopted the term orodispersible tablet as a tablet to be placed in the mouth where it disperses rapidly before swallowing and which disintegrates in less than 3 minutes. The British Pharmacopoeia (The British Pharmacopoeia Commission, 2011) vaguely describes orodispersible as “uncoated tablets intended to be placed in the mouth where they disperse rapidly before being swallowed”. RDTs are solid dosage forms containing the active drug which quickly dissolves or disintegrate into a suspension within the buccal cavity, usually in seconds (Sastry et al., 2000). Other than saliva, they do not require water or need to be chewed for disintegration to occur (Sastry et al., 2000). Currently, this technology is used to formulate drugs to treat cardiovascular diseases, analgesics, neuroleptics, anti-allergics and drugs for erectile dysfunction (Chang, 2000).

As a result of the immediate disintegration/dissolution on placing in the mouth, side effects often caused by first pass metabolites are reduced (Virley and Yarwood, 1990). Drugs susceptible to acidic degradation in the stomach and poorly water soluble drugs can also be administered at lower doses using such formulations (Corveleyn and Remon, 1998). However, good taste and pleasant mouth feel will also be an advantage for a better patient compliance.

One of the major differences between conventional tablets and RDTs is the porous nature of RDTs which aids liquid ingress. This characteristic should not however affect its sensitivity to atmospheric temperature and humidity nor should the porosity result in poor mechanical properties of the tablet (Fu et al., 2004). The mechanical properties of RDTs are dependent on the formulation design and excipients used.

Technologies and Excipients: There are several technologies currently employed in the pharmaceutical industry for commercial production of RDTs. These technologies have been extensively reviewed in the literature (C.C. DeRoche et al., 2003, Fu et al., 2004, Goel et al., 2008, Hirani et al., 2009, Sastry and Nyshadham, 2005, Sastry et al., 2000, Seager, 1998, Virley and Yarwood, 1990). Most of these technologies currently employed for manufacturing commercial RDTs may be categorised under the three core processes: Compaction; Moulding; and Freeze Drying as shown in Figure 1.

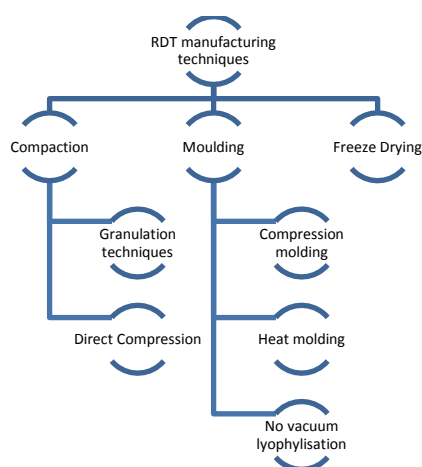


Figure 1. Diagram of the technologies currently used for producing commercial RDTs.

All these technologies aim to maximize the porosity of the final product, to improve the mechanical properties of the final product and to enhance disintegration time. Each technology has its own limitations with regard to the final product characteristics. In general, compaction technologies provide for optimal mechanical strength but sometimes at the expense of disintegration/dissolution time, whereas the products of moulding technology and to some extent freeze-dried are generally considered optimal in terms of disintegration/dissolution profile but often too fragile for patient handling/manipulation.

A summary of some of the technologies available to produce RDTs are listed in Table 1.

Table 1. Summary of the modified technologies used to produce commercial RDTs (Fu et al., 2004)

| Core Technology | Company | Modified Technology |
|-----------------------|-------------------------|---------------------|
| Freeze drying process | Cardinal Health | Zydis® |
| | Janssen Pharmaceuticals | QuickSolv® |
| | Pharmalyoc | Lyoc® |
| Tableting Process | Elan | NanoCrystal™ |
| | Cima Labs | OraSolv®/DuraSolv® |
| | Elan Corp. | Fast Melt® |
| | Ethypharm | FlashTab® |
| | Eurand | AdvaTab™Ziplets® |
| | KV Pharmaceutical | OraQuick® |
| | SPI Pharma | Pharmburst™ |
| | Akina | Frosta® |
| | | |
| Moulding | Yamanouchi | WOWTAB® |

Moulding Technologies RDTs are mainly prepared by compressing water soluble excipients previously wetted with either water or ethanol into moulded plates to form wetted mass. The wet mass is further made into tablets at a pressure which is usually lower than used in making conventional tablets. The physical structure and porosity of the final product will depend on the extent it dissolves in the molten carrier. This is because after the application of heat to remove the solvent, the spaces previously occupied by the solvent molecules forms voids within the matrix. For instance a highly dissolvable excipient will yield a very porous matrix after the solvent has been removed. Unfortunately, these tablets lack the appropriate mechanical properties resulting in erosion and breakage during handling. As shown in Figure 1, at least three different techniques have emerged from the moulding technology; compression moulding, moulding by vacuum without freeze drying and heat moulding.

The heat moulding process is a patented technology (Masaki and Ban, 1995) that combines a suspension of the active drug, agar solution and sugar into a blister packaging well. The wet mass is solidified at room temperature to form a jelly which still contains moisture. Under vacuum, the wet mass is finally dried at approximately 30 °C to remove moisture to leave out voids. It is claimed in the patent that, the use of agar not only acts as a binder, but also has an effect in improving the mechanical strength of the formulation as it is directly part of the formulation matrix.

Unlike the heat moulding process, moulding by vacuum without lyophilisation process evaporates the solvent from the drug suspension at ambient pressure (Dobetti, 2003, Fu et al., 2004). In this process the drug solution or suspension is poured into the required moulds and the mixture is frozen to form a solidified matrix. The solidified mass is finally subjected to

vacuum drying within the collapse and equilibrium freezing temperature range of the excipients leading to a formulation with a partially collapsed matrix (Parakh and Gothoskar, 2003). The difference between this method and freeze drying technology (to be considered in detail in later Sections) is that, in this process, evaporation of free unbound solvent occurs from a solid through the liquid phase into a gas, under controlled conditions, instead of the process of sublimation associated with freeze drying. The vacuum drying helps to improve the density of the matrix and enhance the mechanical stability of the product.

It was shown in the literature that by evaporating the frozen mixture consisting of a gum (e.g. acacia, xanthan), carbohydrate (e.g. dextrose, lactose, maltose or mannitol) and a solvent contained in a tablet mould, RDTs with a disintegration time of about 20 seconds to one minute can be produced (Pebley et al., 1994).

In the compression moulding process, the powder blend is initially moistened with a hydroalcoholic solvent before it is pressed into moulds to form a wet mass. The solvent is subsequently removed by air drying which results in a formulation with a less compact matrix but highly porous in structure when compared to traditional tablets (Parakh and Gothoskar, 2003).

Two major advantages of the moulding technique are:

- The presence of water soluble polysaccharide sugars improves the disintegration time and
- The formulation generally has an acceptable taste as a result of the incorporated sugar.

However, RDTs produced by this technology generally lack good mechanical properties (Fu et al., 2004).

Compaction technologies with some modifications has been extended from producing traditional tablets to RDTs with the technique easier to adapt in manufacturing scale and hence lower manufacturing cost when compared to producing freeze dried RDTs. It also has the advantage having fewer process steps when compared to the other techniques (Shukla et al., 2009).

RDTs produced by this method may possess acceptable disintegration qualities based on the single or corporate actions of disintegrants and in some cases effervescent couples.

There are two major components used in this technique; the disintegrating agents and swelling agents. It has been earlier explained that, the disintegration rate is thought to occur through the combined actions of the disintegrant, swelling agents and the amount of water absorbed (Caramella et al., 1984). The disintegration rate is influenced by the “critical concentration” of the disintegrant. Below the “critical concentration”, the disintegration rate is expected to be inversely proportional to the concentration of the disintegrant. However above the critical concentration, disintegration rate was either expected to increase or remain constant (Ringard and Guyothermann, 1988).

Generally, inclusion of saccharides in compaction technology based RDTs have improve disintegration time, although any individual saccharide can only enhance either the mechanical or disintegration properties. These saccharides have been divided into two categories; high mouldability (e.g. maltose and maltitol) and low mouldability (e.g. lactose and mannitol). Mouldability was used in the context as the ability of the saccharide to be compressed rather than moulding for wet or melt granulation. The term: low mouldability meant the saccharide had low compressibility and was very porous during compression. In contrast, high mouldability meant high compressibility but low porosity.

The Orasolv® technology (Cima Labs) is a patented modified traditional tableting technology used to develop over-the-counter RDT formulations (Wehling et al., 1993) based on the incorporation of effervescent couples as a disintegrant. It is produced using low compression pressure and effervescent disintegration pair, which includes an acid source (citric acid, fumaric acid, malic acid) and a carbonate source (sodium bicarbonate, potassium bicarbonate, potassium carbonate). The disintegrant is water sensitive, thus when in contact with moisture or saliva, CO₂ is evolved. The concentration of disintegrant couple used is usually around 20% to 25% of the total weight of the preparation (Fu et al., 2004). The gas release provides a distinct, pleasant sensation of effervescence (fizzing or bubbling) in the mouth.

Briefly, it was explained that the preparation contains multi-particulate forms that are capable of accommodating high drug dosing. The multi-particulates are made up of the drug dispensed in a suitable polymer which may include ethyl cellulose, methyl cellulose or acrylate with the inclusion of mannitol and magnesium oxide. In this instance, mannitol and magnesium oxide acts as drug release promoters from the polymeric coating (Sastry et al., 2000). The active drug component and mannitol are mixed with the polymeric dispersion under gentle continuous stirring, after which the magnesium oxide is added. The blend is dried for up to one hour at

50°C, de-lumped to ensure a homogeneous blend and dried for another one hour at 50 °C. The multi-particulates are loosely compressed into tablets at 1 – 2 kp hardness. This helps maintain the product fragility and surface coating used to mask poor taste.

Due to the low compaction force, the *in vivo* disintegration time is improved significantly when compared to the conventional tablet. However, the lower compaction force also impacts on the mechanical properties, and therefore are required in specially packaged foil-foil blisters.

Freeze drying technique for making RDTs has shown some improved disintegration properties when compared with the other techniques used. When in contact with moisture, freeze dried RDTs instantaneously disintegrates to release the drug due to the highly porous microstructure of the matrix.

Two major components are incorporated into RDTs formulated by this method. The first component forms the matrix, providing the tablet shape and some mechanical support during manufacturing and patient handling. These are mostly water soluble polymers such as gelatin, dextran, dextrin, polyvinylpyrrolidone and alginate (Sastry et al., 2000, Virley and Yarwood, 1990). They also physically entrap the active drug during the freeze drying process.

The second major component includes sugars (e.g. sucrose, lactose, glucose) and polyols (e.g. xylitol, mannitol). These acts as disintegrants and enhances the mechanical properties of the RDTs. However, to achieve the desirable disintegration and mechanical properties, high concentrations of sugars and polyols are required (Chandrasekhar et al., 2009, Seager, 1998).

Some of the current commercially available and pre-approved RDTs are shown in Table 2. Undoubtedly, the majority of RDTs have been prepared based on the Zydis® technology. There has been an in depth review of this technology by (Fu et al., 2004).

Due to the negative lower temperatures used in this process, water soluble drugs can form eutectic mixtures that cause freezing-point depression. During freezing, glassy solids may be formed which can cause a collapse in the process of drying. This is due to the supporting structure losing its integrity during sublimation (Fix, October, 1998, Jennings, 1999, Seager, 1998). However, drug loading for water insoluble drugs can be as much as 400 mg. The optimum disintegration and mechanical properties are lost when the dose is increased any higher (Fix, October, 1998, Seager, 1998). As a result, RDTs manufactured with this technique require special packaging such as PVC plastic packs, Aclar laminates or aluminium foil-foil. The

main purpose of these packaging is to ensure the product does not absorb any atmospheric moisture.

Table 2. Some examples of commercially available, preapproved or submitted RDT products. Table reproduced from (Fu et al., 2004)

| Brand Name | Active Ingredient | Application | Manufacturer | Technology |
|--------------------------------------|-----------------------|------------------------------------|---------------------------|------------|
| Claritin®RediTabs® | Loratidine | Antihistamine | Schering Corp. | Zydis® |
| Feldene Melt® | Piroxicam | NSAID | Pfizer | |
| Maxalt®-MLT® | Rizatriptan benzoate | Migraine | Merck | |
| Pepcid®ODT | Famotidine | Anti-ulcer | | |
| Zyprexa® | Olanzapine | Psychotic disorders | Eli Lilly | |
| Zofran®ODT | Ondansetron | Anti-emetic | GlaxoSmithKline | |
| Children's Dimetapp® ND | Loratidine | Allergy | Wyeth consumer healthcare | |
| Zubrin™(pet drug) | Tepoxalin | Canine NSAID | Schering Corp. | |
| Zelapar | Selegiline | Parkinson's disease | Elan/Amarin Corp. | |
| Klonopin® Wafers | Clonazepam | Sedation | Roche | |
| Risperdal®M-Tab™ | Risperidone | Schizophrenia | Janssen | |
| Imodium Instant melts | Loperamide HCl | Anti-diarrhoea | | |
| Propulsid®Quicksolv® | Cisapride monohydrate | Gastrointestinal prokinetic agent | | |
| Tempra Quicklets/ Tempra FirsTabs | Acetaminophen | Analgesic | Bristol-Myers Squibb | OraSolv® |
| Remeron® SolTab® | Mirtazapine | Anti-depression | Organon Inc. | |
| Triaminic®Softchews® | Various combinations | Paediatric cold, cough and allergy | Novartis consumer health | |

1.1.2 Summary for technologies used in making RDTs

As shown in Table 2, freeze drying technology could be considered a suitable process for manufacturing RDTs because it delivers a highly porous, often amorphous matrix that will inevitably dissolve rapidly. However, such RDTs are characterised by poor mechanical properties. Conversely the compaction technologies for making RDTs are generally considered optimal relative to mechanical properties but unless formulated with enough disintegrants, will not necessarily disintegrate and dissolve quickly.

The issue with RDTs formulated with freeze dry technology with respect to mechanical strength can be addressed through the addition of high concentration crystallising sugars. These same sugars are used in compaction technology based RDTs as disintegrants. The high concentration of sugars required in the formulation does not make freeze dried RDTs ideal for certain patient groups such as diabetics, paediatrics and patients with chronic diseases. An

alternative is to substitute polyols and sugars with small molecular weight additives that can improve the mechanical and perhaps the disintegration properties of RDTs.

The potential for amino acids to fulfil this role is evident from the number of successful pharmaceutical formulations and literature work. It has been suggested that amino acids would be attractive alternatives to sugars/polyols, not only because of the benefits to certain patient groups but also because there is a possibility that the mechanical properties might be optimised at a lower concentration of total solids, thereby creating the opportunity to increase the dose of the active drug component. However, what is not currently understood is how the choice of specific amino acid or combinations and the concentrations at which optimal mechanical properties and disintegration may be achieved.

1.1.3 Hypothesis

Amino acids have different physical properties which affect their solubility and crystallinity. In amino-acid containing freeze-dried RDTs, it might be that one amino acid would crystallise at a lower concentration than the others but will have poor solubility. Whilst this may enhance mechanical properties, the disintegration and dissolution might be adversely impacted. Likewise another amino acid might remain in solution, to ultimately end-up in an amorphous state at the end of the freeze-drying cycle, thus will have a good disintegration and dissolution profile but would not necessarily contribute much to the mechanical properties. It would be interesting therefore to be able to quantify and characterise the crystallinity achieved from a range of freeze dried amino acids. This will contribute towards better understanding of the relationship between mechanical strength and crystallinity and help select from some of the formulation design choices identified in Figure 2.

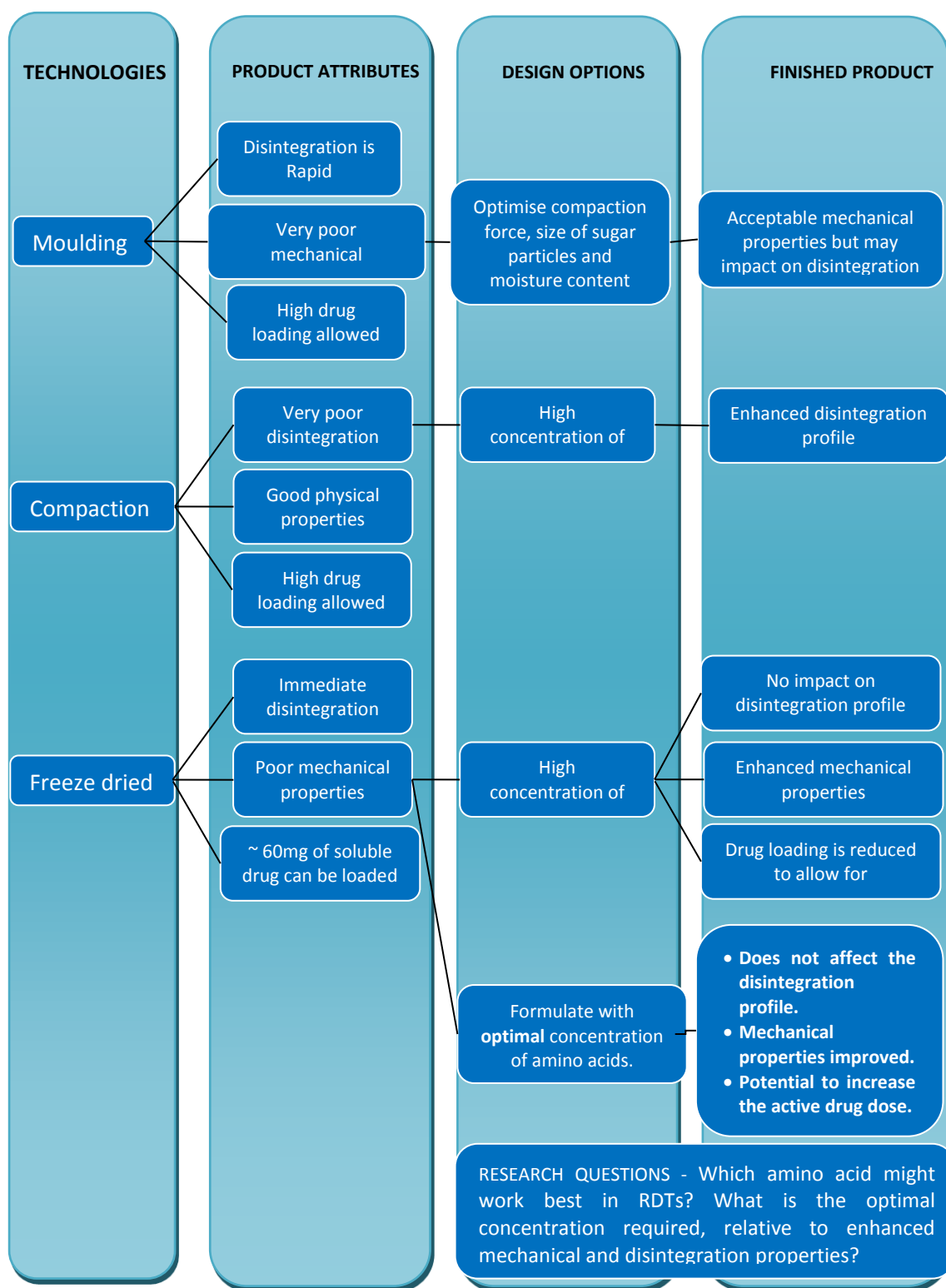


Figure 2. Schematic summary of the technologies used in making rapidly disintegrating tablets and the design options for enhancing the final product quality attributes.

Amino acids are well known biological molecules which have been used extensively in formulations as disintegration enhancers (Fukami et al., 2006), lubricants in oral tablets (Rotthausser et al., 1998) and in freeze-dried products as cryoprotectants (Mohammed et al., 2007) and bulking agent (Akers et al., 1995, Akers et al., 1994).

They are molecules characterised with a common backbone of an amine and carboxyl terminal attached to a central carbon atom. The central carbon atom is attached to a side chain (R group) which determines the characteristics of each specific amino acid. They are also referred to as α amino acid since the amino group is attached to the carbon atom immediately adjacent to the carboxyl group i.e. the α carbon. The α -carbon is attached to four groups and therefore is a chiral carbon atom except in the case of the simplest amino acid, glycine. Hence, all amino acids except glycine can exist in two different stereoisomers, the L and D form with only the L-form present in proteins during translation in the ribosome (Lubec and Rosenthal, 1990). The basic molecular structure of an amino acid is shown in Figure 3.

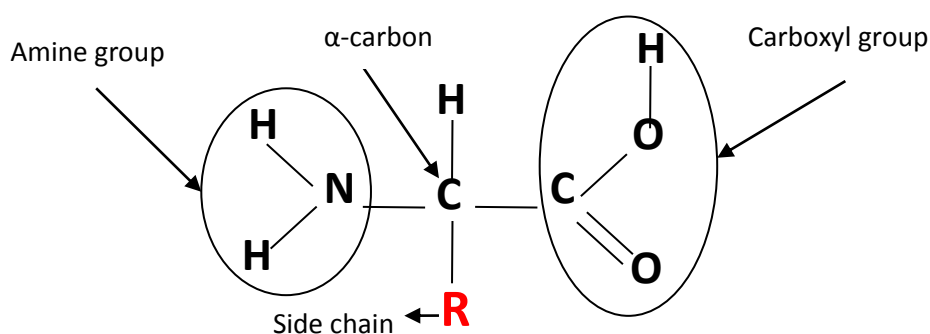


Figure 3. The molecular structure of an α amino acid in the L- stereoisomeric form.

Amino acids are crystalline solids with high range of melting temperatures $\sim 200^\circ\text{C}$ to 300°C (Rodante and Marrosu, 1990, Rodante et al., 1992, Grunenberg et al., 1984). This is because the dominant interaction within individual molecules is ionic rather than hydrogen bonds and other intermolecular interactions. The side group of each amino acid makes the molecule distinct and determines certain physical and chemical properties of the entire amino acid molecule.

One of such characteristics is discussed in context of the impact it might have on the disintegration and mechanical properties of RDTs.

Hydrophilic/Hydrophobic of the R- side chain – The major reason for amino acid as an alternative to sugars is the possibility of enhancing the mechanical properties whilst having negligible effect on the disintegration of RDTs. One of the major characteristics of amino acids

that can impact on the propensity to crystallise and disintegrate in a gelatin/API matrix is the hydrophobicity/hydrophilicity of the side chain. It is well documented that the hydrophobicity/hydrophilicity of the *R*-side-chains can significantly impact on crystallization in the absence of solvent (Liu and Li, 2008) for instance in freeze dried matrix of gelatin/amino acid.

Different amino acids have different hydrophilicity/hydrophobicity due to the chemical properties of the side chain. For instance, by virtue of the hydroxyl group in the organic constituent of serine, it is considered a polar amino acid which may impact on its aqueous solubility. In contrast, alanine is considered a non polar amino acid by virtue of the presence of a methyl group and therefore less soluble in aqueous solution. The solubility profiles of some amino acids have been extensively studied in water and other mixed solvents (Tseng et al., 2009, Held et al., Ji and Feng, 2008).

Another property of an amino acid influenced by the *R*-side chain hydrophobicity/hydrophilicity is the wettability of its crystalline powder. The disintegration process in oral tablets is initiated by wetting the surface of the powder bed. It has been established that, whilst some amino acids required few seconds before wetting onsets, others are wetted instantly. Alhusban *et al.* reported that whilst proline is wetted instantly, alanine and arginine required $1.0 \pm 0.7s$ and $4.9 \pm 2.1s$ respectively (AlHusban et al., 2010b). Fukami *et al.* showed that the wetting profiles of amino acids was dependant on the difference in the physical properties which may be related to the surface properties by using surface penetration methods (Fukami et al., 2005).

Relative to propensity to crystallise, it has been explained that when hydrophobic amino acids such as alanine and proline crystallise from an aqueous solution, the amino group interacts with the carboxyl group via hydrogen bonding, and the hydrophobic side-chains are inclined to assemble together via van der Waals interaction (Kyte, 2003). However, in the presence of a polymer such as gelatin, a non polar molecule (hydrophobic) such as proline and alanine tends to interact with the side chains of the gelatin to form a single stranded triple helix (deWolf and Keller, 1996), which is capable of absorbing more water. Furthermore, a previous study concluded that the metastable polymorphs of L-alanine and L-proline can be formed via sublimation process in freeze drying. This means, for such amino acids, high concentrations must be incorporated into the gelatin matrix to achieve some degree of crystallinity.

In the case of hydrophilic amino acids, when crystallized from aqueous solution, the crystal structure has its own distinct hydrogen interaction arrangements that involve not only the amine and carboxyl groups, but also donating and accepting groups in the *R*- side chain (Janczak et al., 1997). In the presence of water, the amino and carboxyl groups are ionized into the zwitterionic form leading to the presence of both short and long range interaction forces between the charged species.

Hence whilst it will be ideal to use hydrophilic amino acids to enhance mechanical properties, this may impact on disintegration since the required lattice energy will be high when compared to hydrophobic amino acids. In this project, the molecular structure of three different amino acids will be considered relative to their hydrophobicity/hydrophilicity and how this influences their ability to exist as a crystal solid. These will include the *L*-stereoisomers of alanine, proline, and serine.

***L*-alanine** is the simplest α -amino acid with a stereoisomer and is sometimes classified as an aliphatic amino acid due to the α -carbon atom being bound to a methyl (CH_3) side chain. The CH_3 side chain of *L*-alanine (shown in Figure 4) is non-polar but has limited contribution to the overall hydrophobicity of alanine molecule.

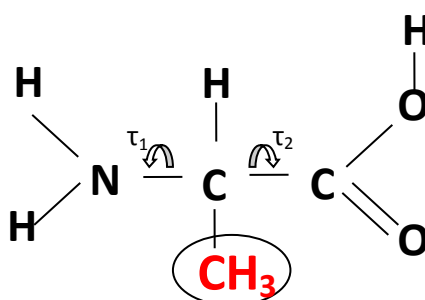


Figure 4. The molecular structure of alanine (Circled is the neutral non polar organic constituent)

In a recent publication which focused on using Born–Oppenheimer molecular dynamics to study *L*-alanine, it was identified that the non-polar side chain defines the direction of movement of the molecule. The study showed that, it was energetically favourable for methyl side group to avoid hydration by migrating to water surface compared to hydrating the entire *L*-alanine molecule. As a result, it was inferred that the first hydration shell of *L*-alanine was localized around the charged carboxyl and ammonium functional groups (Degtyarenko et al., 2007).

However, as shown by Alhusban *et. al.*, crystallisation can be achieved in excess concentration when freeze dried with gelatin. It was reported that alanine has two flexible torsion angles which are relevant to its crystal packing. These are the rotation of the amino group (τ_1) and the carboxyl group (τ_2) as shown in Figure 4. In a density functional theory of isolated molecule calculations, it was observed that conformational energy of crystal alanine was less compared to a more optimised geometry. This was explained that in an isolated molecule, a strong intramolecular hydrogen bond exist whilst in crystal alanine, the amine group orientates in the crystal structures to allow the three amino hydrogen atoms to hydrogen bond with the oxygen atoms which breaks the intramolecular hydrogen bond (Cooper *et al.*, 2007). As a result it was suggested that the crystal packing in alanine induces extreme changes on the molecular conformation. Therefore, with respect to disintegration, it will be expected that crystal alanine/gelatin will have a better disintegration profile when compared to amorphous alanine/gelatin freeze dried cake since lattice energy may be less. In contrast however, Alhusban *et al.*, 2010b showed that in a gelatin matrix containing 10% and 30% w/w of alanine, the disintegration profile of the 30% alanine/gelatin matrix had a shorter disintegration time. Increasing the concentration any further impacted negatively on the disintegration as this increased the degree of crystallinity.

Proline molecule has its α -amino group included in a side chain of a pyrrolidine ring. It lacks an amide proton and as a result it is seen less frequently in both helical and β -strand structures rather than being observed in alternates. When observed in the helix, it is usually located at the first two residues and not in the internal regions, perhaps due to the lack of hydrogen bond donor activities (Richardson and Richardson, 1989) and stereochemical restrictions. Figure 5 shows the molecular structure of proline.

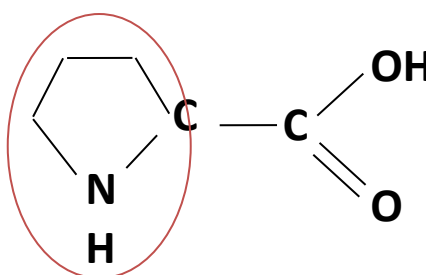


Figure 5. The molecular structure of L-proline which indicates a cyclic side chain.

Although proline has a non-polar side chain, previous work has indicated it is easily wetted and very soluble in water (AlHusban et al., 2010a, AlHusban et al., 2010b) even at sub-zero temperatures (Rasmussen et al., 1997). As such, in the pharmaceutical industry, proline is incorporated into formulations as an osmopectant. Osmopectants are small molecules that can behave as osmolytes in other to help organisms survive the stress of extreme osmotic environments.

Serine has a polar side chain of methoxyl group (shown in Figure 6) making it a hydrophilic molecule. This side group improves the solubility of serine in an aqueous solution although this solubility is dependent on the pH of the solution. The effects of pH on the solubility of some amino acids have been published (Tseng et al., 2009).

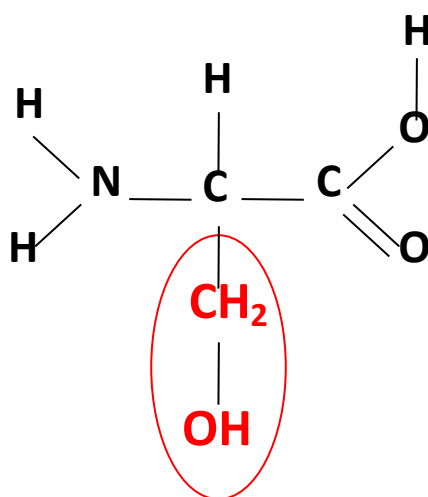


Figure 6. The molecular structure of *L*-serine indicating methoxyl side chain

Generally, the thermal properties of a solution of amino acid are studied and the phase transition correlated with the disintegration. The predictions based on such studies may vary in real solid drug systems containing crystalline amino acids. Furthermore, phase transitions observed in crystalline amino acids are related to the self-assembling of amino acid molecules (Gorbitz, 1989, Vinogradov, 1979). Hence, data analysis based on phase transitions may therefore only give an indication of the material characteristics in aqueous environments but not quantitative values.

Table 3. Summary of some basic properties of the selected amino acids (National Institute of Standards and Technology, 2011).

| Amino acid | Side chain | Polarity (side chain) | Charge(side chain pH 7) | Molecular weight |
|------------|--|-----------------------|-------------------------|------------------|
| Alanine | -CH ₃ (methyl) | Non polar | Neutral | 89.09 |
| Proline | -C ₄ H ₉ N (Pyrrolidine) | Non polar | Neutral | 115.13 |
| Serine | -HOCH ₂ (methoxyl) | Polar | Neutral | 105.09 |

| | High | Intermediate | Low |
|--|---------------|---------------|-------------------|
| Hydropathy Index ¹ | Alanine 1.8 | Serine -0.8 | Proline -1.8 |
| Solubility (g/100ml H ₂ O at 25 °C) | Proline 162.3 | Alanine 16.65 | Serine 5.02 |
| Melting temperature (°C) | Alanine 258 | Serine 246 | Proline 205 - 228 |

Gelatin is a biopolymer derived from the hydrolysis of collagen which is the main protein component of connective tissues (Jones, 1987). There are two main types of gelatin, categorised based on the method of production. Type A is prepared by acid hydrolysis with manufacturing process lasting between seven to ten days. Gelatin from animal skins is usually obtained through this method since they require less time for pre-treatment. Type B in contrast, is made by basic hydrolysis which takes longer. This process is thus suitable for processing gelatin from bovine bones. The basic manufacturing process has been explained in depth by previous publications (Jones, 1987). Briefly, it is explained that, the bones are decalcified by washing with acid to produce ossein, a spongy-like material, which is soaked in lime pits. The gelatin is later extracted from the treated ossein with hot water after few weeks.

One of the most important properties of gelatin is the bloom strength and viscosity. The bloom strength is a measure of how rigid gelatin can withstand standard plunger 4 mm with a certain load using specific proposed conditions as described in the publish work (Choi and Regenstien, 2000). The quality of gelatin for a specific application is dependent on the rheological properties (Stainsby, 1987, Totre et al., 2011). These properties are dependent on the molecular properties of gelatin with respect to the amino acid constituent, which is unique in the different species, and the molecular weight distribution due to processing conditions employed (Gómez-Guillén et al., Totre et al., 2011). The gelling properties of the final product are affected by proline and hydroxyproline contents. Hydroxyproline is thought to help in stabilizing the triple-stranded collagen helix due to its ability to hydrogen-bond via its OH

¹ Hydropathy index ranks the hydrophobicity of amino acid residues. The more positive a value is, the more hydrophobic the amino acid residue is.

group (Burjanadze, 1979). Gelatin is made up of a combination of different polypeptides that usually present a band pattern distribution associated with type I collagen. It has been explained that such gelatin was characterized with ² $\alpha 1/\alpha 2$ chain ratio of ~ 2 with ³ β - and ⁴ γ -components covalently linked to α -chain dimers and trimers respectively (Stainsby, 1987). The decrease in the occurrence of β - and γ -components, with an increase in degradants, are normally due to the intense extracting conditions like pH, temperature and time (Johnston-Banks, 1990).

Gelation and viscosity texture are related properties determined by the structure, molecular size and temperature of the system. Gelatin chain in aqueous solution may be covalently cross-linked to form matrices that can swell to form a gelatine hydrogel.

Gelatin has broad applications in the pharmaceutical industries as a result of its gel forming abilities. It is used in the production of a recognised dosage forms like the soft and hard gelatin capsules, used for tablet coating, binder and granulation, and also applied in encapsulation and micro-encapsulation. Due to its biocompatibility, gelatin has also been used in the production of edible films, as another form of formulation type. It has been documented in previous publications that amongst hydrocolloids, gelatin is unique in forming thermo-reversible gels with the melting point similar to the body temperature (Achet and He, 1995, Gómez-Guillén et al., Totre et al., 2011). Gelatin forms a three dimensional network in water with small regions of intermolecular microcrystalline junctions (Slade and Levine, 1987) that may produce brittle films when dehydrated (Vanin et al., 2005). To improve the flow properties, flexibility and mechanical strength of the network, plasticizer can be added (Aydinli and Tutas, 2000). Currently gelatin films are plasticized by hydroxyl compounds and polyols. Polyols are good plasticizers for protein-based materials because they help to reduce intermolecular interactions while increasing the spaces between molecules (Audic and Chaufer, 2005).

² Three polypeptide units. Since α chain of various types gelatin is different, they are called $\alpha 1$, $\alpha 2$, etc.

³ Dimer of an α chain

⁴ Trimer of an α chain

TOTRE, J., ICKOWICZ, D. & DOMB, A. J. 2011. Properties and homostatic application of gelatin. *In*: DOMB, A. J. & KUMAR, N. (eds.) *Biodegradable polymers in clinical use and clinical development* 1ed. New Jersey: John Wiley & Sons.

1.2 Physical Properties of freeze dried RDTs

Freeze dried RDTs are mostly amorphous cakes with highly porous matrix structure. The quality of the freeze dried cake can be assessed by visual observation. Good cake has non-reduced volume and uniform texture. If shrinkage or collapse of the final product occurs then the volume of the final freeze dried product is less than the volume of the initial frozen matrix. The collapse of the final product will likely be an indication of poor formulation type, wrong parameters used during primary drying, or the presence of excess moisture (Pikal and Shah, 1990).

1.2.1 Moisture content and Glass transition

The moisture content of freeze dried RDTs is an indication of other associated physical and chemical properties of the finished product. For instance, the Zydex technology produces RDTs that may degrade at humidity greater than 65% (Fu et al., 2004).

There are two categories of moisture that is encountered in freeze dried product: residual moisture and bound water. The major differences between these two forms of moisture are interactions that exist between them and the excipients.

Bound water is associated with the stability of the active component or other excipients. There are two forms of bound water; water of hydration and surface water. For instance in freeze-dried gelatin/amino acid base RDT, surface water is involved in defining the configuration of the gelatin polymer.

The residual water or water gained during storage can affect the glass transition temperature, T_g , working as a plasticiser. The higher the moisture content, the lower the T_g . In this case, recrystallization of the amorphous components can occur, which inevitably affects the disintegration and dissolution profiles, which are extremely important for RDTs.

1.2.2 Mechanical properties of freeze-dried product

Freeze dried amino acids are mostly amorphous cakes with large pores which helps ingress of water to collapse the matrix. However, amorphous materials lack long-range order within the

molecular arrangement. Therefore the position of molecules relative to one another is considered to be more random than in a crystal, thus an unstable matrix which is often very fragile and crumbles when handled. Thus with respect to most pharmaceutical excipients and especially those considered in this area of study, post freeze dried cakes are mechanically weak. As a result, special packaging is required which further increases the cost.

The alternative is to therefore include adjuvants that crystallise out during the freeze drying process. The major advantage of this design option is based on the fact that crystalline materials have ordered arrangement of molecules with very low molecular mobility. Inevitably, a pure crystalline material may also have a compromised disintegration profile. Thus the proportion between crystalline and amorphous parts in the freeze dried RDT becomes very important and underpins the need for balance between solubility and mechanical properties.

Therefore it is important to be able to quantify some of the physical properties like crystallinity that can be observed in a complex system of freeze dried gelatin/amino acid in-situ. The feasibility for using different techniques in the characterization of amino acid crystallinity will be compared in the next section.

1.3 Some quantification techniques used to determine crystallinity

Whilst RDTs prepared by freeze drying technology are required to be porous and sometimes amorphous, these dosage forms particularly those prepared with the Zydis® technology may melt between the fingers due to its high sensitivity to moisture. Hence a certain degree of crystallinity may be required to ensure it has acceptable mechanical properties without impacting on the disintegration time. The degree of crystallinity in RDTs is particularly important for future predictions of the stability profile (shelf life), susceptibility to moisture uptake, mechanical properties and the disintegration profile.

Many analytical technologies may be employed to study qualitatively and quantitatively the degree of crystallinity in RDTs. Currently, technologies ranging from powder X-ray diffraction (PXRD) (Davidovich et al., 2004), spectroscopic (Korter et al., 2006, Matei et al., 2005, Mathlouthi et al., 1986) and thermal analytical methods (Grunenberg et al., 1984, Rodante and

Marrosu, 1990, Rodante et al., 1992) have been used to study amino acids, with varying degrees of success. These technologies have been used to understand the relationship between amino acid structure and intermolecular interactions, identify the different stereoisomers and importantly quantifying the degree of crystallinity in solutions. The following section discusses some of the available technologies

1.3.1 Thermal analysis

Differential scanning calorimetry (DSC) is widely used thermal analytical method in the pharmaceutical industry for analysing the purity of materials and characterising materials (crystallisation, polymorphism, state transitions, etc.).

However, an RDT formulation containing a polymorphic material, during thermal analysis could melt to the metastable liquid before re-crystallising to a different polymorphic form e.g. *L alanine* which indicated at least six polymorphs (Liu and Li, 2008). Furthermore the literature explained that it was demanding to maintain phase equilibrium when studying polymorphic materials. Thus during the process, the crystal growth and homogeneity cannot be controlled (Ferguson et al., 2000).

A major limitation of thermal analysis is the decomposition of amino acids at elevating temperature. It has also been explained that the application of heat to amino acids leads to the formation of gases like CO, NH₃, and other linear and cyclic compounds which makes quantitative analysis difficult (Rodante and Marrosu, 1990, Rodante et al., 1992). Moreover, the thermal curves are subject to variations in heating rates, for this reason, the initial decomposition temperature of same amino acid has been reported differently (Grunenberg et al., 1984, Rodante and Marrosu, 1990, Rodante et al., 1992, Wendlandt, 1982).

A typical example of a DSC thermogram of an amino acid is as shown in Figure 7 indicating one asymmetric endothermic peak with dual local maxima near 230-235 °C. This peak can be ascribed to the melting transition with onset Temperature 220 °C. The end temperature of the phase transition and enthalpy of melting cannot be assessed properly due to exothermic decomposition following shortly after (or during) the melting process. The evidences for the decomposition are the following: (i) there is a sharp dropping in heat flow after the endothermic peak. (ii) The base line dropped down significantly from ~18 mW before

transitions to, ~3.2 mW after the transitions. Thus, there is an overlapping of melting and decomposition processes in the same temperature range.

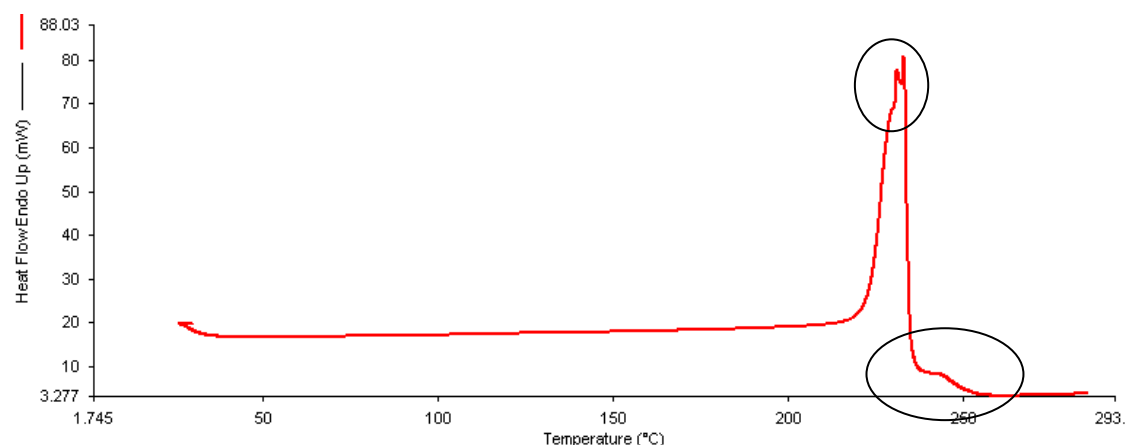


Figure 7. Differential scanning calorimetry thermogram of crystal L-serine. Highlighted areas corresponding to melting endothermic peak and decomposition exotherm.

DSC is widely used for estimating the percentage crystallinity in pharmaceutical materials. The quantitative approach is based on the enthalpy of melting, which can be calculated as the area under the melting peak. There are few sources of inaccuracy in such calculations, one of which is related to heat transfer into pan with material in DSC chamber. It has been explained that for quantitative analysis, one should account for resistance in heat transfer at the interface between the pan and sample and the time differences between the inherent DSC control mechanism (Batch and Macosko, 1991), which is not accounted for when using “area under the peak” method for quantification.

The preliminary analysis has shown that in the case of amino acids, the overlapping of the melting and decomposition processes means DSC technique is not feasible to estimate the degree of crystallinity in semi-crystalline materials such as amino acids. Thus, some other techniques should be considered for the study of the temperature-sensitive materials, like amino-acids.

1.3.2 Spectroscopic Techniques

Currently, spectroscopic and powder X-ray diffraction techniques are more favoured to study the degree of crystallinity and polymorphism in pharmaceutical materials.

Near Infra-Red spectroscopy (NIRS) is a technique which measures the molar absorptivity of materials based on their characteristic molecular overtones and combination vibrations of the mid-infrared bands. It is commonly used to identify intra-molecular bond vibrations originating

from $-\text{CH}$, $-\text{OH}$, $-\text{NH}$ and $-\text{SH}$ (Siesler et al., 2002). The infrared radiation lies within the frequency range of 800 nm to 2500 nm of the electromagnetic spectrum (Donald A. Burns and Ciurczak, 2008). Due to wide absorption range, NIRS is mostly robust for probing large materials with less emphasis on the sample preparation.

NIRS has been used to previously study crystallinity of pharmaceutical materials, polymorphism, moisture content (Bai et al., 2004) in freeze dried cakes (Kamat et al., 1989) and the disintegration profile of RDTs prepared by compaction technique (Narazaki et al., 2004). The major similarities from these separate studies is that, the spectra measured by NIRS is complicated with respect to different bonds sometimes being identified at the same frequency or overlapping each other.

Furthermore, the molar absorptivity measured by NIRS is low, making the technique less sensitive due to the wide frequency range it measures. Relative to crystallinity, it has been explained in previous work that intramolecular vibrations are indirectly affected by crystal changes (Snyder, 1961). Hence a direct technology that probes intermolecular vibrations will be considered for this study.

Raman spectroscopic technology originates from the inelastic light scattering referred to as Raman radiation. The scattering is energy originating as a result of shedding monochromatic light shed onto a material. The scattered energy consists of radiation of the incident frequency and a small fraction of photons with shifted frequencies. This technique like infrared, also measures molecular vibration and changes due to rotational energy. However, in Raman spectroscopy, the vibrations are related to the polarizability of the molecule and not dipole moments. The polarizability is dependent on how tightly electrons are bounded to the central nuclei. Currently, there are two main technologies used in Raman spectroscopy; dispersive Raman and Fourier transfer Raman (FTR). The major difference between these two techniques is the type of laser used and the detection and analysis mechanism. FTR has one major advantage over dispersive Raman due to the possibility of less fluorescence. FTR incorporates lasers capable of exciting longer wavelengths using less energy. This helps to reduce fluorescence interferences, capable of masking Raman signals. An in depth principles of FTR operation has been well documented in the works of (McCreery, 2005).

The characteristics of Raman radiation are dependent on the chemical composition of the material with every material having unique spectra features. Since the intensity of light scatter

is also dependent on the amount of material being analysed, it can be inferred that, this tool can be used for both qualitative and quantities analysis. Figure 9 shows the unique spectra features of gelatin and *L*-serine. It can be observed that at the low frequencies between 0 cm^{-1} to 100 cm^{-1} (terahertz domain), there are distinct features which if resolved can yield rich source of information about the material. The absorption spectra of gelatin showed no distinctive scattering at this same frequency range whilst a distinctive absorption band was observed for crystalline *L*-serine. The absorption bands observed at 3000 cm^{-1} appears to be artefact of the instrument or fluorescence. Furthermore, in the mid infrared region (between 750 cm^{-1} and 950 cm^{-1}) there are also distinct absorption bands.

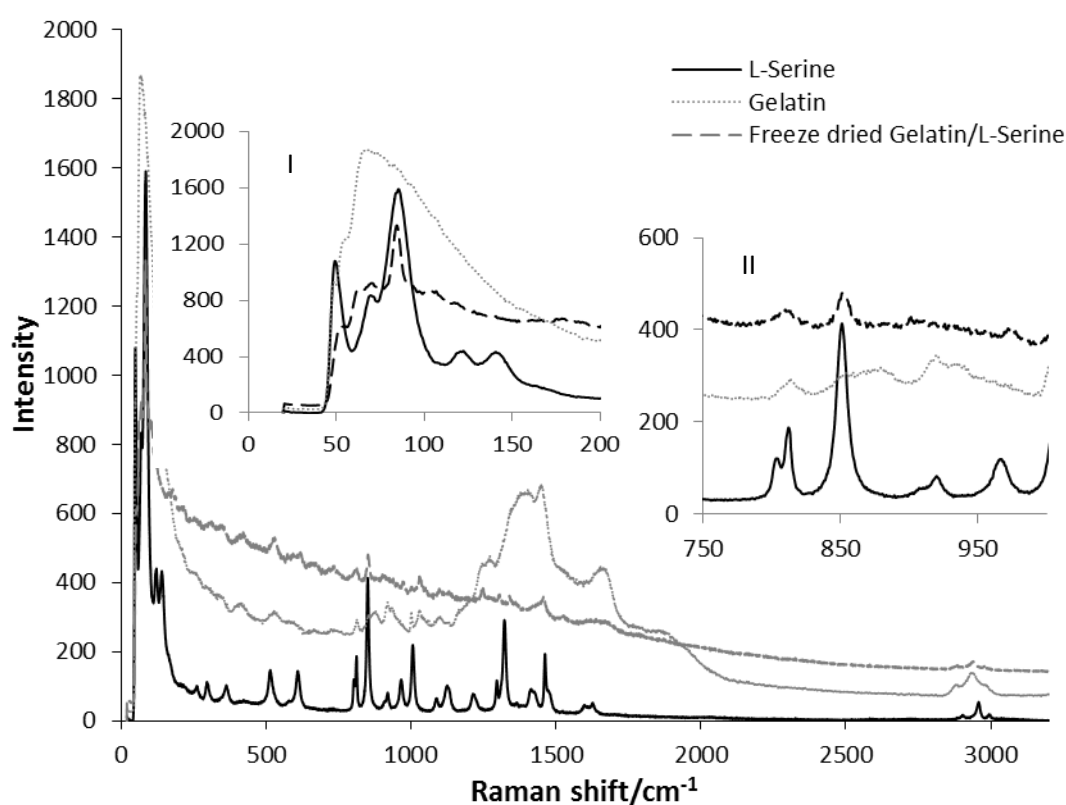


Figure 8. Typical Raman spectra of L-serine and gelatin indicating the distinctive absorption bands. (Insert spectra features at the (I) terahertz domain and (II) portions of the mid IR). Absorption spectra measured at Nottingham University.

This technology may be feasible for measuring vibrational spectrum of both solids and liquid materials as signals are not interfered by water; such, can be used to analyse complex samples including live tissues, and in vivo. Recent technological advances have made it possible for the

Raman signal to be measurable with small probe head linked to a portable Raman apparatus via optical fibre. The technology is also marred by some limitations. For instance, due to heat produced from the intense laser radiation, the samples may be destroyed. The detectors used must be very sensitive to enhance the weak Raman Effect. Similar to bond overlapping associated with measurements by NIR technology, this also makes Raman spectroscopy unattractive technique to some academia.

Terahertz Pulsed Spectroscopy (TPS) is a novel spectroscopic technology that has the ability to directly probe intermolecular interactions. It has been suggested that atomic level representation of amino acids and other biological molecule can be created from using terahertz measurements of frequency vibrations (Markelz et al., 2000, Yamamoto et al., 2005). Previous studies also concluded that different types of crystalline and amorphous materials can be easily differentiated by using their terahertz absorption spectra (Strachan et al., 2004, Strachan et al., 2005, Taday et al., 2003). Therefore, this tool has shown potential for both on-line and off-line qualitative and quantitative study of crystalline amino acids and freeze dried materials. In a recent study (Walther et al., 2003) on polycrystalline saccharides, it was shown that a series of distinct absorption bands were observed whilst for amorphous sugars a broad, featureless absorption spectrum is observed. It was explained that the ordered arrangements of molecules in crystalline materials led to precise lowest intermolecular vibrational modes which are detected by terahertz technology.

Terahertz radiation generated with modified Fourier transform infra-red technology have been used previously to study binary systems like *L*-serine, cysteine, *L* and *D,L*-alanine, *D,L*-valine, and others (Korter et al., 2006, Murli et al., 2006, Yamaguchi et al., 2005, Yamamoto et al., 2005). It was concluded that terahertz radiations were capable of inducing low frequency bond vibrations, crystalline phonon vibrations, and torsion vibrations. The results indicated that the absorption bands in the THz range were sensitive to the crystal structures of the studied amino acids, thus making the terahertz technology feasible in characterising the degree of crystallinity in gelatin/amino acid based freeze dried RDTs. The relevance of terahertz radiation and how this could be useful tool in characterising pharmaceutical materials have also been published in previous reviewed (Chantry, 1971, Shen, Mantsch and Naumann). A detail discussion of the mode of operation for TPS is further described in the Appendix II.

Figure 10 shows typical terahertz absorption spectra of *L* leucine and *L* lysine revealing the distinctive vibrational features which can be identified with the terahertz technology.

Comparable absorption spectra has previously been published in the literature (Matei et al., 2005) using modified far infra-red spectroscopy to generate the terahertz radiation. The absorption band revealed at $\sim 33 \text{ cm}^{-1}$ for lysine was ascribed to hydrogen bond modes. Similarly in leucine, within the frequency range of 5 to 85 cm^{-1} , Matei *et al.* reported five absorption bands at 21 cm^{-1} , 27 cm^{-1} , 43 cm^{-1} , 55 cm^{-1} and 71 cm^{-1} . As shown in Figure 9, four of the predicted absorption bands at located at 21 cm^{-1} , 27 cm^{-1} , 43 cm^{-1} and 55 cm^{-1} were also revealed in this preliminary study.

Thus comparing these mentioned technologies, THz spectroscopy is the most feasible and favourable technology to be used for quantifying crystalline amino acids with minimum prediction errors if combined with a robust statistical method.

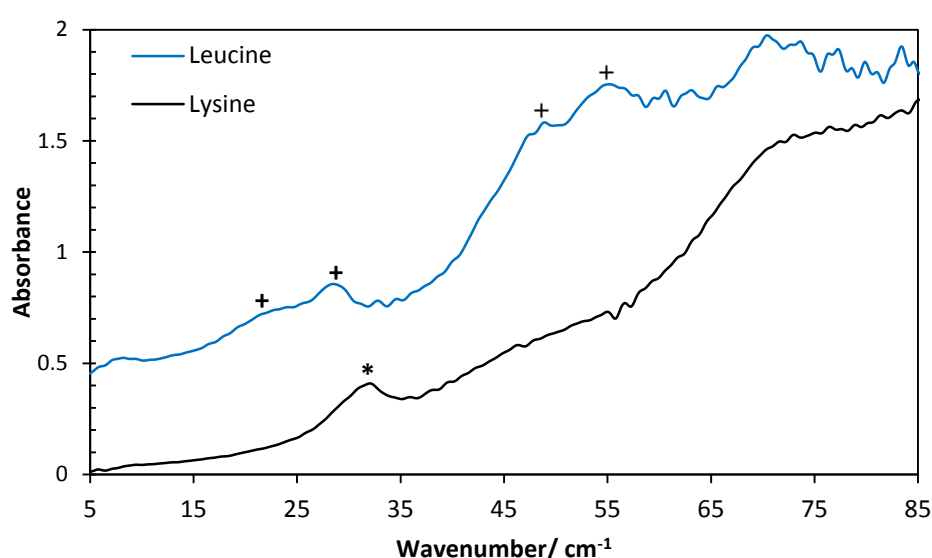


Figure 9. Terahertz absorption spectra of L-leucine and L-lysine offset from 5 cm^{-1} . The spectra of leucine have been shifted upwards 0.5 units for clarity. The distinctive absorption bands are marked with + for leucine and * for lysine.

When combined with an ideal statistical method, the terahertz absorption spectra of materials can be used to create calibration models for future crystallinity predictions. As a result, two different statistical approaches will be considered for this study, namely linear regression and partial least square methods.

Table 4 summarises these analytical technologies.

Table 4 Summary of some technologies used to study the physical properties and quantify degree of crystallinity

| Technologies | Advantages | Disadvantages |
|-------------------------------|---|--|
| DSC | <ol style="list-style-type: none"> 1. Ideally used to determine crystallinity, polymorphism and thermal transitions. 2. Determine the purity of materials | <ol style="list-style-type: none"> 1. Resistance in heat transfer at the interface between the sample pan and sample (Batch and Macosko, 1991). 2. Time differences between the inherent DSC control mechanism (Batch and Macosko, 1991). 3. Only measures thermal properties and not for identifying intermolecular or intramolecular interactions distinctive in different materials. 4. Not suitable for materials susceptible to heat decomposition. 5. Hard to maintain phase equilibrium. For instance, polymorphic material may melt to the metastable liquid before recrystallising to another polymorph (Ferguson et al., 2000). |
| Near Infra-Red | <ol style="list-style-type: none"> 1. Non-destructive to samples. 2. Data covers the transition from visible spectra to the mid infrared region. | <ol style="list-style-type: none"> 1. Absorption bands measured are overtones or combination bands of the fundamental mid infra-red range. 2. Difficult to interpret spectra due to overlap of the near infra-red bands |
| Raman Spectroscopy | <ol style="list-style-type: none"> 1. Can be used with solids and liquids and requires no sample preparation. 2. Not interfered by water and non-destructive. | <ol style="list-style-type: none"> 1. Heat from the laser radiation can damage the sample |
| Terahertz pulsed spectroscopy | <ol style="list-style-type: none"> 1. Non ionizing and non-destructive to the sample. 2. A terahertz absorption spectra shows the intermolecular vibrations that corresponds to motions linked with consistent, delocalized movements of large numbers of atoms and molecules 3. Yamamoto <i>et al.</i> (Yamamoto et al., 2005) suggested an atomic level representation of amino acids and other biological molecule can be created. 4. In transmission mode, data acquisition and measurements is within few seconds. | <ol style="list-style-type: none"> 1. Transient heating can affect the sample during preparation into pellets. 2. Affected by the presence of water molecules, hence requires longer purging times. |

1.4 Data processing for quantitative analysis – Regression analysis

For quantitative analysis of spectral data, specific absorption bands are selected for either the traditional peak area analysis or a more robust statistical analysis. Peak area analysis is simply estimating the area or height under an absorption band where absorption band is the region of the spectrum that shows signs of peaks (in absorbance) or trough (in transmittance) when compared to the reference material. This method is quick but may sometime carry the risks of over or under estimating.

In statistics, regression analysis is use to predict outcomes based on modelling and analysing sets of data that have a common relationship between a dependent variable and one or more independent variables sometimes using linear modelling. The quality of linearity between the two variables is measured from the R-squared value which is defined as; $R^2 = 1 - \frac{SS_{total}}{SS_{residuals}}$

Where SS is the sum of squares

$$SS_{total} = \sum_i (x_i - \bar{x})^2 \text{ and } SS_{residuals} = \sum_i (x_i - f_i)^2$$

x_i is the i^{th} value of the explanatory variable. f_i is the predicted value or associated modelled value and \bar{x} is the mean (Weisberg, 2005, Jones, 2002)

1.4.1 Linear regression (LR)

Linear regression (LR) is a statistical method to modelling the relationship between variable Y and different variables X_1, X_2, \dots, X_n . The data is modelled using a linear function ($Y = aX + b$) to estimate the unknown parameters 'a' and 'b'. The determination of the coefficients is based on creating a linear function between X and Y, so that the deviation of Y is at its minimum (Weisberg, 2005).

This statistical method is used for estimating unknown variables based on a linear calibration model. The method minimizes the sum of squared vertical distances between the observed responses and the predicted response by a linear approximation. This is usually referred to as the residual sum of squares. The modelling from linear regression assumes errors are normally distributed. The normality assumption is used to obtain tests and confidence statements for

smaller sample size such as lab scale. In this particular study, LR calibration models will be based on the assumption that, the relative area of the terahertz absorption band compared with the reference absorption spectra correlates with the concentration of the absorbing component in a binary system in this case amino acids. Thus increasing the concentration of the crystalline amino acid in a binary or a complex system should result in an increase in the absorption bands and hence the area under the band.

Calibration models based on LR is relatively easy to build and test with unknown samples. The method however is not comprehensive. For instance in a real system, there are always more than one variable e.g. the effects of noise on the absorption spectra output, concentration and thickness of the samples. As this approach can only account for a single variable and hence only one can be changed at a time, calibration models are unable to identify relationships between different factors.

1.4.2 Partial Least squares regression (PLSR)

Partial least squares regression (PLSR) is a statistical method used primarily for identifying a response variable (or vector) from within a large set of data that has multi co-linear explanatory variables, especially when the random error variance is large (Garthwaite, 1995). Although the main focus of PLSR has been on prediction of the response variable, the method can be used to produce an estimate with low mean square error (MSE). Generally, PLS offers a unique way of choosing factors in contrast to principal component regression and it requires less computations (Yenia and GÄokta, 2002).

PLSR includes the initial reduction of the number of predictor variables using principal component analysis. This analysis uses an orthogonal transformation to change observations of correlated variables into uncorrelated variables normally referred to as principal components. The principal components are always equal or less than the number of datasets. For instance if analysing a data set that comprises 10 sample measurements, then the number of principal components cannot be greater than 10. The orthogonal transformation always presents the first principal component (PC) as that with the major co-variance between the X and Y matrices, i.e. it explains as much of the variability in the dataset as possible. The succeeding principal components are presented in descending order of reduced PC. Thus using the first PC, PLSR calculates the case values by estimating the unobservable variables as an

exact linear combinations of their experiential values (Fornell and Larcker, 1981). It was explained (Garthwaite, 1995) that the weights (i.e., estimated values for latent variable in each dataset) used for determining the case values are estimated in such a way that the resulting case values identifies most of the variance of the independent variables (X) which is useful for predicting the dependent variable (Y). It is then possible to determine a value that corresponds with each unobservable variable, by calculating the weighted average of its indicators. Hence, PLS is a result of all unobservable variables being approximated by a set of case values which can be estimated using OLSR (Haenlein and Kaplan, 2004).

Cross Validation (CV) is a statistical approach for evaluating how the results of an analysis can be simplified to independent datasets. It is employed to improve the accuracy of predictions in real systems. There are different methods of CV, one of which is called the K-fold cross validation. This approach partitions the original sample into k subsamples. One of the subsamples from K is used as the test set, and the remaining sub-samples (k-1) are as used as the training sets. This cross validation is repeated k times (the *folds*) in the way that each of the subsamples is used once for the test set. In order to reduce variations, the validation results are then averaged over all the folds. For instance as shown in a CV involving three sets of data collected from three independent partitions then K-fold CV will apply (Table 5).

CV involves dividing datasets into complementary subsets. The analysis is performed on one subset (the 'training set') whilst the other datasets (known as the 'testing sets') are used to validate the analysis.

Table 5. An example of K-fold CV of three datasets

| Test Set | Training Set |
|-------------|-----------------------------|
| Partition 1 | Partition 2 and partition 3 |
| Partition 2 | Partition 1 and partition 3 |
| Partition 3 | Partition 1 and partition 2 |

However, this approach is disadvantaged based on the fact that it is time consuming since training sets is repeated. CV aims to measure the goodness of the hypothesis by estimating the confidence intervals of the predictions. In a system that estimates a continuously distributed prediction, the average of the mean squared error (MSE) or the root mean squared error (RMSE) of the three repeated CV can be used to summarise the errors in predictions.

Limit of Detection (LOD) and Limit of Quantitation (LOQ): The limit of detection (LOD) in any analytical technology is the lowest boundary at which analysis is feasible but not necessarily determined as an exact value. The limit of quantitation (LOQ) is the concentration at which quantitative results can be reported with sufficient precision and accuracy. These may be determined using a statistical method or experimental measurements of progressively more dilute concentrations of the material under investigation.

Statistically, they are estimated as: $LOD = \frac{3.3\sigma}{S}$ and $LOQ = \frac{10\sigma}{S}$

Where σ is the standard deviation (In the case of regression analysis, the standard deviation can be taken as the residual standard deviation of a regression line or the standard deviation of y-intercepts of regression lines). S is the slope of the validated curve (ICH, 1996).

Table 6 summarises the statistical approaches which can be used in quantitative analysis.

Table 6 compares linear regression with partial least square regression analysis

| Statistical Analysis | Advantages | Disadvantages |
|---|--|--|
| Linear Regression | <ol style="list-style-type: none"> 1. More reliable as only one variable is used. 2. It is relatively easy to build a model, test and understand the models built with this technique. 3. It strongly describes a process as changing a variable can always answer the "what if" scenarios. | <ol style="list-style-type: none"> 1. This method is not comprehensive as in the real world, there are always more than one variable. 2. As the technique can only account for a single variable and hence only one can be changed at a time, calibration models are unable to identify relationships between different factors. |
| Partial Least Squares Regression (PLSR) | <ol style="list-style-type: none"> 1. Has one or more unknown variable making the analysis more rigorous. 2. Produces more robust models that can withstand the changes of real system. | Hard to understand the iterations and time consuming to build models with PLSR. |

Gap in the Knowledge

Given the importance of crystallinity in defining the mechanical strength and disintegration time of RDTs, there is a requirement to develop suitable analytical techniques to quantify the extent of crystallinity. Of those technologies discussed above, it appears that terahertz technology offers the best opportunity to study the physical properties and quantify precisely the extent of crystallinity in freeze dried cakes. However, very little work has been done with

this technology in studying complex formulations such as freeze dried gelatin/amino acid incorporated in polyethylene pellets.

To achieve the best final RDT product, it is imperative that the product design be tested against different parameters such as varying concentrations, different freezing cycles, inclusion of excipients such as disintegrants, etc. In this study, only the effects of concentration will be considered with respect to the degree of crystallinity in freeze dried cakes. The rationale is based on the fact that if the degree of crystallinity can be controlled by altering concentrations of amino acids then the disintegration and mechanical profiles can be optimised.

Although it is envisaged that the absorption spectra from terahertz technology will yield a rich source of information, the complexity of samples, large datasets, co-linearity and possible outliers will be challenging when making precise and accurate quantifications for future predictions. For this reason, both classical area under the curve and partial least square methods of regression will be considered.

Chapter 2. Aim of the Project

Given the importance of crystallinity in defining the mechanical strength and disintegration time of RDTs, this project aims to develop a robust qualitative and quantitative method for determining the physical properties and extent of crystallinity in a freeze dried gelatin/amino acid matrix which are used in formulating rapidly disintegrating tablets.

2.1 Objectives

The project will be subdivided into three different phases.

- **Phase I Method Development**

The objective is to optimise the method of sample preparation in order to improve the quality of the terahertz spectra recorded by the TPS 3000 instrument. Three main parameters were investigated: compression force used for making the pellets, thickness of the pellets and the effects of particle size on the absorption spectra.

- **Phase II Development and Validation of the Calibration Model**

The rationale of this phase was to study a widely used and cheap pharmaceutical excipient like polycrystalline sucrose as a model system to develop a robust calibration model. Two different methods of building a calibration model will be compared with respect to its R^2 and root mean square error (RMSE), viz. linear regression and partial least square regression. The calibration model with least prediction errors will be used to develop calibration models for the selected amino acids.

- **Phase III Determining unknown crystallinity in freeze dried gelatin/amino acids**

The rationale of this phase is to determine the degree of crystallinity in pellets prepared with freeze dried gelatin/amino acids.

Chapter 3. Experimental Section

3.1 Materials

Sucrose (Fluka UK), gelatin, *L*- serine, *L*- proline, and *L*-alanine (Sigma Aldrich, UK) were individually sieved into three separate particle size ranges: $\geq 250 \mu\text{m}$, $63 \mu\text{m}$ to $150 \mu\text{m}$, and $\leq 63 \mu\text{m}$. These sieve sizes were selected based on previous study indicating that the optimal particle size for study with terahertz is about $80 \mu\text{m}$.

Pellets are the standards analysed when using the transmission TPS module attached to the THz equipment. Pellets are usually prepared from material under investigation and bulking agent, which has to be transparent to the THz radiation. It means that absorption coefficient should be very low, comparable to air. Polyethylene (PE) was chosen as the diluent since it showed these ideal properties. PE is nearly transparent with the frequency-independent refraction index of 1.53 in terahertz region (Walther et al., 2003). High density Polyethylene (PE) powder (TeraView, UK) with particle size $< 80 \mu\text{m}$ (and without further size separation) was used as a bulking agent/diluent for the current study.

3.2 Equipment and software

3.2.1 Equipment/Data acquisition

The equipment used in this study is listed in Table 7 along with a brief description of its use in this project.

Table 7. List of the equipment used for this project

| Equipment | Uses |
|---------------------------------|--|
| Carver® hydraulic press | To prepare pellets using up to 3 tonnes compression force. |
| Gamlen Tablet press | To prepare pellets using up to 500 kg compression force. |
| Heto FD7 freeze dryer | To prepare freeze dried amino acids suspended in gelatin matrix |
| Oxford bench cryo-microscopy | To determine the critical parameters for freeze drying amino acids e.g. critical point and collapse temperature. |
| Terahertz pulsed spectroscopy | |
| - ATR module | To determine the distinct absorption spectra features of sample |
| - Transmission module | To determine the absorption bands required for prediction modelling |
| Callipers | To measure the thickness of pellets |
| CO 7500 Educational Colorimeter | To measure the turbidity of amino acids in gelatin solution |
| Electric heater/stirrer | To continuously agitate gelatin solution whilst controlling temperature |

3.2.2 Software/Data processing

The statistical tools used include Matlab®R2010a, Origin®Pro8 and Microsoft® Excel.

3.3 Methods

3.3.1 Preparation of Solutions

Freeze dried amino acid/gelatin formulations (in solid fraction ratios of 10:90; 30:70; 50:50; 70:30) were prepared from simple aqueous solutions of amino acid and gelatin. The first stage was to prepare a stock solution of 5% w/w gelatin. The solution was made by adding 5 g of gelatin to 95 g of distilled water. The mixture was covered then heated to ~40 °C whilst continuously stirring using an electric heater/stirrer. The second stage was to add the required proportions of amino acids according (Table 8) and continuously stir ~30 °C. On freeze-drying (and removal of the majority of water from each formulation), these solutions result in the following solid fraction ratios of amino acid to gelatin: 10:90; 30:70; 50:50; 70:30.

Table 8. Preparation of amino acids solutions based on the addition of a known weight of amino acid to a fixed weight (100 g) of a 5% gelatin solution. The effective concentration has been calculated assuming that gelatin reduces the available water activity by 10%. Comparison of this effective concentration with the literature value of aqueous solubility shows whether the amino acid concentration would exceed the theoretical solubility threshold.

| Weight of amino acid added to 5% gelatin solution | Effective concentration of amino acid (% w/w) in solution | Solubility of amino acids (%w/w) (Ash, 1996, Weast, 1977) | | | Exceed solubility limit (Y/N) | | |
|---|---|---|------|-----|-------------------------------|-----|-----|
| | | | | | Pro | Ala | Ser |
| 0.55 | 0.58 | 162 | 16.7 | 5.0 | N | N | N |
| 2.14 | 2.27 | 162 | 16.7 | 5.0 | N | N | N |
| 5.00 | 5.30 | 162 | 16.7 | 5.0 | N | N | Y |
| 11.70 | 12.39 | 162 | 16.7 | 5.0 | N | N | Y |

3.3.2 Colorimetry measurements

Prior to freeze drying, simple colorimetric measurements were carried out to determine if there were any un-dissolved amino acids which could yield a cloudy solution. Table 8 show estimates for the effective concentration of amino acid in solution in order to assess which solutions would exceed the theoretical solubility limit. In practice, it was found that each amino acid was soluble at all concentrations studied, which must be a consequence of the solubilisation by gelatin (presumably as a result of hydrophobic bonding). An attempt to establish the extent of precipitation of amino acid on freezing, by this same method, was inconclusive owing to the fact that phase separation of gelatin caused the solution to become un-even, opalescent and pearl-like in appearance.

3.3.3 Method Development for THz Measurements: Freeze Drying

Surrogates for RDTs (i.e. formulations of RDTs without the drug substance) were prepared by freeze drying the above amino acid/gelatin solutions (Table 8) according to an optimized cycle developed on a Heto FD7 freeze dryer.

The optimized cycle for sucrose and the gelatin/amino acids were different. For sucrose, 10% of sucrose solution was frozen at -32 °C for a period of two hours. The primary drying stage commenced at -20 °C for further 12 hours followed by the secondary drying stage which lasted three hours at 20 °C.

For preparation of freeze dried gelatin/amino acid, the selected amino acids were individually added to 5% (w/w) gelatin stock solution. The concentrations of amino acids used were 10%, 30%, 50% and 70% of total freeze-dried (solid) material. The vials were filled with 3g of the amino acid/gelatin solution and frozen at -80°C for 2 hours. The frozen solution was freeze dried according to an optimised regime of pre freezing at -40 °C for 7 hours, primary drying at -35 °C for 86 hours and secondary drying at 20 °C for 15 hours. Similar cycle has been previously used in studies by (AlHusban et al., 2010a, AlHusban et al., 2010b).

The freeze dried amino acid/ gelatin was pelleted at RH 0% and room temperature following the pellet preparation method explained in Section 3.3.5. **In these pellets, 10% of the total weight (400 mg) was the freeze dried gelatin/amino acid matrix. Thus, the concentration of freeze dried amino acids in pellets was 1% (10% amino acid:90% gelatin), 3% (30% amino acid:70% gelatin), 5% (50% amino acid:50% gelatin) and 7% (70% amino acid:30% gelatin).**

3.3.4 Method Development for THz Measurements: Pellet Preparation

Prior to terahertz measurement, the polycrystalline sucrose was first formed into a pellet prepared by compaction with polyethylene (which is transparent to THz energy). It was first necessary to research the impact of the following parameters in the preparation of the pellets prior to implementing a standard method: Compression Force, Pellet Thickness; Particle Size.

Compression force: At any particular compression force, there are at least three properties of powders that ultimately affect the thickness of a pellet formed, viz. fragmentation, plasticity, and elasticity. Plastic materials are those that deform by changing its shape so that there are no new surfaces as a result of fracture. In the case of elasticity, the material rebounds in

reaction to releasing the compression force. Pellets produced from such materials have the propensity to cap during storage and handling. However, if a material can easily be deformed permanently, i.e. fragmented, then at a certain threshold of compression load, it may be assumed that compression force will not affect the thickness of the pellet. It is advantageous for a pellet to exhibit a time dependent behaviour associated with plastic excipients, i.e. deform with minimal brittleness to maintain its thickness. However, most active drugs are characterized with poor compression properties. As a result, easily compressible excipients must be added. It is expected that, if high concentrations of the active is used and it is an elastic powder, therefore the excipients used should be plastic in character. However, when using lower concentrations of amino acid, the characteristic of the diluents become more dominant and dictates the compression properties. The rationale for this study was to identify the compression force at which the polyethylene diluent is maximally compressed. The compression force used in preparing pellets of pure polyethylene was varied from 0.5 to 3 tonnes using a Carver hydraulic press. The material weight was kept constant at 400 mg (± 0.005 mg). THz wave forms were recorded immediately after compaction of the pellet then after 7 days storage at room temperature (in order to assess the possibility of elastic recovery)

Pellet Thickness The mass of PE powder was increased by intervals of 50 mg from 200 mg to 400 mg and the powder compressed with a two tonne of force to prepare pellets. The rationale was to identify the optimal thickness of pellet in relation to the quality of the terahertz spectra. It is known that internal reflections within the boundaries of the pellet will introduce spurious peaks into the terahertz waveform, which in turn, when Fourier transformed into the frequency domain will generate ripples in the electric field vector (as a function of wave number).

Particle size: The particle size of the amino acids was sieved into three different fractions: $\geq 250\mu\text{m}$, $63\mu\text{m}$ to $150\mu\text{m}$, and $\leq 63\mu\text{m}$. The rationale for the choice of these three size fractions is that it has been previously reported that the particle size of polyethylene and the material of interest should be $\leq 80\mu\text{m}$ in order to prevent the Mie effect (namely the scattering of light when the particle size approaches that of the wavelength of the incident light). The spectral range of interest from 5 to 80 cm^{-1} translates to an equivalent particle size range of 10 to $200\mu\text{m}$.

3.3.5 Pellet Preparation for Crystalline Amino Acids and Freeze-Dried Amino Acids

400 mg pellets were produced with a Gamlen Tablet press which can apply a maximum compression force of 500 kg. The pellet thickness was measured using a Vernier calliper to ensure consistency. Pellets were prepared for each crystalline amino acid in concentration of 2 to 20% w/w amino acid and 10% w/w gelatin in polyethylene. The amino acid/PE powder was mixed with a pestle and mortar using geometric dilution. Since gelatin is an amorphous material, all concentrations mentioned in later sections will be in relation to the amino acid contents. For the purpose of cross validation analysis, the samples were distributed into three partitions, with each partition containing four different concentrations of amino acid (Table 10). Pellets prepared from the freeze-dried amino acid/gelatin matrix were manufactured in a concentration of 10% freeze-dried material in polyethylene. **Given that the solid fraction ratios of amino acid to gelatin were 10:90; 30:70; 50:50; 70:30, then the final concentration of amino acid in the pellets of freeze-dried material translates to 1%, 3%, 5% and 7%.** Table 9 summarises the concentrations before and after preparing pellets containing freeze dried gelatin/amino acids. The freeze dried amino acid/ gelatin was pelleted in a glove compartment with ~0% relative humidity and room temperature. Given the recognition of the particle size effects (described in Section 3.3.4) it was considered prudent to pre-grind the freeze-dried materials (in a mortar and pestle, within a glove box) to minimise base line elevation from Mie light scattering.

Table 9. Composition of the different freeze-dried formulations studied

| | Sample N | Amino acid, % | Gel, % | Water, % | PE, % |
|-------------------------|----------|---------------|--------|----------|-------|
| In freeze-dried matrix: | 1 (10%) | 10 | 90 | - | - |
| | 2 (30%) | 30 | 70 | - | - |
| | 3 (50%) | 50 | 50 | - | - |
| | 4 (70%) | 70 | 30 | - | - |
| In pellet | 1 | 1 | 9 | - | 90 |
| | 2 | 3 | 7 | - | 90 |
| | 3 | 5 | 5 | - | 90 |
| | 4 | 7 | 3 | - | 90 |

3.3.6 THz measurements

The measurement for each sample was carried out using a scan frequency of 30 scans per second to provide spectra resolution of 1.2 cm^{-1} . To reduce the signal to noise ratio, coadding of 1800 scans were performed on each sample. The samples are held in a specially made sample holders with diameter of 13 mm and a thickness of up to 0.3 mm. The sample holder helps to finely focus the terahertz radiation on to the sample without touching the edges of the sample as explained in the published work (Dorney et al., 2001). The sample compartment was dried by purging with nitrogen gas whilst repeating measurements on the sample in situ as shown in Figure .

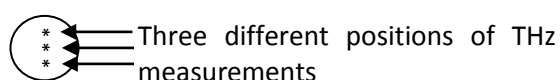


Figure 10. Three different positions on the sample where THz measurements was taking.

The experimental setup and operating principles for TPS have been well documented by (Beard et al., 2002, Dorney et al., 2001, Yamamoto et al., 2005).

3.3.7 Peak Area Analysis

In linear regression modelling, distinct known X_s and unknown Y_s are required to estimate the predictors of each parameter. The known X_s in this study are amino acid concentration whilst unknown Y_s for the purpose of this study are the area under the curve. A major limitation with this technique when used to determine Y_s from terahertz absorption spectra is the selection of the local minima points and the baseline shifts. Traditionally, the trapezoidal rule is used to calculate the definite integral of the peak area. This is based on an assumption that the baseline is linear so that in the calculated area, there is a greater possibility of under or overestimating as shown in Figures 12 A and B.

Table 10. Partition into three datasets of the concentration range for 400 mg Pellets manufactured for each material under test.

| Concentration %w/w | alanine | | | proline | | | serine | | | Sucrose | | |
|-----------------------|---------|---|---|---------|---|---|--------|---|---|---------|---|---|
| | 1 | 2 | 3 | 1 | 2 | 3 | 1 | 2 | 3 | 1 | 2 | 3 |
| 2.5 | | | | | | | | | | | | 1 |
| 3 | | | | | | | 1 | | | | | |
| 3.5 | | | | | | | | | | | 1 | |
| 3.6 | | | | | | | | | | 1 | | |
| 4 | 1 | 1 | | | | | 1 | 1 | 1 | | | |
| 5 | | | | | 1 | | 1 | 1 | | | | |
| 6 | | | 1 | 1 | | 1 | | 1 | | | | |
| 7 | | | | | | | | | 1 | | 1 | 1 |
| 8 | | 1 | | | 1 | 1 | | | | 1 | | |
| 9 | | | | 1 | | | | | | | 1 | |
| 10 | | | 1 | | | | | 1 | 1 | | | 1 |
| 11 | 1 | | | | | | 1 | | | 1 | | |
| 12 | | | | | | | | | 1 | | | |
| 13 | | | | 1 | | | | | | | 1 | |
| 14 | | | 1 | | | 1 | | | | | | 1 |
| 15 | 1 | 1 | | | 1 | | | | | | | |
| 18 | 1 | 1 | | | | | | | | | | |
| 20 | | | 1 | 1 | 1 | 1 | | | | | | |

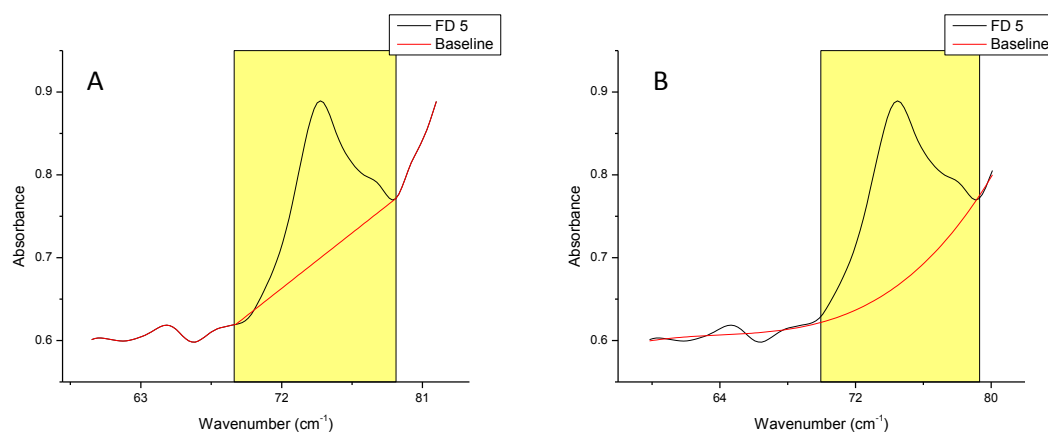


Figure 11. Estimating peak area using (A) Linear function baseline (B) Polynomial function baseline

It will be observed in later chapter that, clearly, the terahertz spectra may also be characterised with polynomial baseline shifts and not just linear shifts. Although the Origin®Pro8 software offers the choice of using polynomial function to estimate the baseline, this option will not be used since from Figure 12B, it can be observed that over estimation will be higher when compared to linear function baseline. To reduce estimation errors, the process will be repeated up to six times and the average used for the linear regression analysis.

Chapter 4. Results

4.1 Phase I - Method development

4.1.1 Pellet Preparation

The following process and material parameters were investigated, in the preparation of the pellets: Compression Force; Diluent (PE) ratio; Particle Size.

Compression Force Figure 13 indicates that at different compression force, the position of the Fresnel and the first reflected peaks are observed at the same scanner position. Given that the thickness of each pellet (as determined from a direct measurement using a micrometer and from the relative measurement provided by the optical delay between the Fresnel peak and the internally reflected peak) does not change with compression force, it might be assumed that this range of compression forces was sufficient to prevent any elastic recovery. This assumption might be further supported by the fact that there is only 0.03% increase in thickness after 7 days. The data appears to suggest that a minimal compression force of 500 kg is sufficient to ensure 100% compaction of the amino acid in polyethylene diluent without affecting the spectra features. This compression force was therefore used in all subsequent pellet manufacture and all THz spectra were acquired on the same day of production. The benefit for all further measurements of minimising the compression force would be to reduce the potential impact of self-heating on the stability of the amino acid.

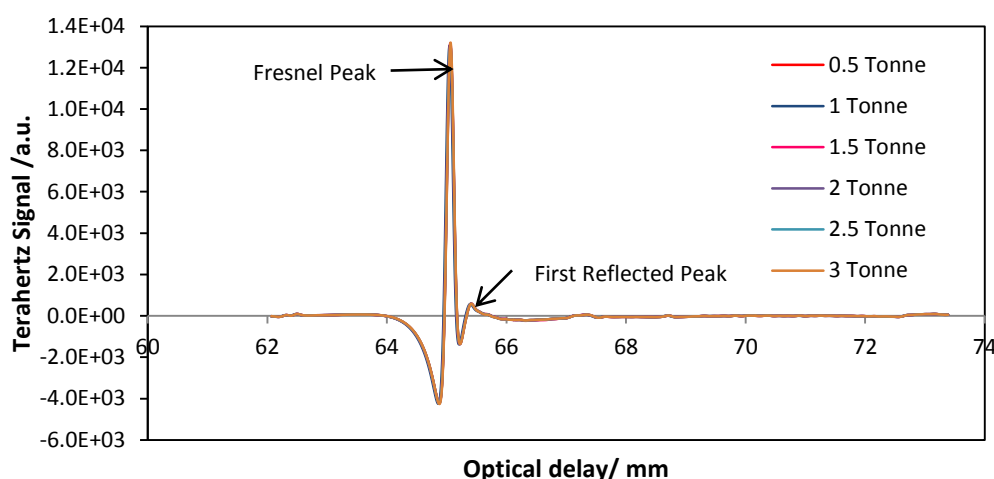


Figure 12. The optical delay response from varying the compression force used to produce amino acid/polyethylene pellets. The spectra presented are average of three different measurements from different positions.

4.1.2 Effects Pellet Thickness

A plot of the recorded thickness for an average of three pellets per material weight against the pellet weight is shown in Figure 14.

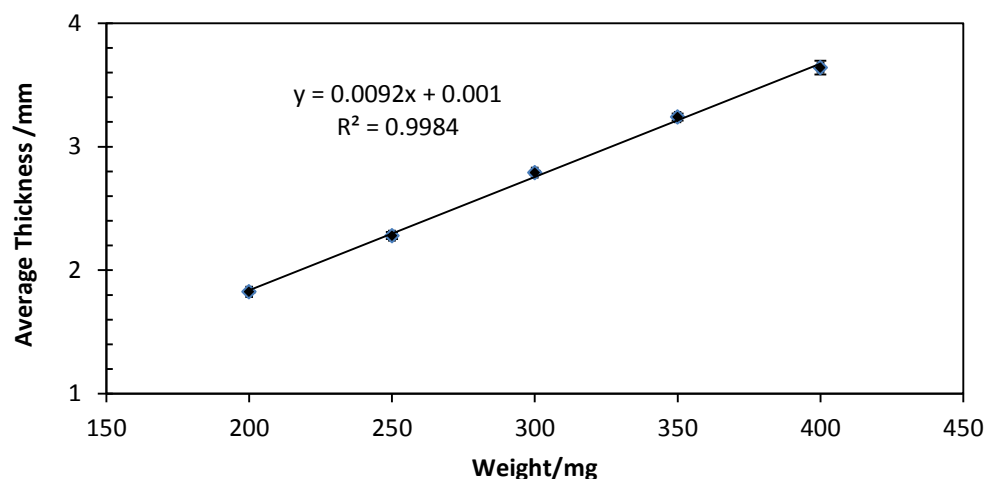


Figure 13. The average thickness of polyethylene pellets against weight

As anticipated, the average thickness of pellet was linearly proportional to weight with an R^2 of 0.99. The pellets prepared from different weight of polyethylene were studied with TPS to establish the dependency of the terahertz waveform on the thickness of the pellet. The raw terahertz waveforms shown in Figure 15 indicate that, the path length of the terahertz beam and hence time delay increases due to added thickness as a result of increasing the mass of polyethylene.

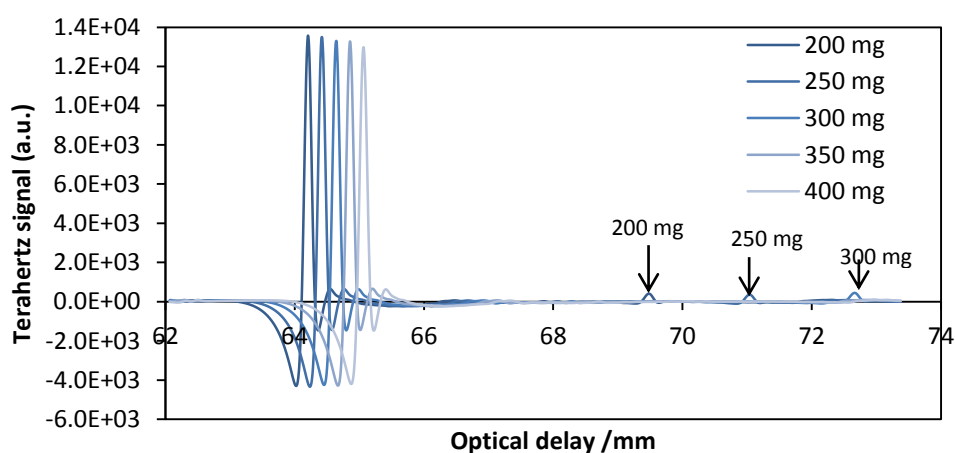


Figure 14. Terahertz waveform and scanner position of different concentration of pellets. Arrows show the spurious internal reflections from the air-pellet interface for the three thinnest pellets (prepared from 200, 250 and 300 mg PE)

Thus the optical delay increases and the position of the Fresnel peak shifts to longer distance as the thickness of the pellet increases and vice versa.

Further peak area analysis of the Fresnel reflected peaks showed that, as we increase the weight of the pellet, and thus the thickness, the peak area and height are reduced as shown in Figure 16. In effect the data is following the Beer-Lambert law in which the negative log of the transmitted energy has a linear dependency with the thickness of the sample.

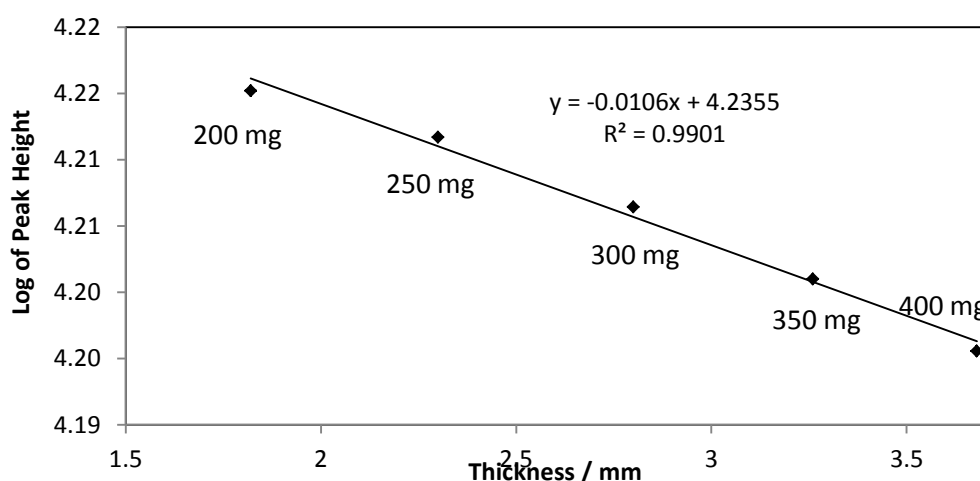


Figure 15. Log of the peak height against the thickness of the diluent.

Whilst this is of superficial interest, the main rationale for these baseline measurements, was to identify the optimal thickness of pellet in relation to the quality of the terahertz spectra. As described in the methods section, the internal reflections from the boundaries of the pellet are seen to introduce spurious peaks into the terahertz waveform (See Figure 15). These reflections are manifest in the experimental time window for the thinnest three tablets (1.82 mm; 2.3 mm; 2.8 mm). As a result, these spurious reflections are then captured by the Fourier transform software with the consequence of introducing ripples into the electric field vector as seen in Figure 17. In order to avoid such artefacts, routine measurements on amino-acid containing materials were therefore undertaken on 400 mg pellets.

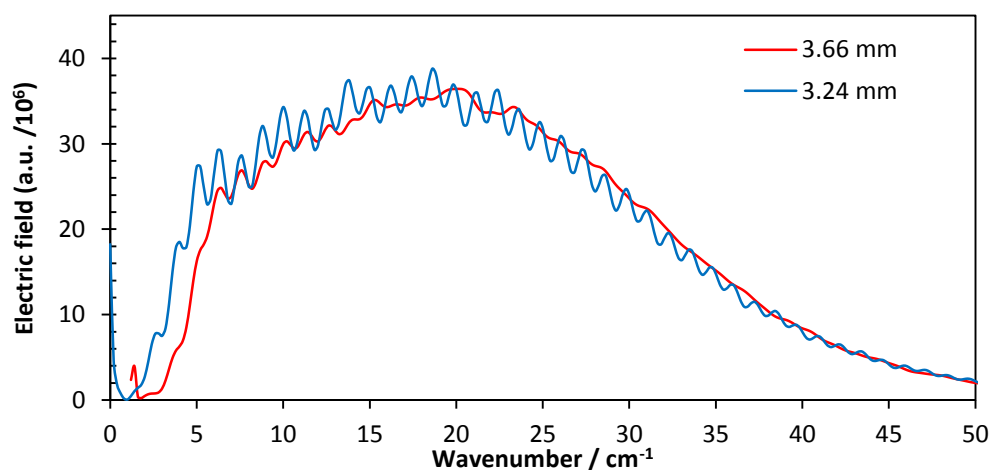


Figure 16. Difference between the sample spectrum of 300 mg tablet with pellet thickness of 3.24 mm and 400 mg with pellet thickness of 3.66 mm. The ripples in the absorption spectrum will cause further issues when recording the spectra from the amino-acid containing samples.

4.1.3 Particle size effects

The effects of particle size on pellets e.g. l-alanine pellet (10% w/w in 400 mg polyethylene pellet) is shown in Figure 18. It was observed that the absorption spectra measured for pellets prepared from powders with particle size 63 - 150 μm showed an elevated baseline, above 40 cm^{-1} , relative to the $\leq 63 \mu\text{m}$ particle size distributions. This is simply due to an increase in light scattering as the particle size is now of a similar magnitude to the wavelength of the incident light. For pellets prepared with powders of particle sizes $\geq 250 \mu\text{m}$, there is a further increase baseline plus the inclusion of various anomalous features (including what might appear to be two broad absorption peaks, centred on 50 cm^{-1} and 65 cm^{-1}) and the introduction of noise within the spectra as low as $\sim 40 \text{ cm}^{-1}$.

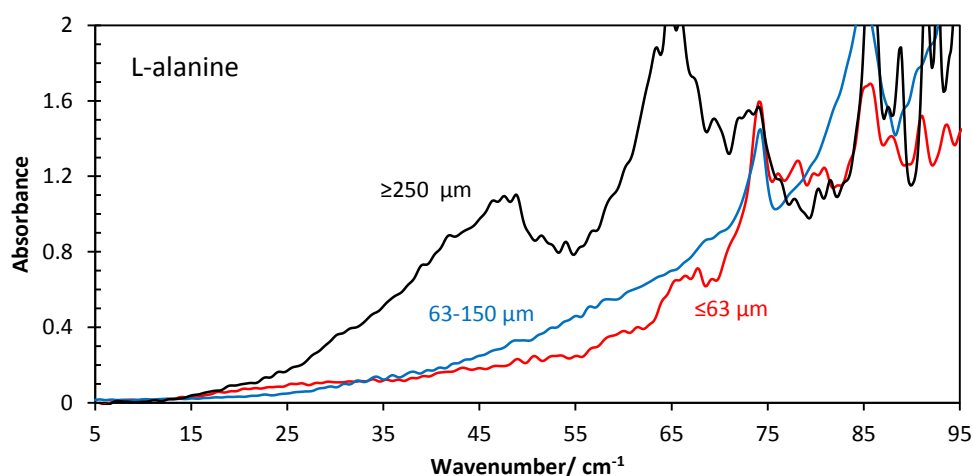


Figure 17. Terahertz absorption spectra of L-alanine indicating the effects of varying the particle size. Each spectrum is the average of three spectra recordings from three different positions

The effects of particle size has been extensively studied using crystalline sucrose (Shen et al., 2008). The study explained that when mixing two powders with different particle size, during handling there is a greater chance of segregation (de-mixing) with the smaller particles settling at the bottom, i.e. resulting in a non-uniform mixture. As a result, between two individual particles of the absorbing constituent, there will be multiple layers of non-absorbing polyethylene with high transmittance. The terahertz beam focused by the terahertz equipment has a sample position to spot size of $\sim 800\ \mu\text{m}$ at 1 THz (Shen et al., 2008). Only a few of the absorbing particles will be in the path of the focused terahertz beam. The average of the individual reflection of the terahertz radiation by the particles is what is recorded and presented as the output. This effect probably explains why the peak height of the 63-150 μm samples is lower than that for the 63 μm sample. The ideal method of avoiding this effect is to prevent powder de-mixing and to prepare pellets with particle sizes $\leq 63\ \mu\text{m}$.

4.1.4 Basic Terahertz Absorption features

Using the optimal parameters identified earlier, the terahertz absorption spectra of polycrystalline sucrose, *L*-alanine, *L*-proline, *L*-serine and gelatin were recorded with TPS and the data shown in Figure 19 to 24 between 5 cm⁻¹ to 95 cm⁻¹.

Polycrystalline Sucrose: The absorption spectra of sucrose shown in Figure 19 shows an absorption band at 48.25 cm⁻¹ and a further distinct band with centered on 60.86 cm⁻¹ and visible shoulders at ~55 cm⁻¹ and ~65 cm⁻¹. The observed shoulders become more pronounced in samples containing high concentrations. These well resolved features has been reported in the literature (Walther et al., 2003). It was explained that, the absorption bands originate from intermolecular vibrational modes of long range order, maintained by the hydrogen bond network of the crystalline structure.

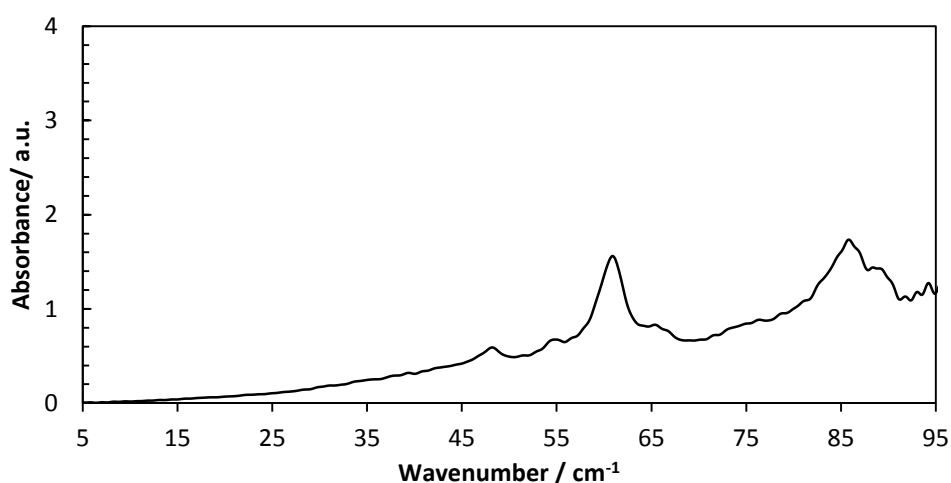


Figure 18. THz absorption spectra of 10% w/w sucrose in PE pellet between 5 cm⁻¹ and 95 cm⁻¹. The data presented is the average of three measurements from three different areas of the pellet.

Amorphous Sucrose: The featureless absorption spectra of amorphous sucrose are shown in Figure 20. It can be observed from this spectrum that the distinct features observed in the polycrystalline sucrose were absent. This is due to lack of long range order molecular arrangements in amorphous materials. Thus amorphous materials will not exhibit phonon vibrations which are recorded by the THz technology. Similar work has also been presented elsewhere and explained (Strachan et al., 2004).

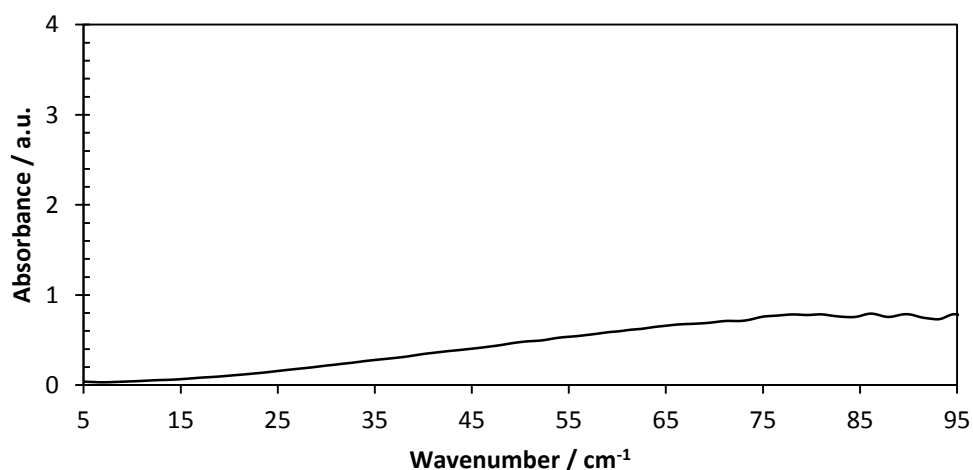


Figure 19. THz absorption spectra of 10% w/w FREEZE DRIED sucrose in PE pellet between 5 cm^{-1} and 95 cm^{-1} . The data presented is the average of three measurements from three different areas of the pellet.

***L-Alanine*:** The terahertz absorption spectra of *L*-alanine presented in Figure 21 revealed two distinct absorption bands with local maxima at $\sim 75 \text{ cm}^{-1}$ and $\sim 85 \text{ cm}^{-1}$.

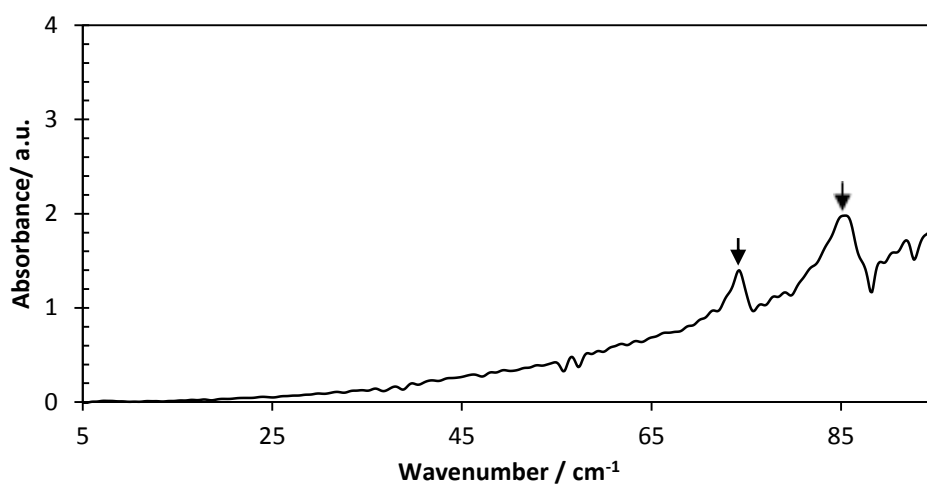


Figure 20. THz absorption spectra of 10% w/w *L*-alanine in PE pellet between 5 cm^{-1} and 95 cm^{-1} . The data presented is the average of three measurements from three different areas of the pellet.

***L-Proline*:** The absorption spectra of *L*-proline presented in Figure 22 revealed a principal absorption band at 66.1 cm^{-1} and a partially obscured band at 42.6 cm^{-1} .

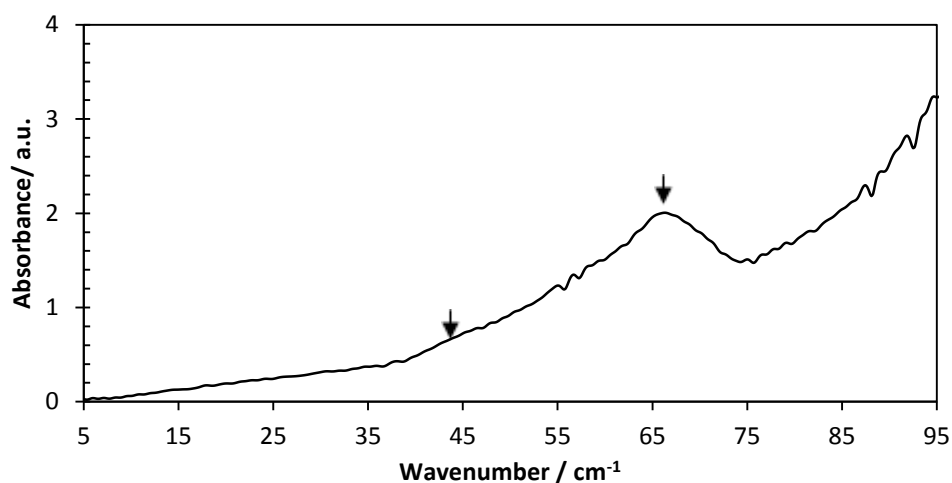


Figure 21. THz absorption spectra of 10% w/w *L*-proline in PE pellet between 5 cm^{-1} and 95 cm^{-1} . The data presented is the average of three measurements from three different areas of the pellet.

***L- Serine*:** The distinct spectra feature of *L*-serine is presented in Figure 23 showing a broad absorption band between 40 cm^{-1} to 80 cm^{-1} and centred on $\sim 67\text{ cm}^{-1}$.

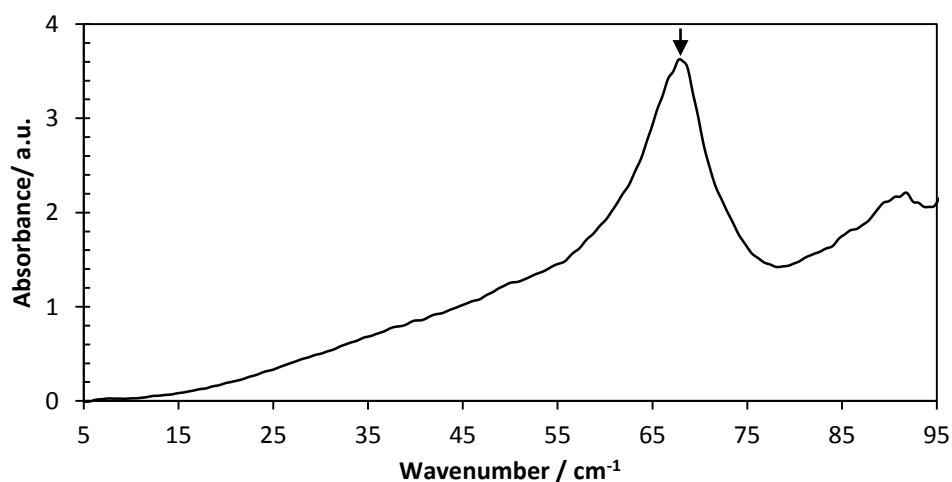


Figure 22. THz absorption spectra of 10% w/w *L*-serine in PE pellet between 5 cm^{-1} and 95 cm^{-1} . The data presented is the average of three measurements from three different areas of the pellet.

Gelatin: The featureless THz spectrum of gelatin is presented in Figure 24. It is evident that the spectrum lacks any distinct peaks within the region studied.

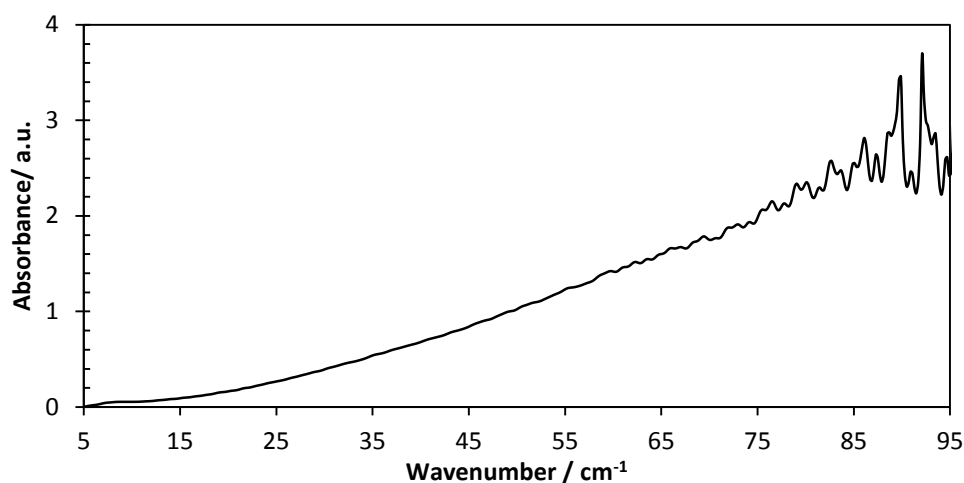


Figure 23. THz absorption spectra of 10% w/w gelatin in PE pellet between 5 cm⁻¹ and 95 cm⁻¹. The data presented is the average of three measurements from three different areas of the pellet.

Thus the presence of gelatin in freeze dried gelatin/amino acid will have negligible response to the THz beam with respect to absorption bands.

It can also be observed from Figures 19 to 24 that, *L*-serine is the most strongly absorbing sample when compared to the other amino acids under study. This is a clear indication that *L*-serine is more likely to be saturated in the PE pellets if the concentration is increased perhaps up to 15% w/w.

4.2 Phase II – Development and Validation of the Calibration Model

4.2.1 THz Measurements of Sucrose

As explained in earlier sections, the idea of CV requires more than two datasets. To achieve a robust calibration model, datasets from three separate partitions will be analysed. Each dataset is the average of three recorded THz measurements at different parts of the pellet. The THz absorption spectra of polycrystalline sucrose are shown in Figure 25, with all concentrations showing the distinctive absorption features of polycrystalline sucrose. Similar spectral features were also recorded for polycrystalline sucrose test samples (Data is shown in appendix 2). Generally, the position of the local maxima of the absorption band is similar for all concentrations and the three partitions. This indicates the frequency at which the absorption band is observed is independent of the concentration. However, the amplitude of the band is sensitive to concentration and increase as with concentration.

The absorption band observed $\sim 83\text{ cm}^{-1}$, as speculated in the earlier chapter, becomes more pronounced at higher concentrations of the polycrystalline sucrose. However, this band is not ideal for quantitative analysis since it is located in the noisy region of the spectra. Thus quantitative analysis will be based on the absorption differences observed between $\sim 45\text{ cm}^{-1}$ to $\sim 66\text{ cm}^{-1}$ for PLSR whilst for LR, the wave numbers between $\sim 50\text{ cm}^{-1}$ to $\sim 66\text{ cm}^{-1}$ will be considered.

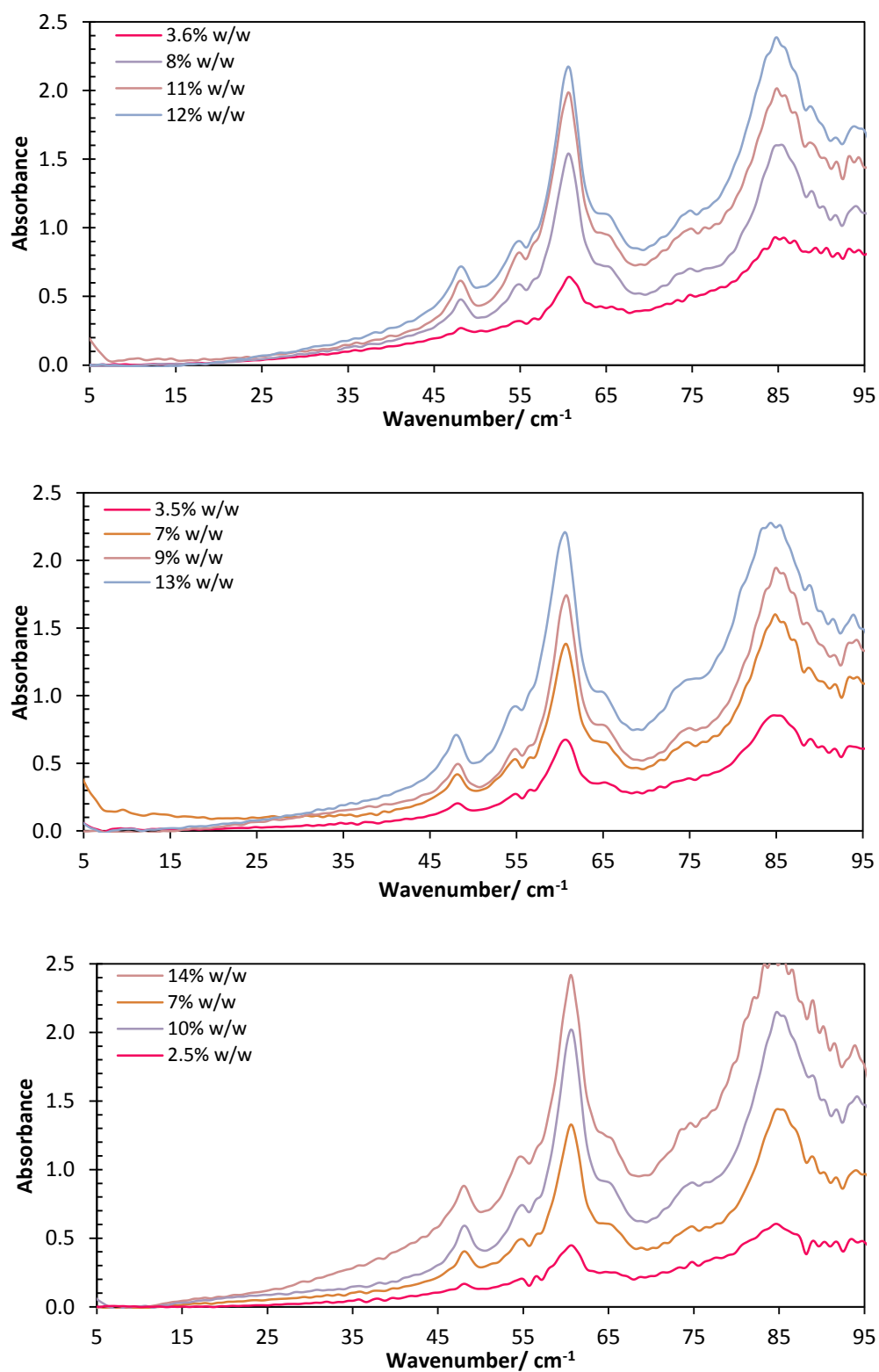


Figure 24. Terahertz absorption spectra of three different partitions of polycrystalline sucrose. Each absorption spectrum is an average of three repeated measurements from three separate positions of the pellets.

Linear Regression: Figure 26 shows the calibration model based on estimated peak area against the concentrations of the twelve test samples (four from each partition)

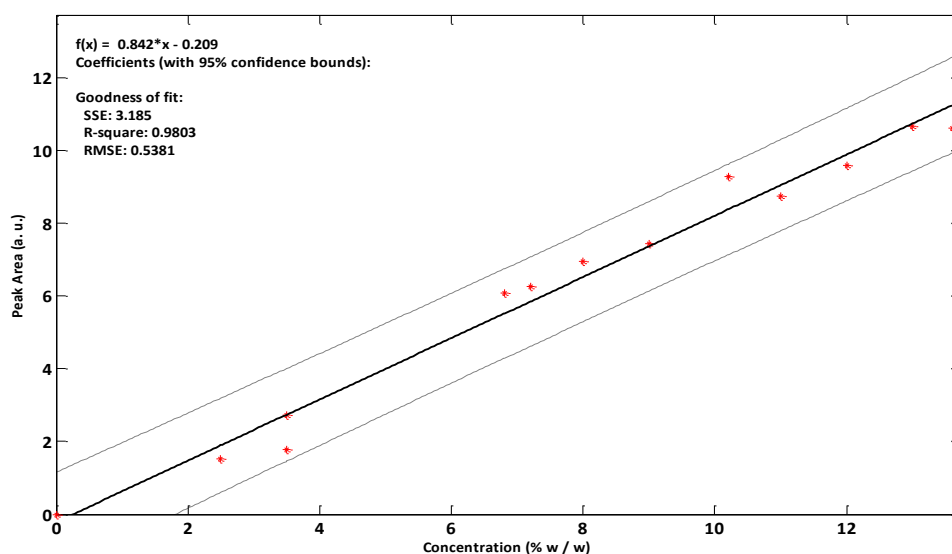


Figure 25. Calibration model based on linear regression of the estimated peak area for polycrystalline sucrose against the actual concentrations with 95% prediction bands.

The calibration model presented in Figure 26 shows a positive correlation between concentrations of sucrose with the peak area. The estimated R^2 was 0.98 with RMSE of $\pm 0.538\%$.

Partial Least Square Regression (PLSR): Unlike peak area analysis (which does not account for equipment noise and other external variables), the PLSR method identifies a number of prediction variables and scores each as a different principal component, the highest score being the factor that contributes the most to the observations. Of the four principal components that were identified, the first PC was used for analysis. Table 11 shows the predictor variables identified and scored based on principal component analysis.

Table 11. Estimated scores from principal component analysis (PCA) using the dimension reduction from the dot product

| PCA | Partition 1 | Partition 2 | Partition 3 |
|------|-------------|-------------|-------------|
| PC 1 | 99.1422 | 97.6048 | 97.9831 |
| PC 2 | 0.7618 | 2.0965 | 1.7457 |
| PC 3 | 0.0520 | 0.2460 | 0.1808 |
| PC 4 | 0.0239 | 0.0328 | 0.0667 |

Based on the PC scorings, PC1 was determined as the best explanatory variables for the data sets. PLSR is therefore modelled based on the PC1 scores for each partition and a linear fit carried out. The predicted parameters in the three separate partitions are shown in Table 12.

Table 12. For a function of $f(x) = p1 \cdot x + p2$, the following parameters were estimated for the three different partitions. The average of the RMSE of these estimates is used as the prediction errors.

| | p1 | p2 | R ² | RMSE |
|--------------------|-------|--------|----------------|-------|
| Partition 1 | 0.074 | -0.609 | 0.999 | 0.012 |
| Partition 2 | 0.071 | -0.585 | 0.998 | 0.018 |
| Partition 3 | 0.069 | -0.564 | 0.998 | 0.019 |

To reduce prediction errors, k-fold CV was carried out using three parameters (Table 13).

Table 13. Parameters used for CV against their respective test sets

| Test Set | p1 | p2 |
|--------------------|--------|---------|
| Partition 1 | 0.0703 | -0.5746 |
| Partition 2 | 0.0716 | -0.5863 |
| Partition 3 | 0.0725 | -0.5970 |

The cross validated model is presented in Figure 27 and a function $f(x) = 1.005x - 0.075$ and R² 0.99 was recorded. With 95% confidence, predictions will have RMSE of 0.227

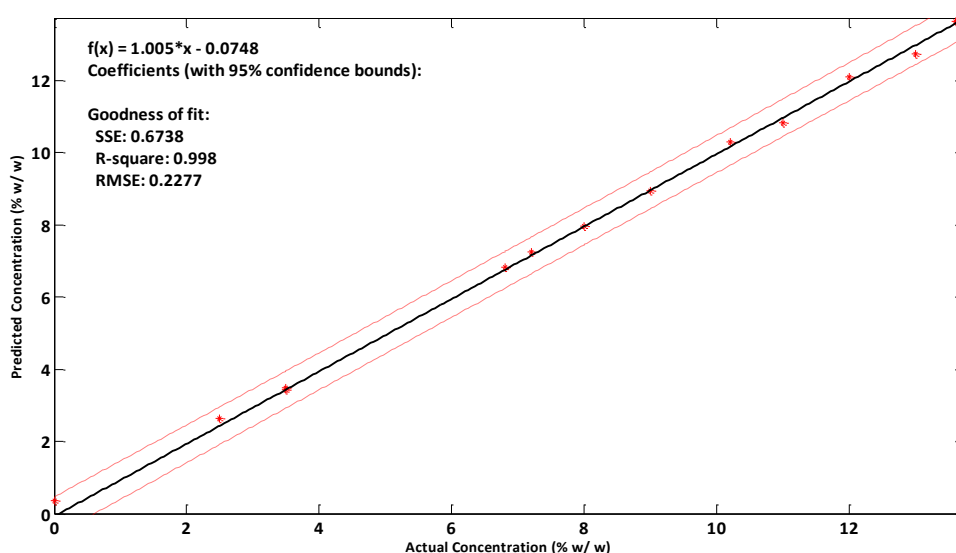


Figure 26. Calibration model based on partial least square regression of the predicted concentration for polycrystalline sucrose against the actual concentrations with 95% prediction bands.

In this analysis, the y-intercept confidence interval ($\alpha=0.05$) included zero and thus, there is no evidence to suggest a non-zero intercept for this model.

4.2.2. Testing Calibration Model

The two different calibration models were validated against polyethylene pellets prepared with various 'test' concentrations of crystalline sucrose. Each pellet was measured up to three

times at three different regions as mentioned in earlier sections. To make accurate predictions, the THz data sets of the “samples prepared with unknown concentrations” recorded was analysed against the data recorded from the ‘test’ concentration samples used to build the calibration models.

Table 14 compares the predicted concentrations based on the calibration models of linear regression and PLSR for the pellets with ‘test’ concentrations. For clarity, the actual concentration of these samples is also shown.

Table 14. Comparing the predicted concentrations using linear regression and PLSR calibration models for pellets prepared with unknown concentrations of sucrose.

| Actual Concentration / % w/w | Predicted Concentration | |
|------------------------------|-------------------------|-------|
| | Linear Regression | PLSR |
| 3.2 | 2.08 | 3.22 |
| 7.35 | 5.32 | 7.40 |
| 10 | 7.45 | 10.10 |
| 13 | 9.64 | 12.92 |
| 10.5 | 7.74 | 10.52 |
| 12.5 | 9.59 | 12.50 |

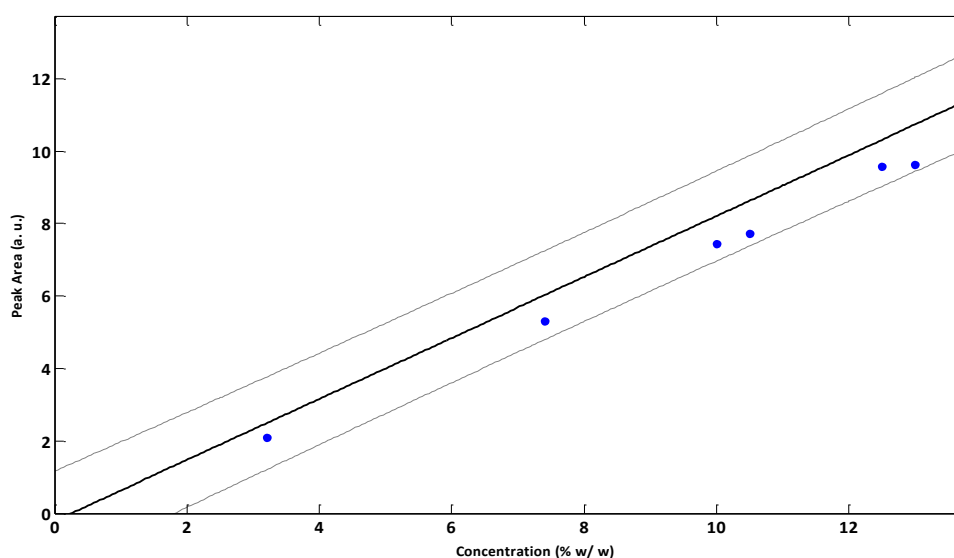


Figure 27. Calibration model based on linear regression of the estimated peak area for polycrystalline sucrose against the actual concentrations with 95% prediction bands fitted with the predicted concentrations in samples prepared with unknown active proportions.

As shown in Table 14 and Figures 27 and 28, the predicted concentrations of the samples prepared with unknown proportions of polycrystalline sucrose were in general agreement with

the actual concentration for both statistical techniques. The predictions based on linear regression were consistently under estimated, with an accuracy of -35% for the 3.2% test sample and -23% for the 12.5% test sample.

In contrast, the predictions based on PLSR showed improved precision and accuracy. The highest prediction error (lowest accuracy due to over prediction) was estimated as +1% in the unknown sample containing 10% w/w of sucrose.

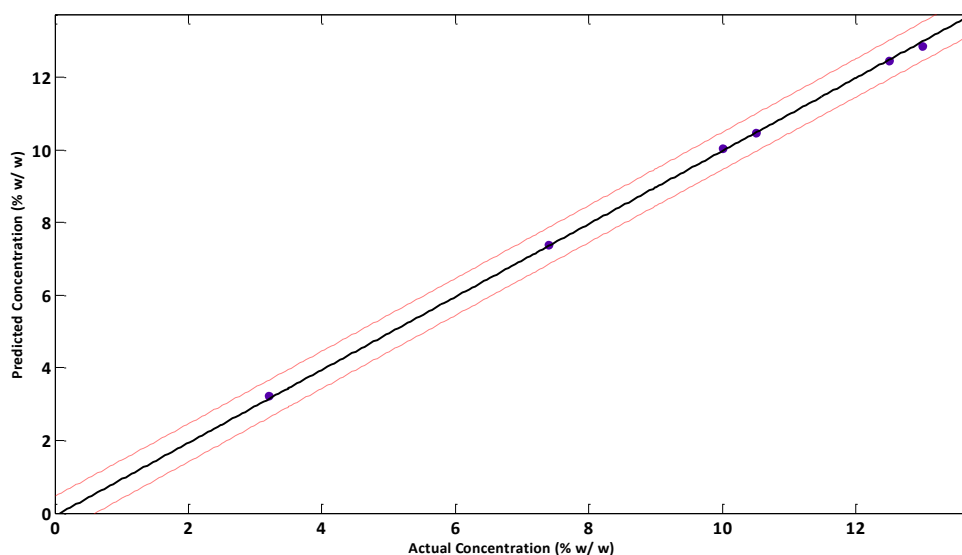


Figure 28. Calibration model based on partial least square regression of the predicted concentration for polycrystalline sucrose against the actual concentrations with 95% prediction bands fitted with the predicted concentrations in samples prepared with unknown active proportions.

Consequently, the fact that PLSR had the lowest RMSE when compared with linear regression is an indication of the sensitivity of PLSR iterations. Hence in the future calibration models, PLSR method will be used.

4.3 Calibration models of amino acids

4.3.1 THz Measurements

As shown in Figures 21 to 24 and explained, the different amino acids showed distinct spectra characteristics due to the difference in their organic constituents. The terahertz absorption spectra for the different concentrations amino acids are shown in Figure 30 to 33. Similar to the observations of sucrose, the amplitude of the absorption bands increased as the concentration of the amino acid in the polyethylene pellet increases.

L-alanine: One of the limitations of terahertz technology observed in this study is the degrading noise to signal ratio observed at frequencies greater than 75 cm^{-1} . Thus for a robust calibration model, the absorption band between 66 cm^{-1} to 76 cm^{-1} was selected for analysis. The absorption spectra for different concentrations of *L*-alanine studied are shown in Figure 30.

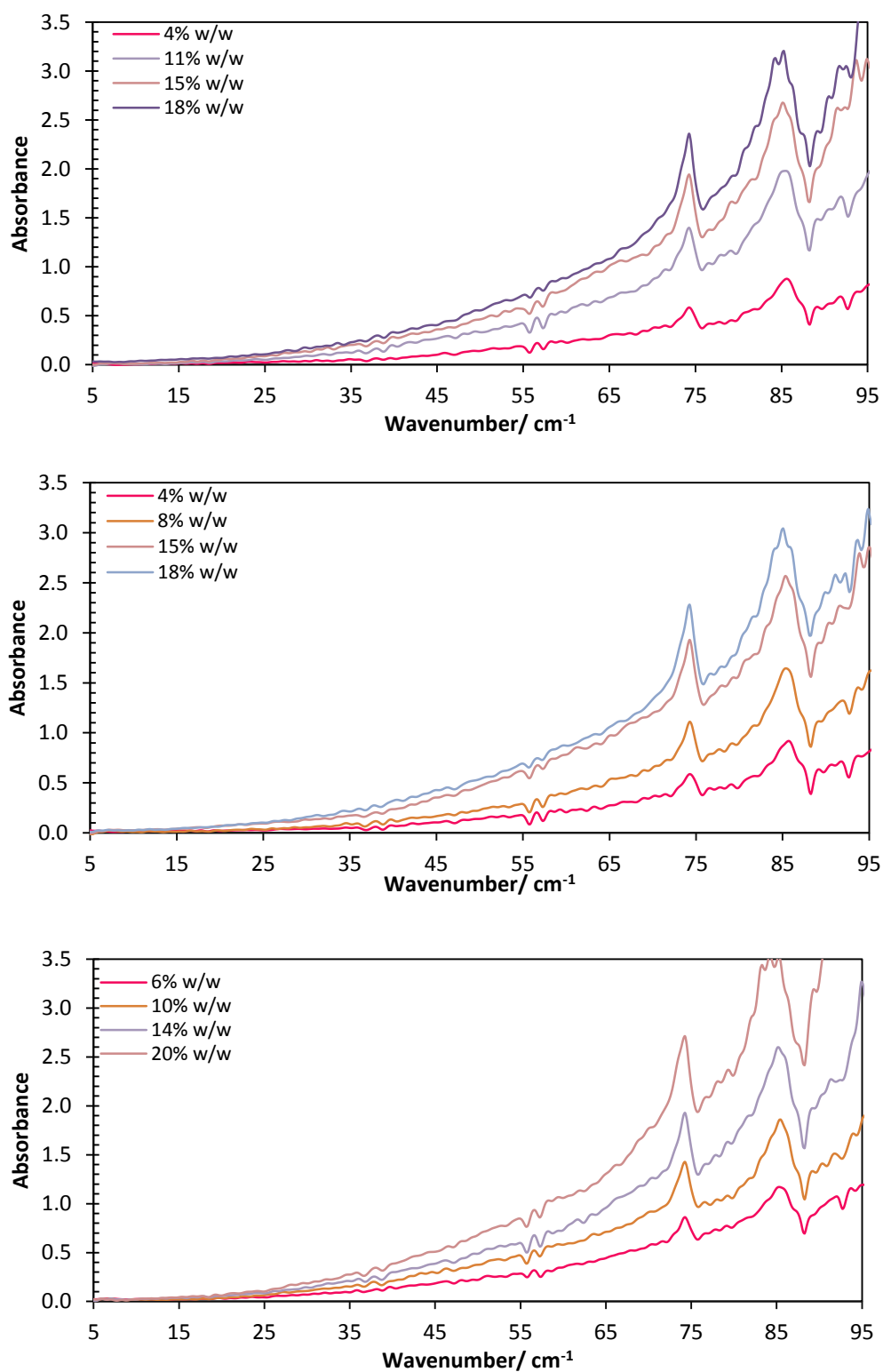


Figure 29. THz terahertz absorption spectra of crystalline *L*-alanine for three separate partitions. Each individual spectrum is an average of three repeated measurements per each sample for each separate partition.

***L*-proline**: The distinct absorption pattern of *L*-proline is also shown in Figure 31.

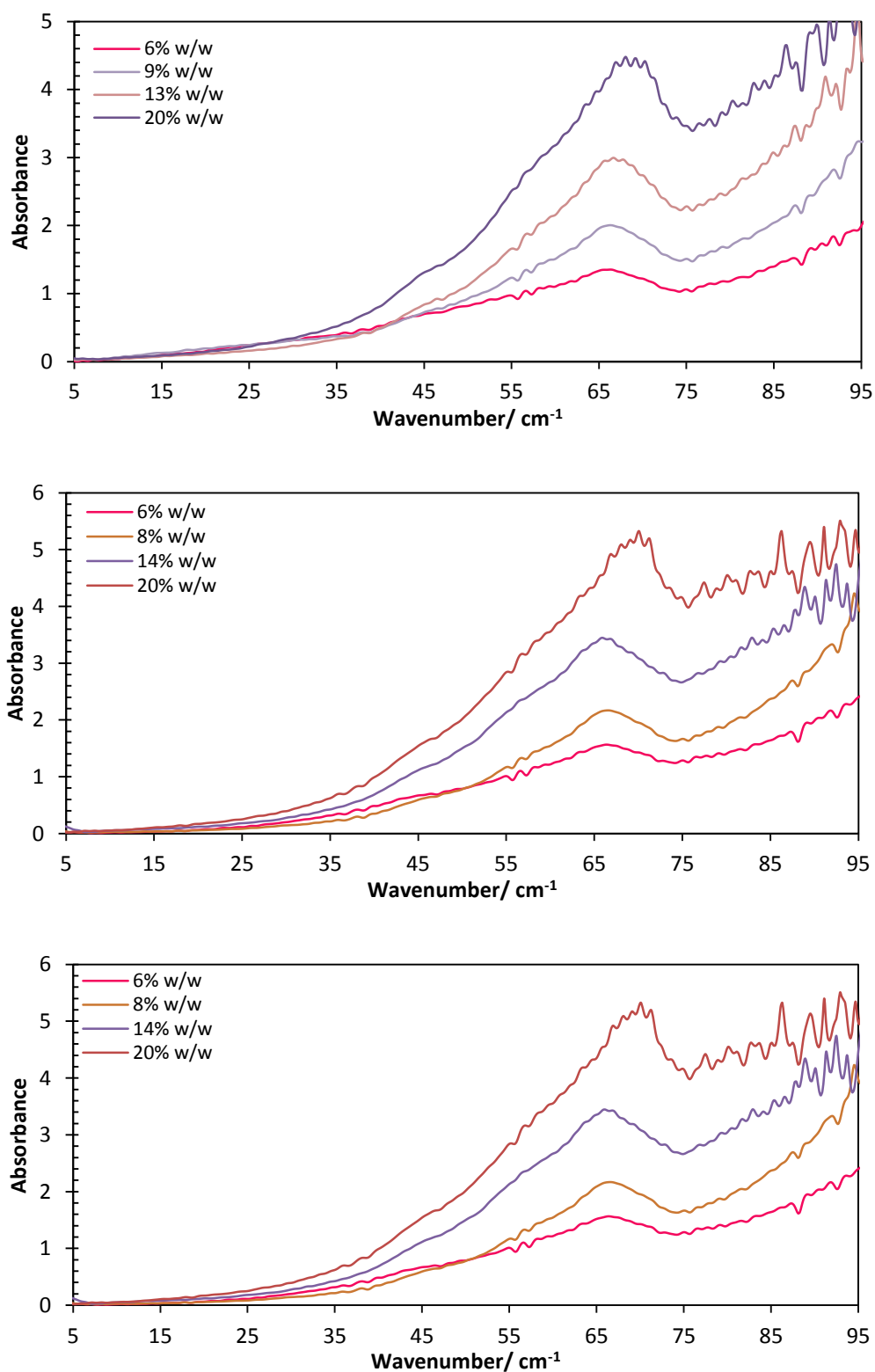


Figure 30. THz absorption spectra of crystalline *L*-proline for three separate partitions. Each individual spectrum is an average of three repeated measurements per each sample for each separate partition.

L-serine: Likewise in Figure 32, the distinct absorption spectra o serine was observed.

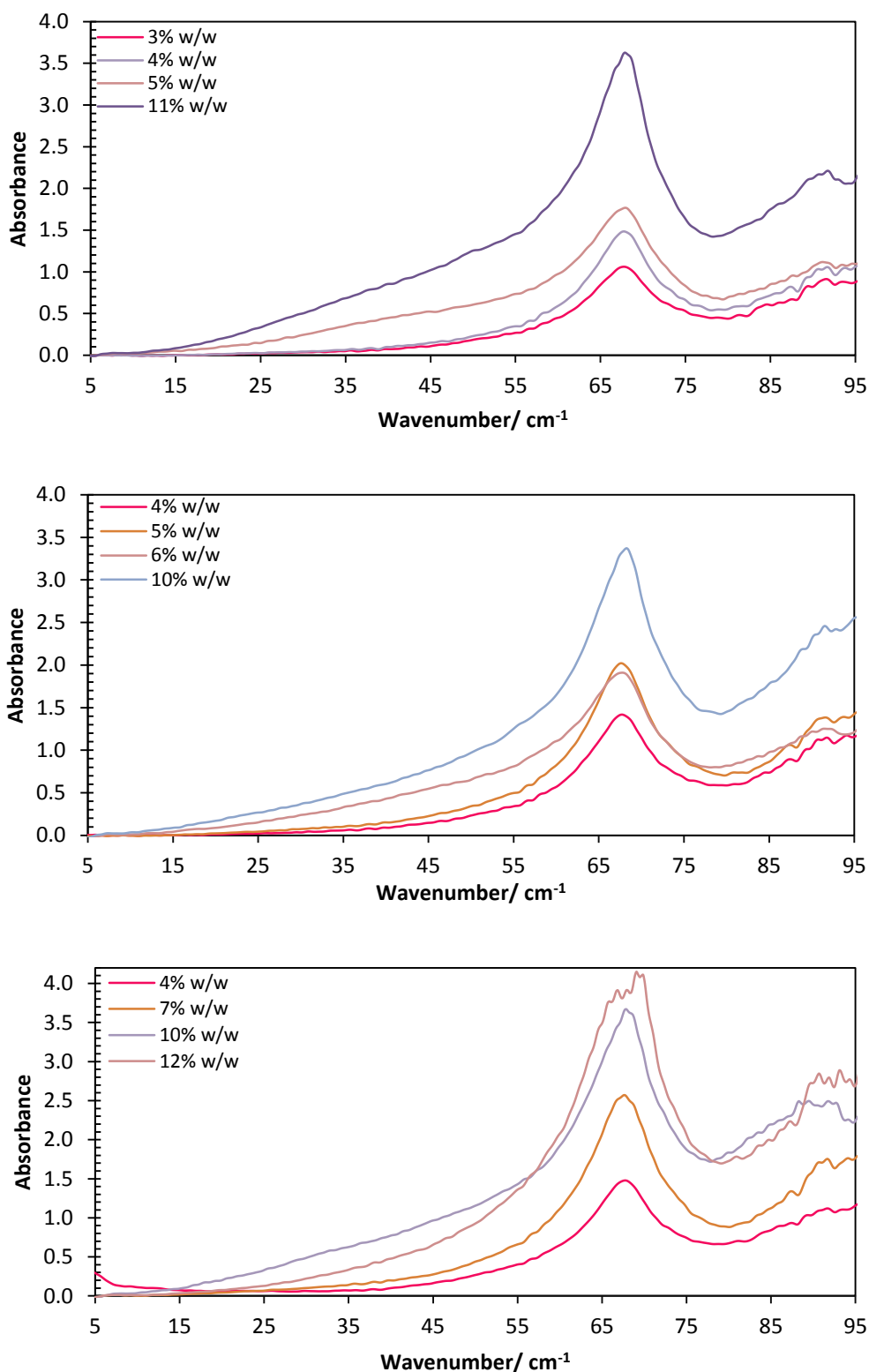


Figure 31. The terahertz absorption spectra of crystalline L-serine for three separate partitions. Each individual spectrum is an average of three repeated measurements per each sample for each separate partition.

4.3.2 Partial Least Squares Regression

L- alanine: The calibration model of *L*-alanine which has been cross validated using three partitions (Table 15) is shown in Figure 33. The function $f(x) = 1.001x - 0.026$ and R^2 0.99 was estimated for this function. With 95% confidence, predictions will have RMSE of 0.156%.

Table 15. Estimated functions of the three different partitions used for *L*-alanine in cross validation.

| Partition | Function: $f(x)$ | RMSE | R^2 |
|-------------|-------------------------|--------|-------|
| Partition 1 | $0.052 \cdot x - 0.429$ | 0.0087 | 0.99 |
| Partition 2 | $0.053 \cdot x - 0.425$ | 0.0100 | 0.99 |
| Partition 3 | $0.052 \cdot x - 0.421$ | 0.0052 | 0.99 |

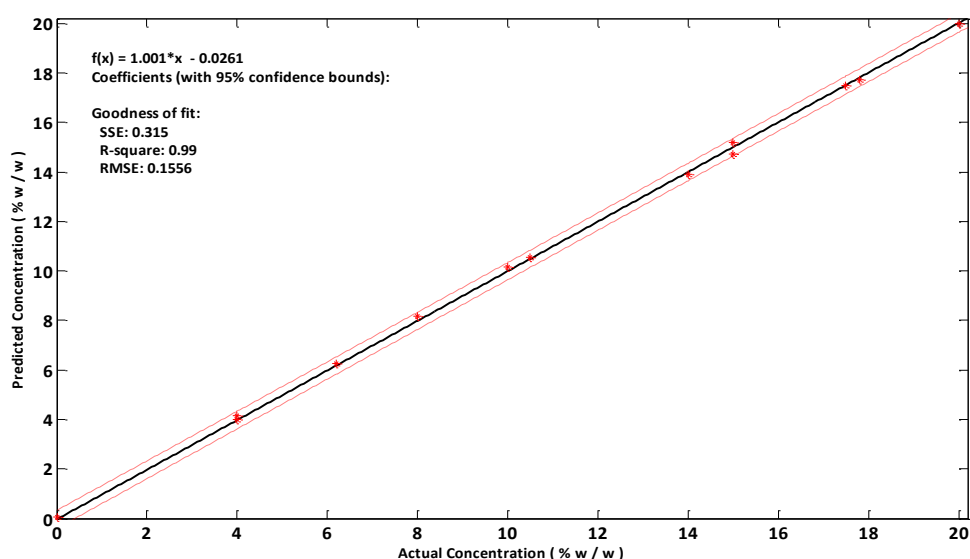


Figure 32. PLSR calibration model of the predicted concentration for *L*-alanine against the actual concentrations with 95% confidence interval bands.

The model was tested with other pellets prepared with unknown proportions of *L*-alanine. However, due to equipment failure, only two of the test samples were deemed acceptable to be used in this analysis.

Table 16. Comparing the actual concentration and the predicted concentrations of samples prepared with unknown proportions of *L*-alanine.

| Actual Concentration (%w/w) | Predicted Concentration (%w/w) |
|-----------------------------|--------------------------------|
| 5 | 4.91 |
| 14 | 13.97 |

As show in Table 16, the predicted concentration of the crystalline alanine incorporated into polyethylene pellets were in agreement with the actual concentration (Figure 34).

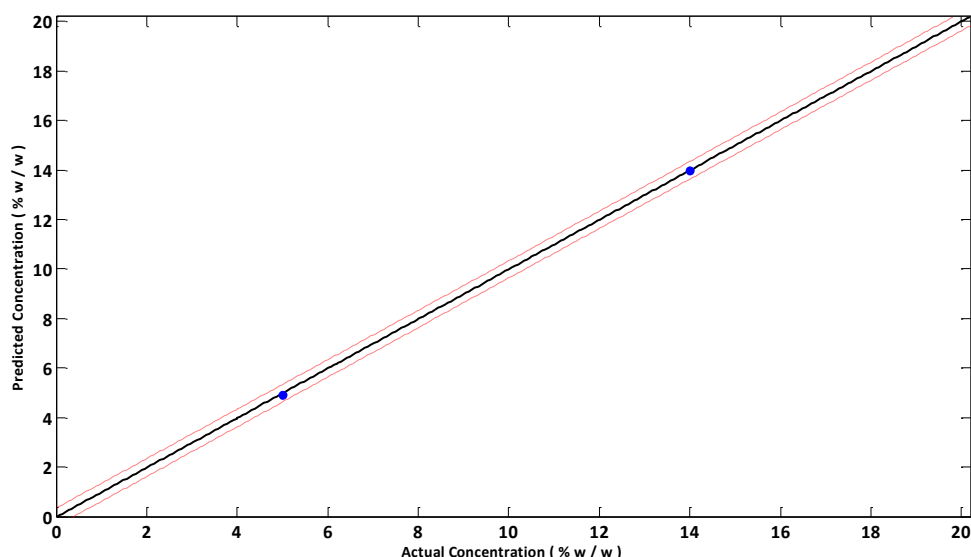


Figure 33. PLSR calibration model of the predicted concentration for *L*-alanine against the actual concentrations with 95% prediction bands. The model is fitted with the predicted concentrations in samples prepared with unknown alanine concentrations.

***L*-proline:** Similarly, the calibration model of *L*-proline is shown in Figure 35 based on the absorption band located between the frequency region 35 cm^{-1} and 75 cm^{-1} . The model was cross validated using three partitions (Table 17) yielding a function $f(x) = 1.001x - 0.026$ and an estimated R^2 of 0.99. With 95% confidence, predictions will have RMSE of 0.196% based on this analysed data.

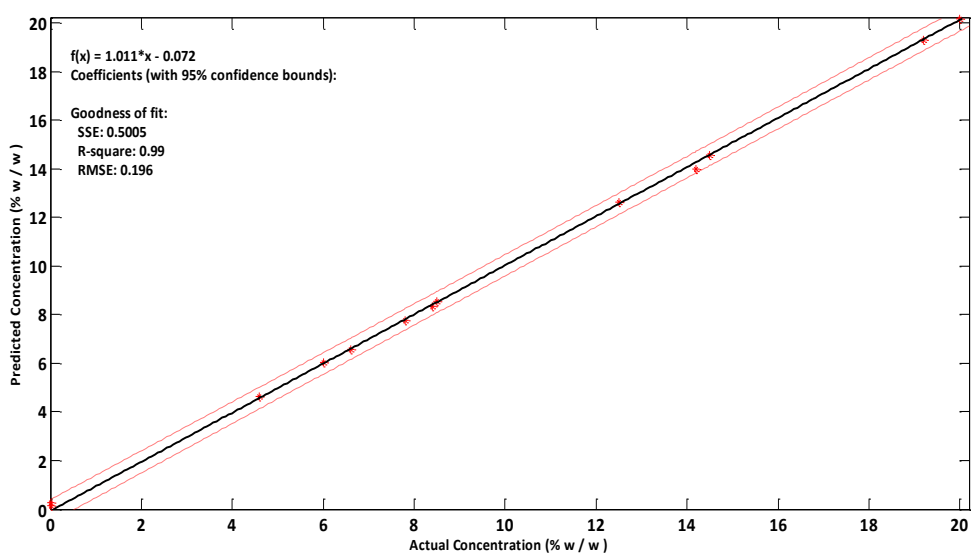


Figure 34. PLSR calibration model of the predicted concentration for *L*-proline against the actual concentrations with 95% confidence interval bands.

Table 17. Estimated functions of the three different partitions used for *l*-proline in cross validation

| Partition | Function: $f(x)$ | RMSE | R^2 |
|-------------|-------------------------|---------|-------|
| Partition 1 | $0.052 \cdot x - 0.434$ | 0.00815 | 0.99 |
| Partition 2 | $0.050 \cdot x - 0.408$ | 0.00716 | 0.99 |
| Partition 3 | $0.050 \cdot x - 0.421$ | 0.00068 | 0.99 |

The model was further tested with other pellets prepared with unknown proportions of *l*-proline and the fitted data is shown in Figure 36. The predicted concentrations are compared with the actual concentration as shown in Table 18. The predicted concentrations of the crystalline proline were in agreement with the actual concentrations. These were however within the 95% prediction bands.

Table 18. Comparing the actual concentration of unknown proline samples with the expected and predicted concentrations using PLSR calibration model

| Actual Conc. (%) | Predicted Conc. (%) | Expected Concentration (%) |
|------------------|---------------------|----------------------------|
| 2 | 2.10 | 2.05 |
| 2.5 | 2.54 | 2.54 |
| 4.5 | 4.51 | 4.52 |
| 5.5 | 5.56 | 5.51 |
| 10.5 | 10.36 | 10.46 |
| 12.5 | 12.67 | 12.44 |
| 13.5 | 13.41 | 13.42 |

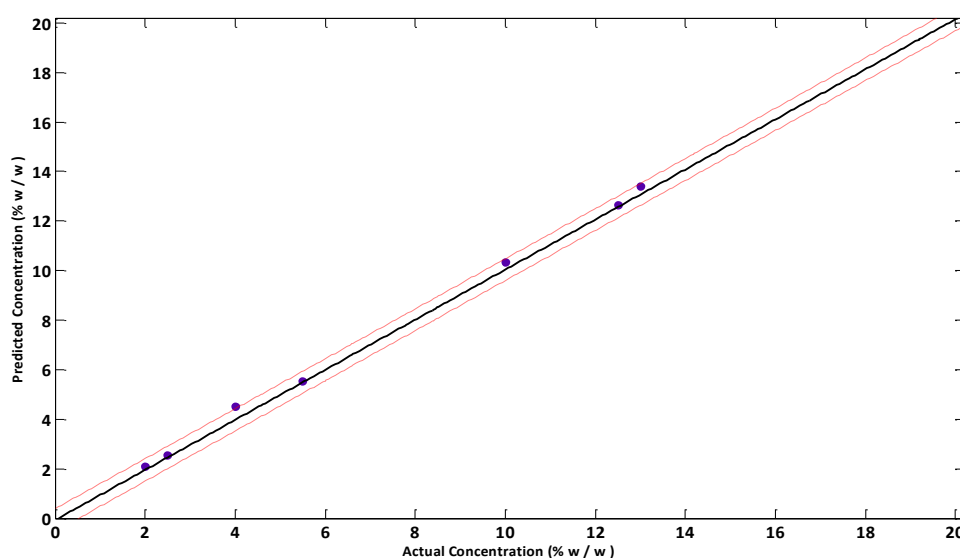


Figure 35. PLSR calibration model of the predicted concentration for *l*-proline against the actual concentrations with 95% prediction bands. The model is fitted with the predicted concentrations in samples prepared with unknown proline concentrations.

L-serine: The PLSR calibration model of *l*-serine is presented in Figure 37 based on the absorption band recorded in the frequency region between 55 cm⁻¹ and 78 cm⁻¹. The overall calibration model recoded $f(x) = 0.998x + 0.0175$ with R^2 0.99. With 95% confidence, predictions will have RMSE of 0.100%. These parameters were estimated using three partitions (Table 19) for the cross validation.

Table 19. Estimated functions of the three different partitions used for l-serine in cross validation

| Partition | Function: $f(x)$ | RMSE | R^2 |
|-------------|-------------------|--------|-------|
| Partition 1 | $0.0749x - 0.421$ | 0.0073 | 0.99 |
| Partition 2 | $0.0778x - 0.441$ | 0.0033 | 0.99 |
| Partition 3 | $0.0758x - 0.426$ | 0.0081 | 0.99 |

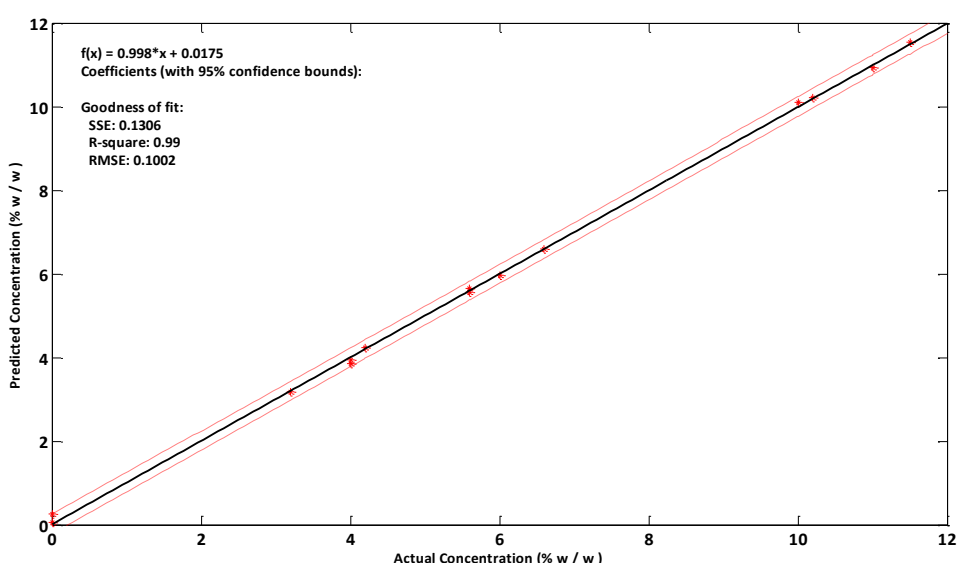


Figure 36. PLSR calibration model of the predicted concentration for l-serine against the actual concentrations with 95% confidence interval bands.

The calibration model was also tested with four samples prepared with unknown concentrations of *l*-serine. The predicted concentration of the crystalline serine is in agreement with both the actual and expected concentration as shown in Table 20 and Figure 38.

Table 20. Comparing the actual concentration of unknown samples with the expected and predicted concentrations using PLSR calibration model

| Actual Conc. (%) | Predicted Conc. (%) | Expected Concentration (%) |
|------------------|---------------------|----------------------------|
| 3.6 | 3.67 | 3.61 |
| 5.0 | 4.95 | 4.81 |
| 7.5 | 7.50 | 7.50 |
| 8.5 | 8.58 | 8.50 |

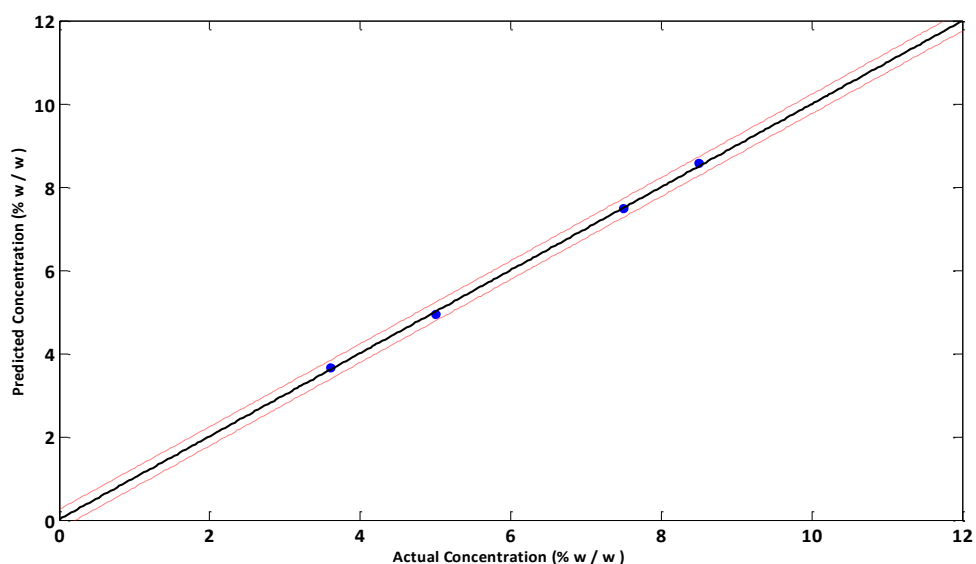


Figure 37. PLSR calibration model of the predicted concentration for *l*-serine against the actual concentrations with 95% prediction bands. The model is fitted with the predicted concentrations in samples prepared with unknown proline concentrations.

Summary

Table 21. Parameters generated from quantitative models using PLSR. All values are expressed in terms of amino acid concentration %w/w

| Sample ID | Alanine | Proline | Serine |
|---------------------------|---------|---------|--------|
| Slope | 1.001 | 1.011 | 0.998 |
| R ² | 0.996 | 0.999 | 0.998 |
| RMSE (%) | 0.156 | 0.196 | 0.100 |
| LOD (3.3 x RMSE/slope) | 0.557 | 1.442 | 0.615 |
| LOQ (10 x RMSE/slope) | 1.686 | 4.369 | 1.864 |

4.4 Phase III– Crystallinity in freeze dried gelatin/amino acid

4.4.1 Colorimetric measurements

Table 22. Colorimetric absorbance recorded for the solution of gelatin, and amino acid/gelatin.

| Concentration (%w/w) | Gelatin (A) | Alanine (A) | Proline (A) | Serine (A) |
|-------------------------|----------------|----------------|----------------|---------------|
| 10 | 0.13 | 0.13 | 0.12 | 0.12 |
| 30 | | 0.12 | 0.13 | 0.12 |
| 50 | | 0.13 | 0.12 | 0.11 |
| 70 | | 0.12 | 0.12 | 0.13 |

Table 19 shows that the relative colorimetric absorbance for gelatin only solution compared to the amino acid/gelatin solution had no significant difference.

4.4.2 THz measurements

The terahertz spectra of freeze dried gelatin/amino acids are as shown in Figures 39 to 41. The 30% to 70% gelatin/serine freeze dried cake all collapsed during the cycle; hence no results will be shown for this concentration. **Given that the solid fraction ratios of amino acid to gelatin were 10:90; 30:70; 50:50; 70:30, then the final concentration of amino acid in the pellets of freeze-dried material translates to 1%, 3%, 5% and 7% in pellets.**

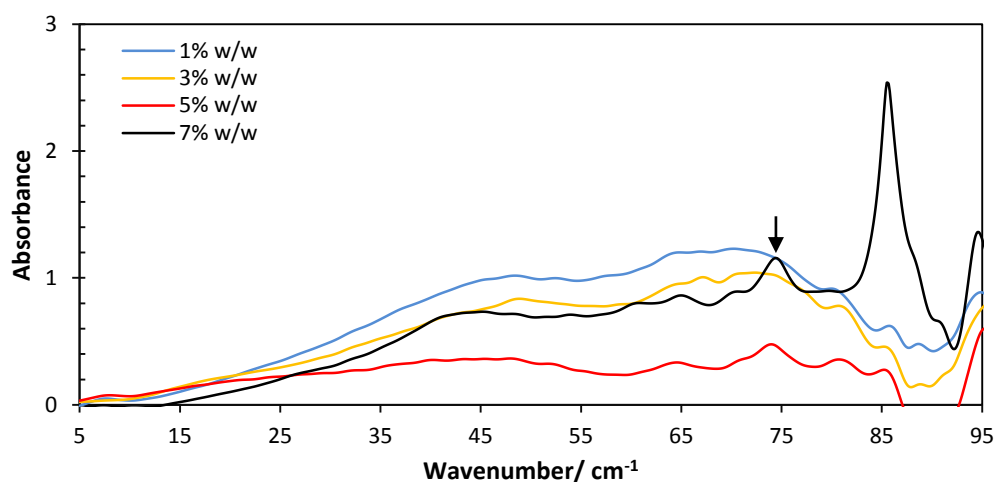


Figure 38. Terahertz absorption spectra of freeze dried gelatin and individual *L*-alanine. Each spectrum is the average of 6 repeated measurements from different areas across the pellet.

From Figure 39, the distinctive spectra features of *L*-alanine can be observed in the THz spectra for alanine/gelatin freeze dried cake at proportions of 50%w/w: 50%w/w (5% w/w in pellets). The THz spectra of *L*-proline/gelatine freeze dried cake shown in Figure 40 revealed no features for all the concentrations studied.

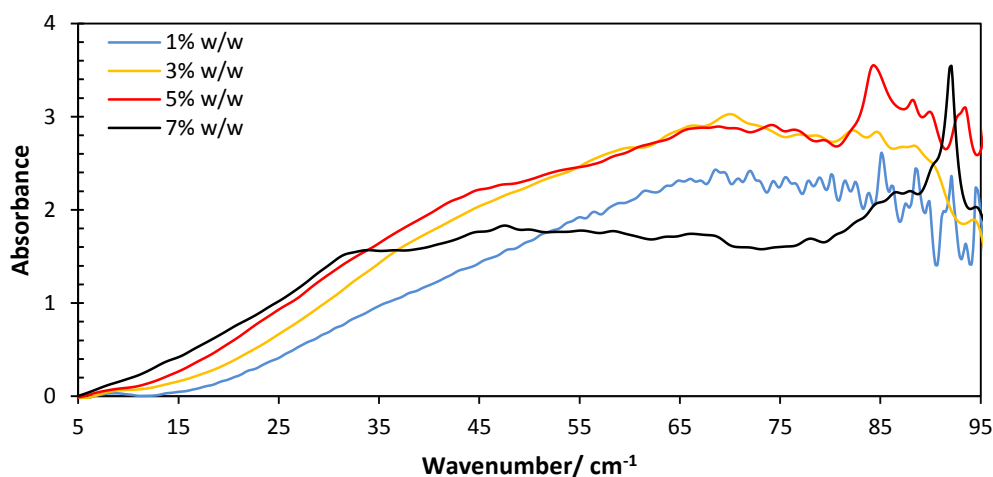


Figure 39. Terahertz absorption spectra of freeze dried gelatin and individual *L*-proline. Each spectrum is the average of 6 repeated measurements from different areas across the pellet.

In Figure 41, the absorption bands synonymous with crystalline serine were also revealed in the *L*-serine/gelatin freeze dried cake in 30% serine: 70% gelatin (3% w/w in pellet) and 50% serine: 50% gelatin (5% w/w in pellet).

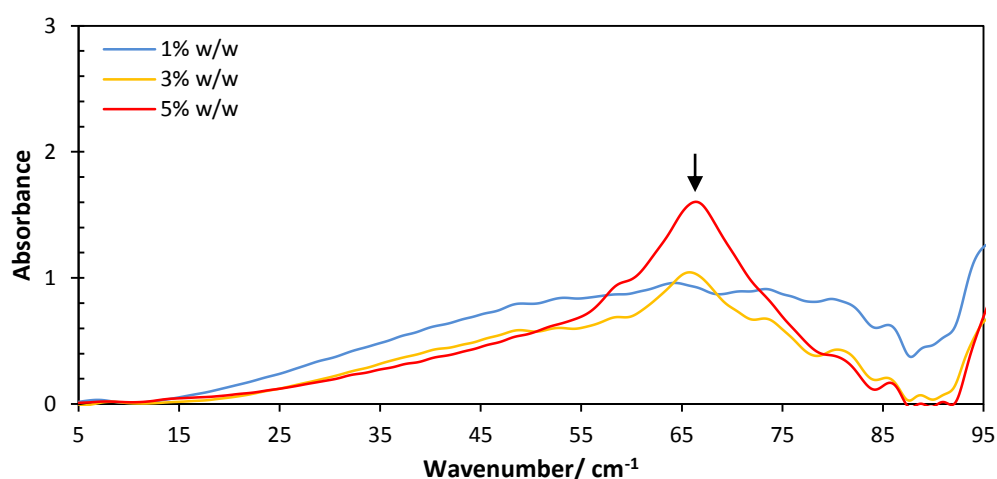


Figure 40. Terahertz absorption spectra of freeze dried gelatin and individual *L*-serine. Each spectrum is the average of 6 repeated measurements from different areas across the pellet.

4.4.3 Determining degree of crystallinity using PLSR

Using PLSR algorithms, the crystallinity in the freeze dried sample pellets were predicted in comparison to the crystalline samples.

L-alanine: The absorption band located between the frequencies of 66 cm^{-1} to 76 cm^{-1} recorded from for polyethylene pellets incorporated with freeze dried gelatine/alanine was analysed against pellets prepared with crystalline alanine. Figure 42 shows a plot of the predicted crystallinity indicating that at 50% w/w and 70%w/w, the degree of crystallinity is estimated to be 61.8% and 71.2% ($\pm 0.16\%$) respectively.

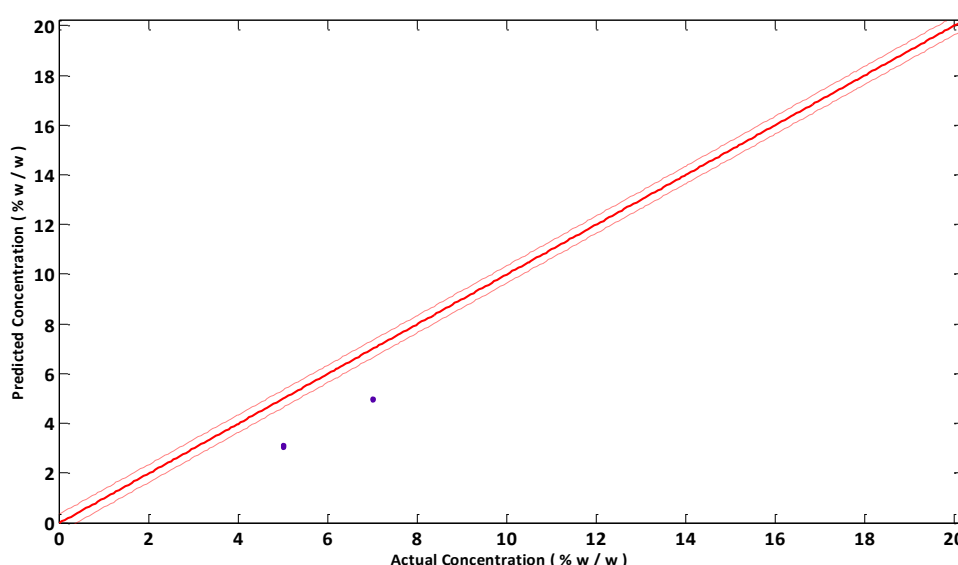


Figure 41. PLSR calibration model of the predicted concentration for l-alanine against the actual concentrations with 95% prediction bands. The model is fitted with the predicted degree of crystallinity in samples prepared with freeze dried gelatin/alanine.

L-proline: In samples prepared with freeze dried gelatine/proline, as shown in Figure 39, by visual observation, the characteristic broad absorption band for proline recorded at 66.1 cm^{-1} and the partially obscured band at 42.6 cm^{-1} as shown in Figure 22 were absent. Hence PLSR analysis was not performed on these datasets and all concentrations are reported as yielding a freeze dried cake with amorphous matrix.

L-serine: The absorption band located between the frequency region of 55 cm^{-1} to 78 cm^{-1} recorded for the polyethylene pellets incorporated with freeze dried gelatine/serine was also

analysed and compared with crystalline serine. The predicted degree crystallinity at 30% w/w and 50%w/w was estimated to be 55% and 96.6% ($\pm 0.1\%$) respectively as shown in Figure 43.

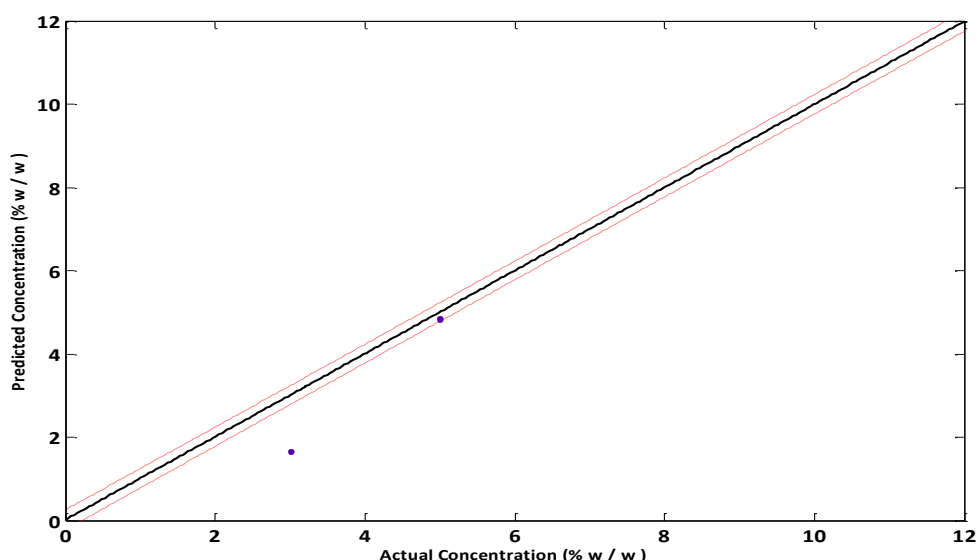


Figure 42. PLSR calibration model of the predicted concentration for l-serine against the actual concentrations with 95% prediction bands. The model is fitted with the predicted degree of crystallinity in samples prepared with freeze dried gelatin/serine.

Table 20 shows a summary of the percentage degree of crystallinity estimated for the freeze dried amino acids using PLSR calibration models.

Table 23. Summary of the degree of crystallinity estimated from the PLSR calibration models built from the related crystalline amino acids (n=3, and RMSE 0.16%, 0.20%, and 0.10% for the respective models of alanine, proline and serine)

| Sample | Concentration (%) | Expected Prediction | Actual Prediction | Degree of crystallinity (%) |
|------------|-------------------|---------------------|-------------------|-----------------------------|
| L-alanine | 1 | 0.95 | 0 | 0 |
| | 3 | 2.95 | 0 | 0 |
| | 5 | 4.95 | 3.09 | 61.8 |
| | 7 | 6.95 | 4.98 | 71.2 |
| L- proline | 1 | 1.07 | 0 | 0 |
| | 3 | 3.07 | 0 | 0 |
| | 5 | 5.08 | 0 | 0 |
| | 7 | 7.09 | 0 | 0 |
| L-serine | 1 | 1.10 | 0 | 0 |
| | 3 | 3.01 | 1.66 | 55.0 |
| | 5 | 5.01 | 4.84 | 96.6 |

Chapter 5. Discussions

5.1 THz studies of;

5.1.1 Crystalline amino acids and gelatin individually in polyethylene

L-alanine: The terahertz absorption spectra of *L*-alanine presented in Figure 21 revealed two distinct absorption bands with local centred on $\sim 75\text{ cm}^{-1}$ and $\sim 85\text{ cm}^{-1}$. Similar data from density functional theory studies (Yamamoto et al., 2005) and terahertz measurements (Yamaguchi et al., 2005) has been published previously.

The terahertz measurements presented by (Yamaguchi et al., 2005) showed that, the D- and L-form of alanine had similar absorption spectra with bands at $\sim 75\text{ cm}^{-1}$ and $\sim 85\text{ cm}^{-1}$. These two absorption bands corresponds to those appearing at 73 cm^{-1} and 85 cm^{-1} in Far Infra-Red spectra also reported previously (Bandekar et al., 1983).

These bands were explained to have originated from the intermolecular vibration modes resulting from hydrogen-bond deformations linked to other modes like COO⁻ torsion, NH³ torsion and the CC α N deformation. The band at 85 cm^{-1} was suggested to be associated with skeletal torsion. In the letters of (Yamamoto et al., 2005), an absorption band predicted by (Krimm, 1987) at 45 cm^{-1} was not observed because this group did not study DL- alanine. This characteristic band was only present in the DL- form of alanine arising from NH out-of-plane angle bend and -C β H₃ bend. This has also been confirmed using Far Infra-Red to study polycrystalline L, D, and DL alanine (Matei et al., 2005, Yamaguchi et al., 2005).

L-Proline: The absorption spectra of *L*-proline presented in Figure 22 revealed a principal absorption band at 66.1 cm^{-1} and a partially obscured band at 42.6 cm^{-1} . The absorption band at 66.1 cm^{-1} has previously been predicted using density functional theory and FIR to be located at 64 cm^{-1} (Matei et al., 2005) which was ascribed to hydrogen bond modes.

Previously published data also showed an absorption band at 76 cm^{-1} (Cooksey et al., 2009) which was not observed in this study. This could in fact be the D- form of proline.

L- Serine: The distinct spectra feature of *L*-serine is presented in Figure 23 showing a broad absorption band between 40 cm^{-1} to 80 cm^{-1} . The effects of low frequency motions of atoms in solid serine and cysteine molecules at 77 K and 298 K using terahertz Fourier Transform Infrared (FTIR) and theoretical spectral calculations has previously been studied and published

(Korter et al., 2006). It was suggested that, the characteristic absorption band observed for *L*-serine was as a result of the internal degree of freedom of the molecule at higher frequencies. However, at lower frequencies, the different intermolecular interactions cause different intermolecular vibrational phonons identified below 3 THz. This study presented five absorption bands based on theoretical calculations at 67 cm^{-1} , 74 cm^{-1} , 85 cm^{-1} , 90 cm^{-1} , and 98 cm^{-1} . However, in this study only one clearly resolved absorption band was identified with local maxima at 67.6 cm^{-1} . This could be the merged peaks earlier report and may be easily identified if THz measurements are recorded using ambient temperatures.

Although a consistent band is observed in this study at 90 cm^{-1} which is in agreement with the reported literature, this cannot conclusively be described as an absorption band since this is noisy region of the spectra and perhaps might be an anomalous artefact of the material and or the technology being used.

Gelatin: The featureless THz spectrum of gelatin is presented in Figure 24. Similar featureless THz spectra has previously been reported (Strachan et al., 2004), and it was explained materials which lack or contained insufficient order of molecular arrangement to continuously cause intermolecular vibrations showed no absorption response in the presence when probed with THz radiations.

5.1.2 Freeze dried amino acids/gelatin in polyethylene

As explained, a comparison between the crystalline amino acids with gelatin suggests that the absence of any terahertz absorption bands in gelatin is due to the lack of sustained phonon mode vibrations. Thus the presence of gelatin in freeze dried amino acid/gelatin will have negligible response to the THz radiation. Therefore the absorption bands observed in Figures 39 to 41 may be ascribed to phonon vibrations characterised in crystalline solids which in this case is the amino acid constituents. It is also recognised that the processes involved in preparing these formulations have the potential to affect the crystallisation process of amino acid. Such effects may include crystal particle sizes, and subtle changes in the crystal structure perhaps through the inclusion of impurities causing defects. These defects may have negative effects on the absorption coefficients of the crystalline amino acids which could influence the estimates which is extrapolated from the calibration data.

Generally, it was observed that as the concentration of amino acid increased, the baseline of the spectra decreased and the signal to noise ratio improved. This can be attributed to the effects of freeze dried gelatin. Amorphous gelatin is electrostatic and therefore particle size reduction was ineffective resulting in a non-uniform blend. At lower concentrations of amino acids, the electrostatic properties of gelatin dominated the characteristics of the entire cake, such that the freeze dried material was always physically springy. This was more prominent in proline/gelatin samples which has been reported to be amorphous after freeze drying (AlHusban et al., 2010b).

In the amino acid/gelatin that contained 10% amino acid and 90% gelatin, the featureless absorption bands similar to what was observed for gelatin (not freeze dried, Figure 24) and freeze dried sucrose (Figure 20) was observed. Furthermore, in the DSC studies by *Alhusban et. al.*, it was reported that at such a lower concentration of crystalline material, *L*-alanine, *L*-serine and *L*-proline show no crystalline characteristics with glass transition temperatures recorded at -21.5 °C, -18.75 °C, and -21.47 °C respectively for solutions of these amino acids (AlHusban et al., 2010a). It was explained that, because amino acids are added to the formulation as a percentage weight per weight, the lower molecular weight amino acids such as *L*-alanine provided higher number of moles compared to the high molecular weight amino acids (*L*-proline). This resulted in a large number of moles within the formulation thereby eventually having a higher cushioning effect which in turn reduces the intermolecular interactions. Hence, the amino acids with the lower molecular weight will be characterised as having higher plasticizing effect.

Upon increasing the concentration of the amino acid to 30% (effectively reducing the concentration of gelatin to 70% and therefore when incorporated into the PE pellet, will be 3 mg amino acid :7 mg gelatin :390 mg PE), the spectra observed for both *L*-alanine (Figures 39) and *L*-proline (Figure 40) retained its featureless characteristic spectra. In contrast, for the sample containing 30% *L*-serine as shown in Figure 41, the distinct absorption band recorded for crystalline *L*-serine shown in Figure 23 was also observed at 66.46 cm^{-1} . As expected, the amplitude of this peak was low perhaps due to the lower concentration or the effects of scattering. Initial thermal studies did not identify any phase transition associated with crystallinity at this concentration (AlHusban et al., 2010b).

In the freeze dried amino acid/gelatin containing 50% w/w of each, the spectra of *L*-alanine showed absorption band at 74.47 cm^{-1} , similar to what was observed in Figure 21 for

crystalline *L*-alanine. The spectrum of freeze dried *L*-serine at 50% w/w also indicated crystalline features initially recorded for crystalline *L*-serine. However, the THz spectrum of *L*-proline showed no distinct features indicating freeze dried *L*-proline/gelatin had retained its amorphous character.

In the previous studies by Alhusban *et. al.* (AlHusban et al., 2010b), it was demonstrated that the crystalline characteristics of *L*-alanine/gelatin in a formulation containing 70% w/w of alanine and 30% w/w of gelatin prohibited the matrix from undergoing the glass transition phase associated with partially crystalline and amorphous materials only. In this study, the THz spectrum for both 50:50 and 70:30 alanine/gelatin shown in Figure 37 also revealed the distinct absorption band recorded at 74.47 cm^{-1} for crystalline *L*-alanine which has been ascribed to long range and orderly internal molecular vibrations. The sharp absorption band revealed $\sim 85\text{ cm}^{-1}$ will be considered as an anomalous peak based on the fact that, pellets prepared from a heterogeneous powder blend (particle size $\geq 250\text{ }\mu\text{m}$) had revealed similar features as shown in Figure 19. In contrast, again the THz spectra of *L*-proline showed no features.

Although lower molecular weight amino acids are thought to exhibit high plasticising and cushioning effects, in this study, one will expect freeze dried *L*-alanine in gelatin to be amorphous unlike *L*-proline. Hence it is ideal to look at the molecular structure of *L*-proline which may be aiding *L*-proline to remain amorphous after freeze drying.

As shown in Figure 5, the *L*-proline structure has a distinctive cyclic structure which infers other specific properties on *L*-proline (Cheng and Chang, 1999). Using the Ramachandran plot, one can identify and show in theory conformations of the backbone dihedral angle ψ against ϕ of amino acids. For instance in a simpler amino acid e.g. glycine which has hydrogen atom as its side constituent, it will be characterised with a smaller van der Waals radius when compared to amino acids with big side chains e.g. eth-, propyl- etc. Hence in a molecule like glycine, there are less conformational restrictions. *L*-proline in contrast has a larger five member ring side chain that restricts possible conformations. Thermodynamically, it might be favourable to have a hydrophobic interaction with gelatin in the presence of water to stay in the solution without precipitating out. In a previous study that looked at the local tendencies for a backbone dihedral angles in proteins, it was suggested that, the dihedral distribution for a molecule might may be significantly affected by the type and conformation of its neighbouring molecules (Betancourt and Skolnick, 2004). In a formulation of gelatin (similar to synthetic high

polymer) and *L*-proline, a physical crosslink of triple stranded helix can be formed as explained in previous publication. This means the effective concentrations of both constituents are altered in favour of the highly wettable and soluble proline (deWolf and Keller, 1996). The freeze dried cake of gelatin like any other large polymer is expected to be amorphous. In a highly concentrated solution of *L*-proline, which has a high solubility and wetting threshold, the freeze dried product may therefore be expected to exhibit amorphous characters.

5.2 Calibration models

As observed in Figure 26, the calibration model based on peak area analysis showed RMSE of 0.538 compared to 0.228 of PLSR model for polycrystalline sucrose (Figure 27). Thus the error margins which accompany linear regression based on area under the peak were wide thereby increasing prediction errors.

For the calibration models for amino acids (summary in Table 21), RMSEs of 0.156%, 0.20% and 0.10% were also estimated for PLSR models of alanine, proline and serine respectively. This indicates a very low dispersion of variance in the three partitions and also a suggestive of a good model fit for these amino acids. Unlike peak area analysis based models, the estimated slope based on PLSR model may not be used to determine which of these amino acids has higher THz absorption.

Based on these PLSR calibration models using the data obtained from this study, it may be surmised that the LODs for the various amino acids in real formulations are in the region of 0.56 and 1.44 whilst LOQs are also in the region 1.69 and 4.37. The relevance of these estimates is that, the test samples (freeze dried amino acids/gelatin) are generally above the LOD and within the LOQ.

However, it should be recognised that these values were determined under conditions ideal for the implementation of the TPS technology and therefore might not be necessarily applicable to “real” complex formulations. Furthermore it is also assumed that the peak intensities per unit concentration are the same for materials which are presented in the calibration model and those in the actual; samples are effectively the same.

5.3 Degree of crystallinity in freeze dried amino acids

The recorded absorbance data shown in Table 22 indicated that, the difference between the absorbance of gelatin solution and amino acid/gelatin solution was negligible. An average absorbance of 0.123 (± 0.006) was measured. Further visual observation also did not show any sediment of crystalline amino acids at the bottom of the gelatin solution. Thus, there is no evidence of light scattering from un-dissolved particulates of amino acids. Hence, it is assumed that all amino acids at the concentration studied were soluble in the gelatin solution. The major proof to determine if gelatin itself is enhancing the solubility of the amino acids in the solution state is to do a solubility testing. In this project, solubility test were carried out with unsuccessful results. As shown in Table 8, particularly for serine, where the aqueous solubility was exceeded, it may be inferred that the presence of gelatin has improved the solubility through some solubilisation mechanism.

It is assumed that, the process of freeze drying effectively reduces the moisture present, hence theoretically it was expected that some of the amino acid dissolved into the gelatin solution will be precipitated out. However, based on all the calibration models and terahertz measurements, the degree of crystallinity predicted for the freeze dried amino acids/gelatin containing 10% amino acid indicated no crystalline activity (Figures 39 to 41).

The increased concentration of alanine to 50% w/w and 70% w/w showed an estimated degree of crystallinity to be ~62% and ~72% ($\pm 0.16\%$) respectively. Similarly in 30% w/w and 50% w/w serine/gelatin freeze dried cake, the degree of crystallinity was estimated to be 55% and ~97% ($\pm 0.10\%$) respectively.

Chapter 6. Conclusion

This work has look at the feasibility of using terahertz technology to determine and quantify crystallinity in polycrystalline saccharides, amino acids and freeze dried gelatin/amino acid mixtures.

It was identified that the TPS when combined with other statistical tools may be a useful tool for estimating and perhaps predicting the degree of crystallinity in materials, which in future may be used as a guide in selecting ideal concentrations which could affect the final product qualities. In the sucrose data analysed, the PLSR calibration models showed reduced prediction errors in the form of RMSE when compared to LR. However, it is also recognised that the PLSR algorithms are very sensitive and may potentially result in over fitting.

The degree of crystallinity is particularly important in RDTs since it has a direct effect on the mechanical properties and disintegration time of a formulation. At a lower concentration of 30% w/w, freeze dried *L*-serine showed 55% ($\pm 0.10\%$) crystallinity compared to 61.8% ($\pm 0.16\%$) crystallinity estimated in the 50% w/w freeze dried *L*-alanine formulations.

The relevance of this project is that, whilst at 50% w/w and 70% w/w, *L*-serine and *L*-alanine respectively might be capable of maintaining the mechanical integrity of amino acid based freeze dried RDTs (owing to the high crystallinity) this may impact negatively on the disintegration time. In contrast, *L*-proline suspended in a gelatin matrix is less likely to crystallise indicating it has a high wetting profile. Thus, in a complex formulation of proline and alanine (or serine) with the optimum proportions, it is expected that the alanine or serine component will provide ideal mechanical properties whilst the proline component helps to enhance the disintegration time.

Chapter 7. Future work

In this project, it has been shown that TPS can provide a reliable estimate of the degree of crystallinity in mixtures of freeze-dried amino acid and gelatin.

The impact of this crystallinity on mechanical strength and dissolution times to define the optimal concentration of individual amino acids or indeed to define the optimal concentration in mixtures of amino acids will be the principal study in the future work. Routine dissolution tests and mechanical strength measurements are required on a range of mixtures in order to isolate the optimal formulation.

It may also be ideal to investigate the impacts of varying the ratios of proline and alanine or serine suspended in gelatin matrix will have on degree crystallinity and correlate to the disintegration profiles. Complementary analysis with Dielectric Impedance spectroscopy can also provide rich source of information about the molecular mobility of moisture during the freeze drying process of amino acids. This can help to control the critical parameters that impacts on crystallinity and hence disintegration process.

Possible mechanisms of crystallization in these complex solutions can also yield rich information as to which parameters can be controlled in other to control the degree of crystallinity. It is currently unknown when the amino-acid come out of solution? One may only presume it to be during the freezing stage. Therefore method based on a thermal method (e.g. DSC) may be used to look into the freeze-thaw behaviour.

Synopsis

Background: Rapidly Disintegrating Tablets (RDTs) are solid dosage forms containing the drug which quickly dissolves or disintegrate into a suspension within the buccal cavity, usually in seconds. Those RDTs which are produced by freeze drying technology have a highly porous and amorphous matrix. As a result these products provide rapid dissolution/disintegration but are fragile and present potential handling issues for the patient. Freeze-dried rapidly disintegrating Tablets (RDTs) are invariably formulated with gelatin, polyols and sugars e.g. mannitol and sucrose. However, the sugar component is required in high concentration to achieve formulations with acceptable mechanical properties. While the increased concentration of sugar does not have a deleterious effect on disintegration, the principle drawback from using sugars *per se* is that the formulation becomes unsuitable for treating chronic diseases, such as diabetics and obesity, or for use by pediatrics and those patients suffering with allergies. Recent research has shown the feasibility of using individual or a combination of amino acids as a replacement component for sugars in RDT formulations. Although there are reports of enhanced mechanical properties it has been noted that high concentrations will have a negative effect on disintegration time. What has emerged from this work is the notion of an optimal concentration of amino acid, i.e. one that is sufficiently high to provide the desired mechanical strength but not too high to impact disintegration time. This creates a further opportunity to reduce the loading of excipients and to increase the drug loading which is advantageous. However, there has not been any systematic quantitative study of the influences of amino acids on these RDTs to identify the optimal concentrations required, i.e. that concentration which results in sufficient crystallinity to provide for adequate mechanical strength but at the same time does not impact adversely the disintegration time. In order to determine what might present as the optimal concentration it is first necessary to establish a measurement technique that can quantify the degree of crystallinity in each formulation. DSC is used routinely for crystallinity determinations in solids but for amino-acids this is not possible owing to the fact that the melting endotherm co-exists with the degradation endotherm.

Aim In this study, the degree of amino acid crystallinity in gelatin/amino acid based RDTs was investigated using terahertz pulsed spectroscopy. Three amino acids were investigated: alanine (89 g mol^{-1}), serine (105 g mol^{-1}), proline (115 g mol^{-1}). The order of decreasing hydrophobicity of the amino acid residue is proline > serine > alanine. In simple aqueous

solution, the solubility follows the order proline (162 %w/v at 25 °C), followed by alanine (17 % w/v at 25 °C) then serine (5 % w/v at 25 °C).

Hypotheses One might expect that the degree of crystallinity in the final product, i.e. the freeze-dried solid matrix of gelatin and amino acid, would follow the inverse of the rank order aqueous solubility, viz. serine > alanine > proline. It is also expected that the crystalline component would inevitably form during the freezing stage of the freeze-drying process, whereby much of the free water supporting the solubility of the amino acid would be removed through the formation of ice.

However, this hypothesis ignores the potential impact of specific interactions between the amino acid and gelatin. There might be a counter argument based on the hydropathy index whereby, on freezing, the most hydrophobic amino acid (alanine) would be expected to crystallise to the lesser degree from a co-solution with gelatin when compared with a simple aqueous solution. This is because the hydrophobic amino acid-gelatin interaction will increase the both solubility of the amino acid and the propensity for the amino acid to remain in solution during freezing.

Methods The three amino acids were studied by terahertz pulsed spectroscopy (in the frequency band 0.1 to 3 THz; 3 to 100 cm^{-1}), both in the pure crystalline form (as received from the manufacturer) and in the form of a co-freeze-dried matrix with gelatin. Freeze dried amino acid/gelatin formulations (in solid fraction ratios of 10:90; 30:70; 50:50; 70:30) were prepared in accordance with an optimal regime developed for a HETO FD8 freeze-drier. Prior to terahertz measurement, each material was first formed in a pellet prepared by compaction with polyethylene (which is transparent to THz energy). Pellets with crystalline amino acids were manufactured in concentration of 2 to 20% amino acid in polyethylene. Pellets prepared from the freeze-dried amino acid/gelatin matrix were manufactured in a concentration of 10% freeze-dried material in polyethylene. Given that the solid fraction ratios of amino acid to gelatin were 10:90; 30:70; 50:50; 70:30, then the final concentration of amino acid in the pellets of freeze-dried material translates to 1%, 3%, 5% and 7%. Following a short study to develop the optimal method of sample preparation, a calibration model was developed based on partial least squared regression (PLSR) and used in all subsequent analysis of THz spectra, whether acquired from the pure crystalline material or the freeze-dried material.

Results Each pure crystalline form of amino acid displayed one or two resonance peaks at characteristic wave numbers, which were in general agreement with the literature (with alanine at 75 cm^{-1} and 85 cm^{-1} ; proline at 48 cm^{-1} and 66 cm^{-1} ; and serine centred on 67 cm^{-1}). Generally, it was observed from the TPS spectra that the area under each absorption band (as determined by the PLSR method) had a linear dependence on the concentration of amino acid in the pellet, thereby providing the opportunity to create a calibration model for the crystallinity of the amino acid. Given that the position and shape of the principal absorption bands were independent of the form in which the amino acid was presented within the pellet (i.e. as the pure crystalline material or from the freeze dried matrix) then it seems reasonable to use the calibration model from the crystalline material to estimate the degree of crystallinity in the amino-acids which had been co-freeze-dried with gelatin. Limits of detection (LOD) and Limits of quantitation (LOQ) were estimated using formulae provided by the ICH Q2 guidelines. These estimates showed that the LOD with this technology based on the data recorded for pelleted amino acid, were 0.557% for alanine, 0.615% for serine and 1.442% for proline. This indicates that TPS is quite sensitive for the determination of % crystallinity in amino acids at the low concentrations of interest. The corresponding LOQ values were 1.686%, 1.864% and 4.369% respectively.

Irrespective of the amino acid in question (viz. alanine, proline, or serine) all freeze-dried formulations containing 10% amino acid and 90% gelatin were found to have no crystallinity with respect to the amino acid component. On increasing the amino acid to 30% (thereby reducing the gelatin concentration accordingly to 70%) those formulations manufactured from alanine and proline still maintained their amorphous state whilst serine showed evidence of crystallisation behaviour. The latter may be inferred from the fact that the serine formulation displayed distinct absorption bands similar to what was recorded in the crystalline serine reference. Only on increasing the concentration of amino acid to 50% did the spectra of alanine display the distinct absorption bands of their crystalline reference counterparts whilst at this same concentration proline retained its amorphous character.

The degree of crystallinity in serine and alanine was estimated using calibration models built from partial least square regression (PLSR). The degree of crystallinity in the 30% *L*-serine formulation was estimated to ~55% ($n=3$). In the formulation containing 50% *L*-alanine, degree of crystallinity was estimated to be ~62% ($n=3$) whilst at the same concentration, *L*-serine was

estimated to have been ~97% (n=3) crystallised. Further increasing the concentration to 70% in *L*-alanine yielded an estimated crystallisation of 71% (n=3).

Discussion Overall, one might consider an effective 'solubility' of the amino acid within the freeze-dried matrix to be derived from the degree of crystallinity quantified by terahertz spectroscopy. This work has shown a rank of proline > alanine > serine. Unsurprisingly, the same rank order exists for the aqueous solubility, with serine being the least soluble ($\sim 5 \text{ g ml}^{-1}$) and proline being the most soluble ($\sim 162 \text{ g ml}^{-1}$). The impact of hydrophobic interactions between the amino acid and gelatin are therefore less dominant in defining the crystallinity of the amino acid within the freeze-dried material.

The relevance of this project is that, whilst at 50% w/w and 70% w/w, *L*-serine and *L*-alanine respectively are capable of maintaining the mechanical integrity of amino acid based freeze dried RDTs, this may impact negatively on the disintegration time. In contrast, *L*-proline suspended in a gelatin matrix is less likely to crystallise indicating it has a high wetting profile. Thus, in a complex formulation of proline and alanine (or serine) with the optimum proportions, it is expected that the alanine or serine component will provide ideal mechanical properties whilst the proline component helps to enhance the disintegration time.

Chapter 8. References

- ACHET, D. & HE, X. W. 1995. DETERMINATION OF THE RENATURATION LEVEL IN GELATIN FILMS. *POLYMER*, 36, 787-791.
- AKERS, M. J., MILTON, N., BYRN, S. R. & NAIL, S. L. 1995. GLYCINE CRYSTALLIZATION DURING FREEZING - THE EFFECTS OF SALT FORM, PH AND IONIC STRENGTH. *PHARMACEUTICAL RESEARCH*, 12, 1457-1461.
- AKERS, M. J., MILTON, N., NAIL, L. L. & NAIL, S. L. 1994. GLYCINE CRYSTALLIZATION DURING FREEZE DRYING: EFFECTS OF PH AND IONIC STRENGTH. *PHARMACEUTICAL RESEARCH (NEW YORK)*, 11, S134.
- ALHUSBAN, F., ELSHAER, A., KANSARA, J., SMITH, A., GROVER, L., PERRIE, Y. & MOHAMMED, A. 2010A. INVESTIGATION OF FORMULATION AND PROCESS OF LYOPHILISED ORALLY DISINTEGRATING TABLET (ODT) USING NOVEL AMINO ACID COMBINATION. *PHARMACEUTICS*, 2, 1-17.
- ALHUSBAN, F., PERRIE, Y. & MOHAMMED, A. R. 2010B. FORMULATION AND CHARACTERISATION OF LYOPHILISED RAPID DISINTEGRATING TABLETS USING AMINO ACIDS AS MATRIX FORMING AGENTS. *EUR. J. PHARM. BIOPHARM.*
- ASH, J. E. 1996. *THE MERCK INDEX*, MERCK & CO.
- AUDIC, J.-L. & CHAUFER, B. 2005. INFLUENCE OF PLASTICIZERS AND CROSSLINKING ON THE PROPERTIES OF BIODEGRADABLE FILMS MADE FROM SODIUM CASEINATE. *EUROPEAN POLYMER JOURNAL*, 41, 1934-1942.
- AYDINLI, M. & TUTAS, M. 2000. WATER SORPTION AND WATER VAPOUR PERMEABILITY PROPERTIES OF POLYSACCHARIDE (LOCUST BEAN GUM) BASED EDIBLE FILMS. *LEBENSMITTEL-WISSENSCHAFT UND-TECHNOLOGIE*, 33, 63-67.
- BAI, S. J., RANI, M., SURYANARAYANAN, R., CARPENTER, J. F., NAYAR, R. & MANNING, M. C. 2004. QUANTIFICATION OF GLYCINE CRYSTALLINITY BY NEAR-INFRARED (NIR) SPECTROSCOPY. *JOURNAL OF PHARMACEUTICAL SCIENCES*, 93, 2439-47.
- BANDEKAR, J., GENZEL, L., KREMER, F. & SANTO, L. 1983. THE TEMPERATURE-DEPENDENCE OF THE FAR-INFRARED SPECTRA OF L-ALANINE. *SPECTROCHIMICA ACTA PART A: MOLECULAR SPECTROSCOPY*, 39, 357-366.
- BATCH, G. L. & MACOSKO, C. W. 1991. DSC SAMPLE TEMPERATURE CONTROL WHILE MEASURING REACTION KINETICS. *THERMOCHIMICA ACTA*, 188, 1-15.
- BEARD, M. C., TURNER, G. M. & SCHMUTTENMAER, C. A. 2002. TERAHERTZ SPECTROSCOPY. *JOURNAL OF PHYSICAL CHEMISTRY B*, 106, 7146-7159.

- BETANCOURT, M. R. & SKOLNICK, J. 2004. LOCAL PROPENSITIES AND STATISTICAL POTENTIALS OF BACKBONE DIHEDRAL ANGLES IN PROTEINS. *JOURNAL OF MOLECULAR BIOLOGY*, 342, 635-649.
- BURJANADZE, T. V. 1979. HYDROXYPROLINE CONTENT AND LOCATION IN RELATION TO COLLAGEN THERMAL STABILITY. *BIOPOLYMERS*, 18, 931-938.
- C.C. DEROCHE ET AL. YEAR. CONSUMER PREFERENCE FOR ORALLY DISINTEGRATING TABLETS OVER CONVENTIONAL FORMS OF MEDICATION: EVOLVING METHODOLOGY FOR MEDICATION INTAKE IN DYSPHAGIA. *IN: 12TH ANNUAL MEETING OF THE DYSPHAGIA RESEARCH SOCIETY, 2003 SAN FRANCISCO, CA.*
- CARAMELLA, C., COLOMBO, P., CONTE, U., GAZZANIGA, A. & LA MANNA, A. 1984. ROLE OF SWELLING IN THE DISINTEGRATION PROCESS. *INTERNATIONAL JOURNAL OF PHARMACEUTICAL TECHNOLOGY AND PRODUCT MANUFACTURE*, 5, 1-5.
- CHANDRASEKHAR, R., HASSAN, Z., ALHUSBAN, F., SMITH, A. M. & MOHAMMED, A. R. 2009. THE ROLE OF FORMULATION EXCIPIENTS IN THE DEVELOPMENT OF LYOPHILISED FAST-DISINTEGRATING TABLETS. *EUROPEAN JOURNAL OF PHARMACEUTICS AND BIOPHARMACEUTICS*, 72, 119-129.
- CHANG, R.-K., GUO, X., BURNSIDE, B.A., COUCH, R.A 2000. FAST-DISSOLVING TABLETS. *PHARMACEUTICAL TECHNOLOGY* 24, 52-58.
- CHANTRY, G. W. 1971. *SUBMILLIMETRE SPECTROSCOPY: A GUIDE TO THE THEORETICAL AND EXPERIMENTAL PHYSICS OF THE FAR INFRARED*, LONDON, ACADEMIC PRESS INC. LTD.
- CHENG, S.-F. & CHANG, D.-K. 1999. PROLINE-INDUCED KINK IN A HELIX ARISES PRIMARILY FROM DIHEDRAL ANGLE ENERGY: A MOLECULAR DYNAMICS SIMULATION ON ALAMETHICIN. *CHEMICAL PHYSICS LETTERS*, 301, 453-457.
- CHOI, S. S. & REGENSTEIN, J. M. 2000. PHYSICOCHEMICAL AND SENSORY CHARACTERISTICS OF FISH GELATIN. *JOURNAL OF FOOD SCIENCE*, 65, 194-199.
- COOKSEY, C. C., GREER, B. J. & HEILWEIL, E. J. 2009. TERAHERTZ SPECTROSCOPY OF L-PROLINE IN REVERSE AQUEOUS MICELLES. *CHEMICAL PHYSICS LETTERS*, 467, 424-429.
- COOPER, T. G., JONES, W., MOTHERWELL, W. D. S. & DAY, G. M. 2007. DATABASE GUIDED CONFORMATION SELECTION IN CRYSTAL STRUCTURE PREDICTION OF ALANINE. *CRYSTENGCOMM*, 9, 595-602.
- CORVELEYN, S. & REMON, J. P. 1998. FORMULATION OF A LYOPHILIZED DRY EMULSION TABLET FOR THE DELIVERY OF POORLY SOLUBLE DRUGS. *INTERNATIONAL JOURNAL OF PHARMACEUTICS*, 166, 65-74.
- COUNCIL OF EUROPE 2001. *EUROPEAN PHARMACOPOEIA 2002*, COUNCIL OF EUROPE.

- DAVIDOVICH, M., J. Z. GOUGOUTAS, R. P. SCARINGE, I. VITEZ & YIN, S. 2004. DETECTION OF POLYMORPHISM BY POWDER X-RAY DIFFRACTION: INTERFERENCE BY PREFERRED ORIENTATION. *AMERICAN PHARM REV*, 7, 10-17.
- DEGTYARENKO, I. M., JALKANEN, K. J., GURTOVENKO, A. A. & NIEMINEN, R. M. 2007. L-ALANINE IN A DROPLET OF WATER: A DENSITY-FUNCTIONAL MOLECULAR DYNAMICS STUDY. *THE JOURNAL OF PHYSICAL CHEMISTRY B*, 111, 4227-4234.
- DEWOLF, F. A. & KELLER, R. C. A. 1996. CHARACTERIZATION OF HELICAL STRUCTURES IN GELATIN NETWORKS AND MODEL POLYPEPTIDES BY CIRCULAR DICHROISM. *IN: ZRINYI, M. (ED.) GELS*. BERLIN 33: DR DIETRICH STEINKOPFF VERLAG.
- DOBETTI, L. 2003. *FAST DISINTEGRATING TABLETS*. UNITED STATES PATENT APPLICATION 6596311.
- DONALD A. BURNS & CIURCZAK, E. W. (EDS.) 2008. *HANDBOOK OF NEAR-INFRARED ANALYSIS*, FLORIDA: CRC PRESS.
- DORNEY, T. D., BARANIUK, R. G. & MITTLEMAN, D. M. 2001. MATERIAL PARAMETER ESTIMATION WITH TERAHERTZ TIME-DOMAIN SPECTROSCOPY. *JOURNAL OF THE OPTICAL SOCIETY OF AMERICA A-OPTICS IMAGE SCIENCE AND VISION*, 18, 1562-1571.
- FERGUSON, B. & ZHANG, X. C. 2002. MATERIALS FOR TERAHERTZ SCIENCE AND TECHNOLOGY. *NATURE MATERIALS*, 1, 26-33.
- FERGUSON, H. F., FRURIP, D. J., PASTOR, A. J., PEEREY, L. M. & WHITING, L. F. 2000. A REVIEW OF ANALYTICAL APPLICATIONS OF CALORIMETRY. *THERMOCHIMICA ACTA*, 363, 1-21.
- FIX, J. A. YEAR. ADVANCES IN QUICK-DISSOLVING TABLETS TECHNOLOGY EMPLOYING WOWTAB. *IN: IIR CONFERENCE ON DRUG DELIVERY SYSTEMS*, OCTOBER, 1998 WASHINGTON DC, USA.
- FORNELL, C. & LARCKER, D. F. 1981. EVALUATING STRUCTURAL EQUATION MODELS WITH UNOBSERVABLE VARIABLES AND MEASUREMENT ERRORS. *JOURNAL OF MARKETING RESEARCH*, 18, 39-50.
- FU, Y. R., YANG, S. C., JEONG, S. H., KIMURA, S. & PARK, K. 2004. ORALLY FAST DISINTEGRATING TABLETS: DEVELOPMENTS, TECHNOLOGIES, TASTE-MASKING AND CLINICAL STUDIES. *CRITICAL REVIEWS IN THERAPEUTIC DRUG CARRIER SYSTEMS*, 21, 433-475.
- FUKAMI, J., OZAWA, A., YOSHIHASHI, Y., YONEMOCHI, E. & TERADA, K. 2005. DEVELOPMENT OF FAST DISINTEGRATING COMPRESSED TABLETS USING AMINO ACID AS DISINTEGRATION ACCELERATOR: EVALUATION OF WETTING AND DISINTEGRATION OF TABLET ON THE BASIS OF SURFACE FREE ENERGY. *CHEMICAL & PHARMACEUTICAL BULLETIN*, 53, 1536-1539.

- FUKAMI, J., YONEMOCHI, E., YOSHIHASHI, Y. & TERADA, K. 2006. EVALUATION OF RAPIDLY DISINTEGRATING TABLETS CONTAINING GLYCINE AND CARBOXYMETHYLCELLULOSE. *INTERNATIONAL JOURNAL OF PHARMACEUTICS*, 310, 101-109.
- GARTHWAITE, P. H. 1995. AN INTERPRETATION OF PARTIAL LEAST SQUARES. *JOURNAL OF THE AMERICAN STATISTICAL ASSOCIATION*, 89, 122-127.
- GOEL, H., RAI, P., RANA, V. & TIWARY, A. K. 2008. ORALLY DISINTEGRATING SYSTEMS: INNOVATIONS IN FORMULATION AND TECHNOLOGY. *RECENT PAT DRUG DELIV FORMUL*, 2, 258-74.
- GÓMEZ-GUILLÉN, M. C., GIMÉNEZ, B., LÓPEZ-CABALLERO, M. E. & MONTERO, M. P. FUNCTIONAL AND BIOACTIVE PROPERTIES OF COLLAGEN AND GELATIN FROM ALTERNATIVE SOURCES: A REVIEW. *FOOD HYDROCOLLOIDS*, IN PRESS, CORRECTED PROOF.
- GORBITZ, C. 1989. HYDROGEN-BOND DISTANCES AND ANGLES IN THE STRUCTURES OF AMINO ACIDS AND PEPTIDES. *ACTA CRYSTALLOGRAPHICA SECTION B*, 45, 390-395.
- GRUNENBERG, A., BOUGEARD, D. & SCHRADER, B. 1984. DSC- INVESTIGATIONS OF 22 CRYSTALLINE NEUTRAL ALIPHATIC AMINO ACIDS IN THE TEMPERATURE RANGE 233 TO 423 K. *THERMOCHIMICA ACTA*, 77, 59-66.
- HAENLEIN, M. & KAPLAN, A. M. 2004. A BEGINNER'S GUIDE TO PARTIAL LEAST SQUARES ANALYSIS. *UNDERSTANDING STATISTICS*, 3, 283-297.
- HELD, C., CAMERETTI, L. F. & SADOWSKI, G. MEASURING AND MODELING ACTIVITY COEFFICIENTS IN AQUEOUS AMINO-ACID SOLUTIONS. *INDUSTRIAL & ENGINEERING CHEMISTRY RESEARCH*, 50, 131-141.
- HIRANI, J. J., RATHOD, D. A. & VADALIA, K. R. 2009. ORALLY DISINTEGRATING TABLETS: A REVIEW. *TROPICAL JOURNAL OF PHARMACEUTICAL RESEARCH*, 8, 161-172.
- ICH 1996. VALIDATION OF ANALYTICAL PROCEDURES: TEST AND METHODOLOGY. *IN: INTERNATIONAL CONFERENCE ON HARMONISATION OF TECHNICAL REQUIREMENTS FOR REGISTRATION OF PHAMACEUTICALS FOR HUMAN USE (ICH) (ED.) INTERNATIONAL CONFERENCE ON HARMONISATION OF TECHNICAL REQUIREMENTS FOR REGISTRATION OF PHAMACEUTICALS FOR HUMAN USE (ICH), ED.*
- IKEDA, Y., ISHIHARA, Y., MORIWAKI, T., KATO, E. & TERADA, K. 2010. A NOVEL ANALYTICAL METHOD FOR PHARMACEUTICAL POLYMORPHS BY TERAHERTZ SPECTROSCOPY AND THE OPTIMIZATION OF CRYSTAL FORM AT THE DISCOVERY STAGE. *CHEMICAL & PHARMACEUTICAL BULLETIN*, 58, 76-81.
- JANCZAK, J., ZOBEL, D. & LUGER, P. 1997. L-THREONINE AT 12 K. *ACTA CRYSTALLOGRAPHICA SECTION C-CRYSTAL STRUCTURE COMMUNICATIONS*, 53, 1901-1904.

- JENNINGS, T. A. 1999. THE PRIMARY DRYING PROCESS. *LYOPHILIZATION: INTRODUCTION AND BASIC PRINCIPLES*. INTERPHARM PRESS.
- Jl, P. & FENG, W. 2008. SOLUBILITY OF AMINO ACIDS IN WATER AND AQUEOUS SOLUTIONS BY THE STATISTICAL ASSOCIATING FLUID THEORY. *INDUSTRIAL & ENGINEERING CHEMISTRY RESEARCH*, 47, 6275-6279.
- JOHNSTON-BANKS, F. A. 1990. GELATINE. IN: HARRIS, P. (ED.) *FOOD GELS*. LONDON: ELSEVIER APPLIED SCIENCE.
- JONES, D. 2002. *PHARMACEUTICAL STATISTICS*, LONDON, PHARMACEUTICAL PRESS.
- JONES, R. T. 1987. GELATIN STRUCTURE AND MANUFACTURE. IN: RIDGWAY, K. (ED.) *HARD CAPSULES: DEVELOPMENT AND TECHNOLOGY*. LONDON: PHARMACEUTICAL PRESS.
- KAMAT, M. S., LODDER, R. A. & DELUCA, P. P. 1989. NEAR INFRARED SPECTROSCOPY DETERMINATION OF RESIDUAL MOISTURE IN LYOPHILIZED SUCROSE THROUGH INTACT GLASS VIALS. *PHARMACEUTICAL RESEARCH*, 6, 961-965.
- KORTER, T. M., BALU, R., CAMPBELL, M. B., BEARD, M. C., GREGURICK, S. K. & HEILWEIL, E. J. 2006. TERAHERTZ SPECTROSCOPY OF SOLID SERINE AND CYSTEINE. *CHEMICAL PHYSICS LETTERS*, 418, 65-70.
- KRIMM, S. 1987. PEPTIDES AND PROTEINS. IN: SPIRO, T. G. (ED.) *IN: BIOLOGICAL APPLICATIONS OF RAMAN SPECTROSCOPY*. NEW YORK: JOHN WILEY & SONS.
- KYTE, J. 2003. THE BASIS OF THE HYDROPHOBIC EFFECT. *BIOPHYSICAL CHEMISTRY*, 100, 193-203.
- LABORATORY OF TERAHERTZ SPECTROSCOPY. 2010. *TERAHERTZ SPECTROSCOPY* [ONLINE]. PRAGUE. AVAILABLE: <http://department.fzu.cz/lts/> [ACCESSED 14/01 2011].
- LINDGREN, S. & JANZON, L. 1991. PREVALENCE OF SWALLOWING COMPLAINTS AND CLINICAL FINDINGS AMONG 50-79 YEARS OLD MEN AND WOMEN IN URBAN POPULATION. *DYSPHAGIA*, 6, 187-192.
- LIU, Z. & LI, C. 2008. SOLVENT-FREE CRYSTALLIZATIONS OF AMINO ACIDS: THE EFFECTS OF THE HYDROPHILICITY/HYDROPHOBICITY OF SIDE-CHAINS. *BIOPHYSICAL CHEMISTRY*, 138, 115-119.
- LUBEC, G. & ROSENTHAL, G. A. 1990. *AMINO ACIDS: CHEMISTRY, BIOLOGY AND MEDICINE*, ESCOM.
- MANTSCH, H. H. & NAUMANN, D. TERAHERTZ SPECTROSCOPY: THE RENAISSANCE OF FAR INFRARED SPECTROSCOPY. *JOURNAL OF MOLECULAR STRUCTURE*, 964, 1-4.
- MARKELZ, A. G., ROITBERG, A. & HEILWEIL, E. J. 2000. PULSED TERAHERTZ SPECTROSCOPY OF DNA, BOVINE SERUM ALBUMIN AND COLLAGEN BETWEEN 0.1 AND 2.0 THZ. *CHEMICAL PHYSICS LETTERS*, 320, 42-48.

- MASAKI, K. & BAN, K. 1995. *INTRABUCCALLY DISINTEGRATING PREPARATION AND PRODUCTION THEREOF*. UNITED STATES PATENT APPLICATION 256034.
- MATEI, A., DRICHKO, N., GOMPF, B. & DRESSEL, M. 2005. FAR-INFRARED SPECTRA OF AMINO ACIDS. *CHEMICAL PHYSICS*, 316, 61-71.
- MATHLOUTHI, M., CHOLLI, A. L. & KOENIG, J. L. 1986. SPECTROSCOPIC STUDY OF THE STRUCTURE OF SUCROSE IN THE AMORPHOUS STATE AND IN AQUEOUS SOLUTION. *CARBOHYDRATE RESEARCH*, 147, 1-9.
- MOHAMMED, A. R., COOMBES, A. G. A. & PERRIE, Y. 2007. AMINO ACIDS AS CRYOPROTECTANTS FOR LIPOSOMAL DELIVERY SYSTEMS. *EUROPEAN JOURNAL OF PHARMACEUTICAL SCIENCES*, 30, 406-413.
- MURLI, C., VASANTHI, R. & SHARMA, S. M. 2006. RAMAN SPECTROSCOPIC INVESTIGATIONS OF DL-SERINE AND DL-VALINE UNDER PRESSURE. *CHEMICAL PHYSICS*, 331, 77-84.
- NARAZAKI, R., HARADA, T., TAKAMI, N., KATO, Y. & OHWAKI, T. 2004. A NEW METHOD FOR DISINTEGRATION STUDIES OF RAPID DISINTEGRATING TABLET. *CHEM PHARM BULL (TOKYO)*, 52, 704-7.
- NATIONAL INSTITUTE OF STANDARDS AND TECHNOLOGY. 2011. *ALANINE, LEUCINE, LYSINE, PROLINE AND SERINE* [ONLINE]. AVAILABLE: <http://webbook.nist.gov/chemistry/name-ser.html> [ACCESSED 25/08 2011].
- PARAKH, S. R. & GOTHOSKAR, A. 2003. A REVIEW OF MOUTH DISSOLVING TABLET TECHNOLOGIES. *PHARMACEUTICAL TECHNOLOGY*, 27, 92 - 100.
- PEBLEY, W. S., JAGER, N. E. & THOMPSON, S. J. 1994. *RAPIDLY DISTINTEGRATING TABLET*. UNITED STATES PATENT APPLICATION 995196.
- PIKAL, M. J. & SHAH, S. 1990. THE COLLAPSE TEMPERATURE IN FREEZE DRYING: DEPENDENCE ON MEASUREMENT METHODOLOGY AND RATE OF WATER REMOVAL FROM THE GLASSY PHASE. *INTERNATIONAL JOURNAL OF PHARMACEUTICS*, 62, 165-186.
- RASMUSSEN, P. H., JÄRGENSEN, B. & NIELSEN, J. 1997. AQUEOUS SOLUTIONS OF PROLINE AND NaCl STUDIED BY DIFFERENTIAL SCANNING CALORIMETRY AT SUBZERO TEMPERATURES. *THERMOCHIMICA ACTA*, 303, 23-30.
- RICHARDSON, J. S. & RICHARDSON, D. C. 1989. PRINCIPLES AND PATTERNS OF PROTEIN CONFORMATION. IN: FASMAN, G. D. (ED.) *PREDICTION OF PROTEIN STRUCTURE AND PRINCIPLES OF PROTEIN CONFORMATION*. NEW YORK: PLENUM PRESS.
- RINGARD, J. & GUYOTHERMANN, A. M. 1988. CALCULATION OF DISINTEGRANT CRITICAL CONCENTRATION IN ORDER TO OPTIMIZE TABLETS DISINTEGRATION. *DRUG DEVELOPMENT AND INDUSTRIAL PHARMACY*, 14, 2321-2339.

- RODANTE, F. & MARROSU, G. 1990. THERMAL-ANALYSIS OF SOME ALPHA-AMINO-ACIDS USING SIMULTANEOUS TG-DSC APPARATUS - THE USE OF DYNAMIC THERMOGRAVIMETRY TO STUDY THE CHEMICAL-KINETICS OF SOLID-STATE DECOMPOSITION. *THERMOCHIMICA ACTA*, 171, 15-29.
- RODANTE, F., MARROSU, G. & CATALANI, G. 1992. THERMAL ANALYSIS OF SOME [ALPHA]-AMINO ACIDS WITH SIMILAR STRUCTURES. *THERMOCHIMICA ACTA*, 194, 197-213.
- ROTTHAUSER, B., KRAUS, G. & SCHMIDT, P. C. 1998. OPTIMIZATION OF AN EFFERVESCENT TABLET FORMULATION USING A CENTRAL COMPOSITE DESIGN OPTIMIZATION OF AN EFFERVESCENT TABLET FORMULATION CONTAINING SPRAY DRIED L-LEUCINE AND POLYETHYLENE GLYCOL 6000 AS LUBRICANTS USING A CENTRAL COMPOSITE DESIGN. *EUROPEAN JOURNAL OF PHARMACEUTICS AND BIOPHARMACEUTICS*, 46, 85-94.
- SASTRY, S. V. & NYSHADHAM, J. R. 2005. PROCESS DEVELOPMENT AND SCALE-UP OF ORAL FAST-DISSOLVING TABLETS. IN: GHOSH, T. K. & PFISTER, W. R. (EDS.) *DRUG DELIVERY TO THE ORAL CAVITY: MOLECULES TO MARKET*. NEW YORK, NY: CRC PRESS.
- SASTRY, S. V., NYSHADHAM, J. R. & FIX, J. A. 2000. RECENT TECHNOLOGICAL ADVANCES IN ORAL DRUG DELIVERY - A REVIEW. *PHARMACEUTICAL SCIENCE & TECHNOLOGY TODAY*, 3, 138-145.
- SEAGER, H. 1998. DRUG-DELIVERY PRODUCTS AND THE ZYDIS FAST-DISSOLVING DOSAGE FORM. *JOURNAL OF PHARMACY AND PHARMACOLOGY*, 50, 375-382.
- SHEN, Y.-C. TERAHERTZ PULSED SPECTROSCOPY AND IMAGING FOR PHARMACEUTICAL APPLICATIONS: A REVIEW. *INTERNATIONAL JOURNAL OF PHARMACEUTICS*, IN PRESS, CORRECTED PROOF.
- SHEN, Y.-C., TADAY, P. F. & PEPPER, M. 2008. ELIMINATION OF SCATTERING EFFECTS IN SPECTRAL MEASUREMENT OF GRANULATED MATERIALS USING TERAHERTZ PULSED SPECTROSCOPY. *APPLIED PHYSICS LETTERS*, 92.
- SHUKLA, D., CHAKRABORTY, S., SINGH, S. & MISHRA, B. 2009. MOUTH DISSOLVING TABLETS I: AN OVERVIEW OF FORMULATION TECHNOLOGY. *SCI. PHARM.*, 77, 309-326.
- SIESLER, H. W., OZAKI, Y., KAWATA, S. & HEISE, H. M. (EDS.) 2002. *NEAR-INFRARED SPECTROSCOPY: PRINCIPLES, INSTRUMENTS, APPLICATIONS*, WEINHEIM: WILEY-VCH
- SLADE, L. & LEVINE, H. 1987. POLYMER CHEMICAL PROPERTIES OF GELATIN. IN: PEARSON, A. M., DUTSON, T. R. & BAILEY, A. J. (EDS.) *ADVANCES IN MEAT RESEARCH: COLLAGEN AS A FOOD*. NEW YORK: VAN NOSTRAND REINHOLD INC.

- SNYDER, R. G. 1961. VIBRATIONAL SPECTRA OF CRYSTALLINE N-PARAFFINS: II. INTERMOLECULAR EFFECTS. *JOURNAL OF MOLECULAR SPECTROSCOPY*, 7, 116-144.
- STAINSBY, G. 1987. GELATIN GELS. *IN: PEARSON, A. M., DUTSON, T. R. & BAILEY, A. J. (EDS.) ADVANCES IN MEAT RESEARCH: COLLAGEN AS A FOOD*. NEW YORK: VAN NOSTRAND REINHOLD INC.
- STRACHAN, C. J., RADES, T., NEWNHAM, D. A., GORDON, K. C., PEPPER, M. & TADAY, P. F. 2004. USING TERAHERTZ PULSED SPECTROSCOPY TO STUDY CRYSTALLINITY OF PHARMACEUTICAL MATERIALS. *CHEMICAL PHYSICS LETTERS*, 390, 20-24.
- STRACHAN, C. J., TADAY, P. F., NEWNHAM, D. A., GORDON, K. C., ZEITLER, J. A., PEPPER, M. & RADES, T. 2005. USING TERAHERTZ PULSED SPECTROSCOPY TO QUANTIFY PHARMACEUTICAL POLYMORPHISM AND CRYSTALLINITY. *JOURNAL OF PHARMACEUTICAL SCIENCES*, 94, 837-846.
- TADAY, P. F., BRADLEY, I. V., ARNONE, D. D. & PEPPER, M. 2003. USING TERAHERTZ PULSE SPECTROSCOPY TO STUDY THE CRYSTALLINE STRUCTURE OF A DRUG: A CASE STUDY OF THE POLYMORPHS OF RANITIDINE HYDROCHLORIDE. *JOURNAL OF PHARMACEUTICAL SCIENCES*, 92, 831-838.
- TERAVIEW LIMITED 2009. TPS SPECTRA 3000 USER'S GUIDE.
- THAKUR, R. R. & KASHI, M. 2011. AN UNLIMITED SCOPE FOR NOVEL FORMULATIONS AS ORALLY DISINTEGRATING SYSTEMS: PRESENT AND FUTURE PROSPECTS. *JOURNAL OF APPLIED PHARMACEUTICAL SCIENCE*, 1, 13-19.
- THE BRITISH PHARMACOPOEIA COMMISSION 2011. FORMULATED PREPARATIONS: GENERAL MONOGRAPHS - TABLETS *BRITISH PHARMACOPOEIA Vol III* NORWICH: THE STATIONERY OFFICE.
- TOTRE, J., ICKOWICZ, D. & DOMB, A. J. 2011. PROPERTIES AND HOMOSTATIC APPLICATION OF GELATIN. *IN: DOMB, A. J. & KUMAR, N. (EDS.) BIODEGRADABLE POLYMERS IN CLINICAL USE AND CLINICAL DEVELOPMENT* 1ED. NEW JERSEY: JOHN WILEY & SONS.
- TSENG, H.-C., LEE, C.-Y., WENG, W.-L. & SHIAH, I. M. 2009. SOLUBILITIES OF AMINO ACIDS IN WATER AT VARIOUS PH VALUES UNDER 298. *FLUID PHASE EQUILIBRIA*, 285, 90-95.
- UNITED STATES PHARMACOPEIAL CONVENTION 2009. GENERAL CHAPTER <1151> PHARMACEUTICAL DOSAGE FORMS. *IN: PHARMACOPEIAL FORUM BY AUTHORITY OF THE UNITED STATES PHARMACOPEIAL CONVENTION*, M. A. W. D. C. M.-., 2005, (ED.) 5 ED. PHARMACOPEIAL FORUM: UNITED STATES PHARMACOPEIAL CONVENTION INC.
- VANIN, F. M., SOBRAL, P. J. A., MENEGALLI, F. C., CARVALHO, R. A. & HABITANTE, A. M. Q. B. 2005. EFFECTS OF PLASTICIZERS AND THEIR

- CONCENTRATIONS ON THERMAL AND FUNCTIONAL PROPERTIES OF GELATIN-BASED FILMS. *FOOD HYDROCOLLOIDS*, 19, 899-907.
- VINOGRADOV, S. N. 1979. HYDROGEN BONDS IN CRYSTAL STRUCTURES OF AMINO ACIDS, PEPTIDES AND RELATED MOLECULES. *INTERNATIONAL JOURNAL OF PEPTIDE AND PROTEIN RESEARCH*, 14, 281-289.
- VIRLEY, P. & YARWOOD, R. 1990. ZYDIS- A NOVEL, FAST DISSOLVING DOSAGE FORM. *MANUFACTURING CHEMIST*, 61, 36-37.
- WALTHER, M., FISCHER, B. M. & UHJ JEPSEN, P. 2003. NONCOVALENT INTERMOLECULAR FORCES IN POLYCRYSTALLINE AND AMORPHOUS SACCHARIDES IN THE FAR INFRARED. *CHEMICAL PHYSICS*, 288, 261-268.
- WEAST, R. C. 1977. *CRC HANDBOOK OF CHEMISTRY AND PHYSICS: A READY-REFERENCE BOOK OF CHEMICAL AND PHYSICAL DATA*, CRC PRESS.
- WEHLING, F., SCHUEHLE, S. & MADAMALA, N. 1993. *EFFERVESCENT DOSAGE FORM WITH MICROPARTICLES*. UNITED STATES PATENT APPLICATION 5178878.
- WEISBERG, S. 2005. SIMPLE LINEAR REGRESSION. *IN: WEISBERG, S. (ED.) APPLIED LINEAR REGRESSION*. THIRD ED. NEW JERSEY: JOHN WILEY.
- WENDLANDT, W. W. 1982. THERMAL ANALYSIS. *ANALYTICAL CHEMISTRY*, 54, 97R-105R.
- YAMAGUCHI, M., MIYAMARU, F., YAMAMOTO, K., TANI, M. & HANGYO, M. 2005. TERAHERTZ ABSORPTION SPECTRA OF [L]-, [D]-, AND [DL]-ALANINE AND THEIR APPLICATION TO DETERMINATION OF ENANTIOMETRIC COMPOSITION. *APPLIED PHYSICS LETTERS*, 86, 053903.
- YAMAMOTO, K., TOMINAGA, K., SASAKAWA, H., TAMURA, A., MURAKAMI, H., OHTAKE, H. & SARUKURA, N. 2005. TERAHERTZ TIME-DOMAIN SPECTROSCOPY OF AMINO ACIDS AND POLYPEPTIDES. *BIOPHYSICAL JOURNAL*, 89, L22-L24.
- YAO-CHUN, S. 2011. TERAHERTZ PULSED SPECTROSCOPY AND IMAGING FOR PHARMACEUTICAL APPLICATIONS: A REVIEW. *INTERNATIONAL JOURNAL OF PHARMACEUTICS*, 417, 48-60.
- YENIA, Ä. & GÄOKTA, A. 2002. A COMPARISON OF PARTIAL LEAST SQUARES REGRESSION WITH OTHER PREDICTION METHODS. *HACETTEPE JOURNAL OF MATHEMATICS AND STATISTICS*, 31, 99 - 111.

Appendix I

Publication 1 – PharmSci Annual Conference 2010

Study of Amino Acids and Gelatin as a Matrix for Lyophilised Rapid Disintegrating Tablets using Terahertz Pulsed Spectroscopy.



Joseph Darkwah, I. Ermolina, G. Smith

Leicester School of Pharmacy, De Montfort University, Leicester. LE1 9BH, UK.

1 INTRODUCTION

Previously, Rapid Disintegrating Tablets (RDTs) have been formulated with gelatin, polyols and sugars e.g. mannitol. RDTs produced by lyophilisation technology possess a high level of porosity and amorphous character of the matrix. However, the sugars are required in high concentrations for better mechanical strength, but then the formulation becomes unsuitable for the treatment of some chronic diseases, e.g. diabetics and obesity or for children and those with allergies (e.g. lactose intolerance). Recent research has focused on the use of amino acids as a replacement component for polyols and sugars. Moreover, this offers the potential for improved mechanical strength at lower concentrations compared to sugars. However, there is an intrinsic stability issue with both types of RDTs, i.e. conversion from amorphous to crystalline state (devitrification), which impacts the mechanical property, solubility and hence dissolution time. Stability of these formulations is affected by moisture content and storage conditions.

This study investigates the use of terahertz Pulsed Spectroscopy (TPS) for quantifying morphological changes associated with the devitrification process and recrystallization. The study is based on the fact that crystalline amino acids show distinct phonon resonances when probed with terahertz radiation whereas the amorphous amino acids does not.

2. AIM

The aim of this study is to quantify the recrystallization of amino acids in standard pellets gelatin loaded films, and freeze dried gelatin/amino acid pellets.

3. MATERIALS and METHODS

Three types of formulations were studied: pellets with crystalline amino acids, gelatin/amino acid films and pellets with freeze dried gelatin/amino acid matrix. Gelatin and amino acids (L-Serine, L-Alanine, L-Lysine and L-Leucine) were obtained from Sigma Aldrich UK.

Pellets Up to 10% of the crystalline amino acid was incorporated into 400mg ($\pm 0.005\%$) polyethylene pellets (Carver hydraulic press with load of 2 tons). These pellets were used as the standard formulation for calibration of TPS measurements.

Films Films of thickness 0.3 ± 0.07 mm were prepared by casting 10% aqueous gelatin loaded with amino acids at concentrations of 33% total solid material and then evaporation of water overnight. The thickness of each sample was estimated by micrometer as an average value out of six measurements at different points of pellet.

Pellets with Freeze Dried Amino acid/Gelatin (PFD) Gelatin/Amino acid solution was frozen at -80°C for 2 hrs. The frozen solution was freeze dried at an optimum regime (HETO FD8 - pre freeze at -40°C for 7 hrs, primary drying at -35°C for 86 hrs and secondary drying at 20°C for 15 hrs)

Terahertz Pulsed Spectroscopy (TPS 3000, Teraview Cambridge, UK) was used in transmission mode to measure the spectra of absorbance at the ambient temperature. The sample chamber was purged with dry nitrogen for 10 minutes prior to measurements to avoid moisture uptake.

ACKNOWLEDGEMENT

East Midlands Development Agency for funding the TeraView TPS3000 spectrometer

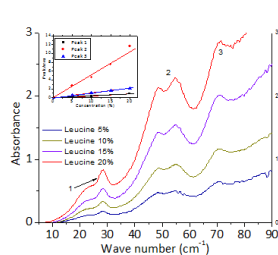


Fig 1. TPS spectra of Leucine pellets of different concentration. Inclusion shows area dependence of area of three main peaks vs. Concentration.

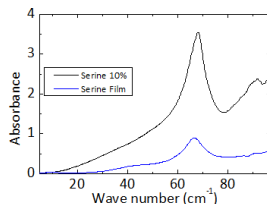


Fig 2. Comparing characteristic peaks of pellets with gelatin films loaded with 33% tsm Amino acid

Table 1 Normalised peak area for the serine film and pellets

| | Concentration % | Thickness mm | Peak Area | Normalized Peak Area (concentration) | Normalized Peak Area by thickness |
|--------|-----------------|--------------|-----------|--------------------------------------|-----------------------------------|
| Film | 22 | 0.30 | 5.56 | 5.56 (22%) | 67.8 (3.66 mm) |
| Pellet | 10 | 3.66 | 22.7 | 73.1 (22%) | 73.1 (3.66 mm) |

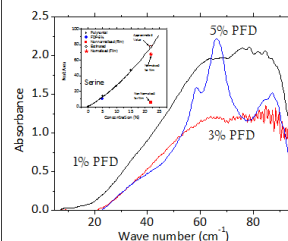


Fig 3. TPS spectra of Serine pellets produced from freeze dried gelatin/amino acid. Inclusion shows calibration curve for estimating crystallinity.

3. RESULTS AND DISCUSSION

The shape of spectra is independent of particle size below $\sim 80\mu\text{m}$. Both the amplitude of the peak and the area under the peak are dependent on the concentration of amino acid, method of preparation (film and pellets) and thickness of sample.

- In pellets, the peak area (PA) is linearly proportional to concentration of amino acid for all four amino acids (See Fig 1 for Leucine)

- To compare the results for film and pellets, the peak area was normalized per thickness of sample and concentration of amino acid.

- The position of the principal absorption peak (wave number) and shape (at small concentration of amino acids) were independent of sample preparation (i.e. pellet or film) as shown in Fig 2.

- The high baseline may possibly be due to different matrix, pure gelatin in films and PE in case of pellets.

- PFD formulation were prepared for Serine and Alanine. In both formulations the amino acids retain their amorphous states at 10% total solid material (tsm). Increasing the concentration to 30% tsm, Alanine retained its amorphous state whilst Serine showed crystallisation behaviour.

- At 50% tsm, both amino acids indicated the distinct peaks reported by Matei et al. and Korter et al. respectively.

- The spectra for Serine at 50% tsm showed an additional peak indicating at 30% tsm, crystallisation may not be completed as shown in Fig 3.

- The crystallinity in PFD was estimated using calibration curve, which was near $\sim 100\%$. (See Inclusion in Fig 3)

- From Table 1 the percentage of crystallinity for the serine film was calculated as 88% ($67.8/73.1$)

5. CONCLUSION

- TPS seems to be a capable tool for estimating the crystalline part of the material in films, which relate to dissolution of crystalline amino acids in films important for RDTs

- In Serine/gelatin film, we observed $\sim 88\%$ crystallisation of the amino acid although the concentration of amino acid was much higher than as contained in freeze dried matrix

- In freeze dried gelatin/Serine matrix, we observed $\sim 100\%$ devitrification of amino acid.

REFERENCES

- [1] AlHusban F. et al, Formulation and characterisation of lyophilised RDTs using amino acids as matrix forming agents, *Eur J Pharm a and Biopharm*, **75**, 254, 2010.
- [2] Matei A. et al, Far infra red spectra of amino acids, *Chem Phys*, **316**, 61, 2005.
- [3] Korter T.M. Et al, Terahertz spectroscopy of solid serine and cysteine, *Chem. Phys. Lett*, **418**, 65, 2006.

PHARMACEUTICAL
TECHNOLOGIES GROUP



Identifying the characteristics of the terahertz absorption spectra of a crystalline binary system containing proline and serine.

J. Darkwah, I. Ermolina, G. Smith

Leicester School of Pharmacy, De Montfort University, Leicester, LE1 9BH, UK.

INTRODUCTION 3

The feasibility of adding proline to lyophilized formulations of serine/gelatin mixtures has been studied and reported in [1], in the formulation of gelatin/amino acid based, orally disintegrating tablets (ODT). Studies showed that the inclusion of a high concentration of proline could increase the wettability of the matrix. However, high concentrations of both serine and proline reduce the total porosity of the matrix thereby increasing the disintegration time. This is thought to be due an increase in the crystalline content of the matrix. Hence, it is desirable to be able to quantify the degree of crystallinity in-situ in order to optimize the characteristics of the product.

Terahertz pulsed spectroscopy (TPS) has been used in previous studies to quantify the degree of crystallinity in individual crystalline and lyophilized amino acids [2]. It was observed that lyophilized gelatin matrices containing greater than 50% w/w of amino acid (total solid material) exhibited 100% crystallinity of the amino acid.

AIM

The aim of this study was to measure the terahertz absorption spectra of a binary system of serine and proline and to compare the peak area of measured absorption spectra with theoretical/calculated areas from the individual components.

MATERIALS and METHOD

Serine (Ser), and proline (Pro) (Sigma Aldrich UK) were sieved and fractions (<63 μm) collected for analysis. Ser (8% w/w), Pro (8% w/w) and a mixture of Ser and Pro (5% w/w each) was incorporated into a non-absorbing polyethylene powder. The powders were compressed into pellets (400 mg \pm 0.005) using a CT5 press at compressional force of 0.5 ton. The absorption spectra of each amino acid were measured using a TPS 3000 (Teraview Cambridge, UK). The sample compartment was purged with dry nitrogen for 10 minutes prior to each measurement.

The peak area of the measured spectra was integrated using Origin® Pro software. The integration analysis was repeated six times and the average used for further analysis.

RESULTS and DISCUSSION

- Figure 1A shows the absorption band for Ser at 67.6 cm^{-1} .
- To compare the results for Ser and Pro, absorption spectra of Pro was normalised to the absorbance maximum for Ser.
- In Pro (normalised to the absorbance maximum for serine), a principal absorption band is observed at 66.1 cm^{-1} and a partially obscured band at 42.6 cm^{-1} .

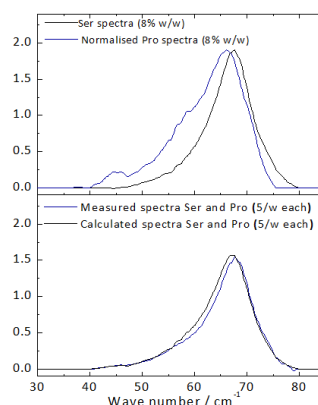


Figure 1 (A) comparison of the terahertz absorption spectra of Ser and Pro (normalized to the absorbance maximum for Ser), (B) comparison of the measured and calculated spectra of the mixture of Ser (5% w/w) and Pro (5% w/w).

- The absorption spectrum of the binary system showed a single absorption band at 67.7 cm^{-1} . The position of this absorption band is similar to that measured for a simple system containing Ser. The additional peak partially observed in pure Pro at 42.6 cm^{-1} has been obscured further.
- The theoretical absorption band of the mixture was calculated from the individual absorption spectra of Ser and Pro.
- The estimated area for the measured spectra of Ser/Pro mixture was 17.7 whilst the calculated area from the theoretical absorption spectra was 18.4. The percentage difference between these two areas is ~4%.

Table 1 shows the integrated peak area of the individual proline (8% w/w), serine (8% w/w) and the combination of serine and proline (5% w/w of each). The data presented is an average of six separate measurements.

| Sample | Peak Area | Variance |
|----------------|-----------|----------|
| Proline | 9.23 | 0.10 |
| Serine | 20.33 | 0.02 |
| Serine/Proline | 17.736 | 0.001 |

- The frequencies of the principal absorption bands for Ser and Pro are dependent on the intermolecular phonon vibrations which are distinct in all amino acids (as reported in [2])
- The difference in intensity of the absorption bands for proline and serine relates to the stronger vibration bonds observed in serine.

CONCLUSIONS

- The area of the absorption bands for the terahertz spectrum of a binary system containing Ser and Pro can be estimated from the summation of the absorbance spectra of the individual components.
- This indicates the feasibility for developing a numerical model to deconvolute the contributions from each component (in a binary mixture) from which the respective concentrations of the individual components can be determined.

REFERENCES

- [1] F. Alhusban, et al. "Investigation of formulation and process of lyophilised orally disintegrating tablets using novel amino acid combination" *Pharmaceutics*. (2010), 1-17
- [2] J. Darkwah, I. Ermolina, G. Smith, "Terahertz pulsed spectroscopy study of amino acids in gelatin". *J. Pharm. and Pharmacol.*, 62 (2010), 1477-78.

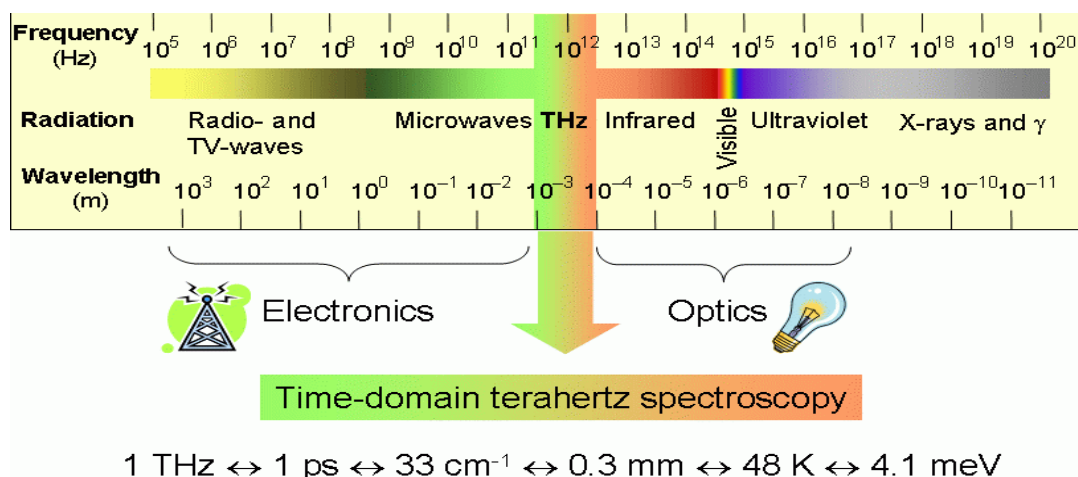
ACKNOWLEDGMENT

To the East Midlands Development Agency for funding the Terahertz pulsed spectroscopy.

Appendix II

Terahertz Pulsed Spectroscopy modus operandi

Terahertz radiation lies within the frequency range of 0.1 THz and 10 THz of the electromagnetic spectrum (Yao-Chun, 2011) located between microwaves and infrared radiation as shown below.

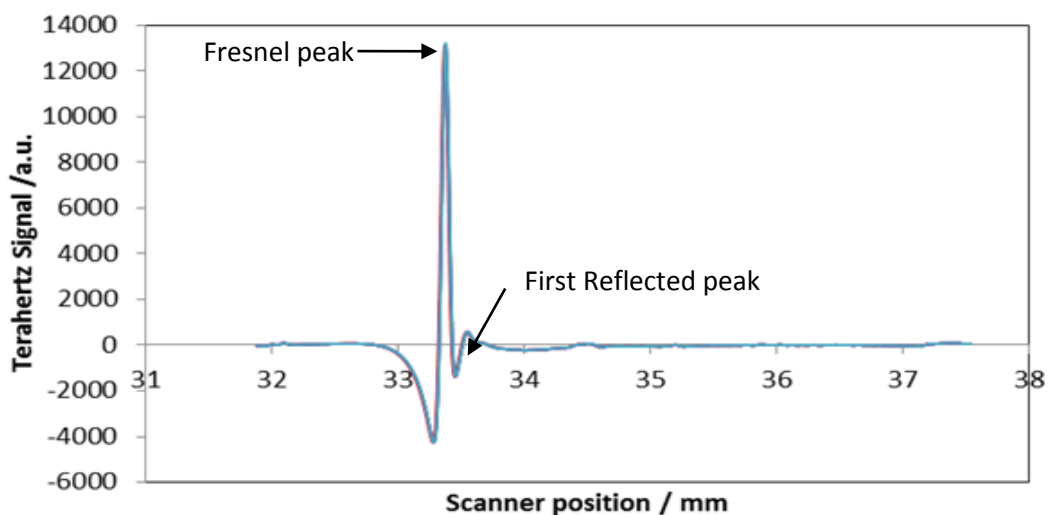


The electromagnetic spectrum highlighting the position in the spectrum where terahertz radiation is observed. Accessed from (Laboratory of Terahertz Spectroscopy, 2010)

The relevance of terahertz radiation and how this could be useful tool in characterising pharmaceutical materials has also been reviewed (Chantry, 1971, Shen, Mantsch and Naumann). Previously, the generation of terahertz radiation has been generated from incoherent blackbody sources such as mercury arc lamp or from sources with temperatures $\geq 10 \text{ K}$ both of which proved to be insensitive when used at the terahertz frequency. As a result, sensitive cryogen cooled bolometers were required to detect the signals (Ikeda et al., 2010). The poor sourcing and environment created noisy spectra making the technology unattractive and hard to use in quantifying crystallinity and identifying polymorphic excipients.

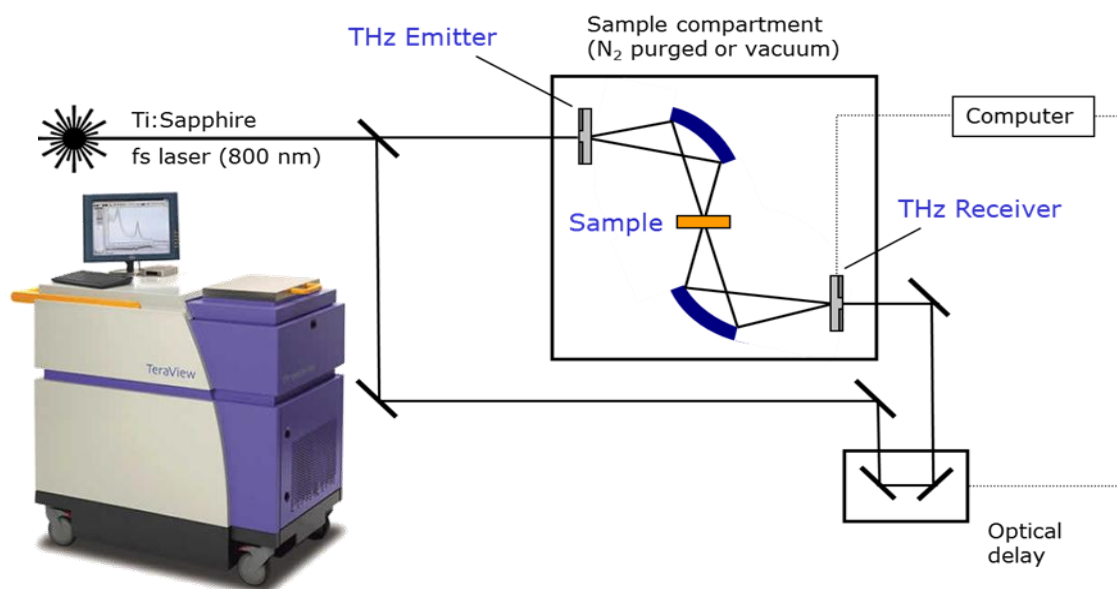
Recent advance in technology has seen development of better emitting sources and detectors (Ferguson and Zhang, 2002). The commercially available TPS technology is based on photoconductive switch. The photoconductive emitters produce broadband pulses in femtoseconds using ultrafast laser to excite biased Gallium Arsenide antenna (GaAs). The emitted power is distributed over a frequency range of about 0.06THz to 3THz. By adjusting the current density of the biased semiconductor in sub-picosecond timescale, the photoconductive antenna produce pulsed terahertz emissions. The change in current density occurs as a result of altering the carrier density through a femtosecond laser illumination and

increasing the rate of light generated carriers in an external electric field. A similar photoconductive antenna circuit is employed for coherent terahertz radiation detection. A current equivalent to terahertz electric field is measured by gating the photoconductive gap using a femtosecond pulse attuned to terahertz emission. To obtain the amplitude of the terahertz wave, a varied optical path length to a receiver is used so that the terahertz time domain can be measured. The typical waveform of a material is as shown



Typical terahertz waveform of pharmaceutical materials indicating the Fresnel peak and the First Reflected peak.

A schematic representation of TPS is as shown.



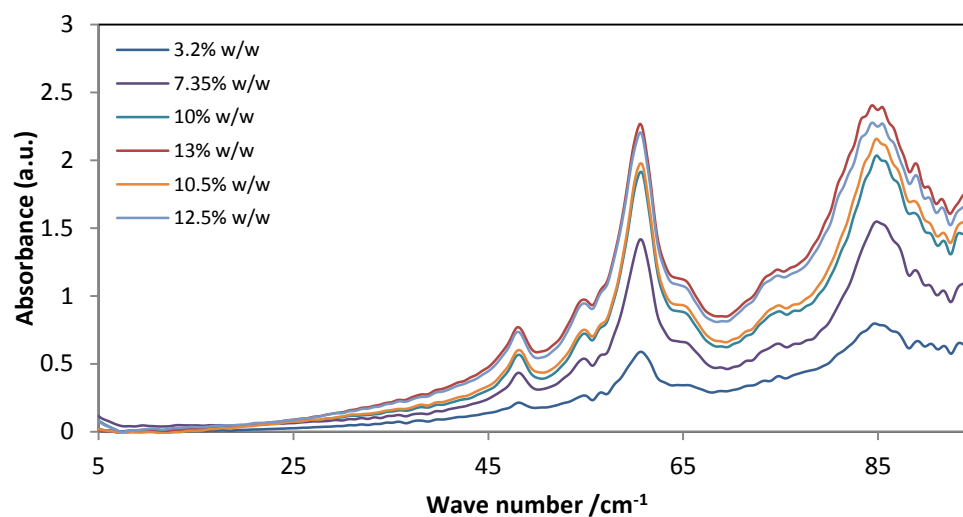
Schematic representation of the geometry of TPS. Bottom left is the TPS 3000 equipment used. Diagram copied from (Teraview Limited, 2009)

The ability of terahertz radiation to probe lattice and hydrogen bond vibrations (Chantry, 1971) has made it a powerful tool fingerprint crystalline materials. In fact it has been suggested that an atomic level representation of amino acids and other biological molecule can be created using their terahertz spectra (Yamamoto et al., 2005). In a recent study (Walther et al., 2003) on polycrystalline saccharides, it was shown that a series of distinct absorption bands were observed whilst for amorphous sugars a broad, featureless absorption spectrum is observed. The ordered arrangements of molecules in crystalline materials lead to precise lowest intermolecular vibrational modes which are detected by terahertz technology. In a different study (Taday et al., 2003), it was also observed that two distinct terahertz spectra of ranitidine hydrochloride due to two different polymorphic forms can be easily observed with this technology.

The terahertz pulsed technology has some major advantages when compared to the other types of analytical technologies. For instance, TPS technology is non-destructive and non-ionizing to the sample when compared to the DSC technology. Unlike the near infrared technology, the terahertz absorption spectra shows the intermolecular vibrations that corresponds to motions linked with consistent, delocalized movements of large numbers of atoms and molecules and not overtones or combination bands of the fundamental mid infrared range. TPS has other modules (i.e. Attenuated Total Reflectance, Terahertz Pulsed Imaging and Terahertz Cryostat) attached to it depending on the users' requirements. All of which has their specific advantages. For instance, the ATR module requires sample quantity of about 10 mg – 15 mg and this sample can be in its raw state.

Terahertz technology like any other technology has some associated drawbacks. The samples are mostly required in discs or pellets unlike the near infrared or the Raman spectroscopic technologies. During sample preparation, transient heating can affect alter the molecular characteristics of the samples. Especially in the case of TPS, this drawback can be avoided when using imaging or the ATR module. The sensitivity of the terahertz radiation is also affected by the presence of water molecules; hence the sample chamber requires longer purging times when using the transmission module.

THz absorption spectra of Sucrose test samples.



THz spectra of L-proline test samples

